



National Library  
of Canada

Bibliothèque nationale  
du Canada

Acquisitions and  
Bibliographic Services Branch

Direction des acquisitions et  
des services bibliographiques

395 Wellington Street  
Ottawa, Ontario  
K1A 0N4

395, rue Wellington  
Ottawa (Ontario)  
K1A 0N4

*Your file* *Votre référence*

*Our file* *Notre référence*

## NOTICE

The quality of this microform is heavily dependent upon the quality of the original thesis submitted for microfilming. Every effort has been made to ensure the highest quality of reproduction possible.

If pages are missing, contact the university which granted the degree.

Some pages may have indistinct print especially if the original pages were typed with a poor typewriter ribbon or if the university sent us an inferior photocopy.

Reproduction in full or in part of this microform is governed by the Canadian Copyright Act, R.S.C. 1970, c. C-30, and subsequent amendments.

## AVIS

La qualité de cette microforme dépend grandement de la qualité de la thèse soumise au microfilmage. Nous avons tout fait pour assurer une qualité supérieure de reproduction.

S'il manque des pages, veuillez communiquer avec l'université qui a conféré le grade.

La qualité d'impression de certaines pages peut laisser à désirer, surtout si les pages originales ont été dactylographiées à l'aide d'un ruban usé ou si l'université nous a fait parvenir une photocopie de qualité inférieure.

La reproduction, même partielle, de cette microforme est soumise à la Loi canadienne sur le droit d'auteur, SRC 1970, c. C-30, et ses amendements subséquents.

**NEW CHEMILUMINESCENT METHODS IN CHROMATOGRAPHIC  
DETECTION**

by

Kevin Blain Thurbide

Submitted in partial fulfillment of the requirements  
for the degree of Doctor of Philosophy

at

Dalhousie University

Halifax, Nova Scotia, Canada

October, 1994

© Copyright by Kevin Blain Thurbide, 1994



National Library  
of Canada

Bibliothèque nationale  
du Canada

Acquisitions and  
Bibliographic Services Branch

Direction des acquisitions et  
des services bibliographiques

395 Wellington Street  
Ottawa, Ontario  
K1A 0N4

395, rue Wellington  
Ottawa (Ontario)  
K1A 0N4

*Your file* *Votre référence*

*Our file* *Notre référence*

THE AUTHOR HAS GRANTED AN IRREVOCABLE NON-EXCLUSIVE LICENCE ALLOWING THE NATIONAL LIBRARY OF CANADA TO REPRODUCE, LOAN, DISTRIBUTE OR SELL COPIES OF HIS/HER THESIS BY ANY MEANS AND IN ANY FORM OR FORMAT, MAKING THIS THESIS AVAILABLE TO INTERESTED PERSONS.

L'AUTEUR A ACCORDE UNE LICENCE IRREVOCABLE ET NON EXCLUSIVE PERMETTANT A LA BIBLIOTHEQUE NATIONALE DU CANADA DE REPRODUIRE, PRETER, DISTRIBUER OU VENDRE DES COPIES DE SA THESE DE QUELQUE MANIERE ET SOUS QUELQUE FORME QUE CE SOIT POUR METTRE DES EXEMPLAIRES DE CETTE THESE A LA DISPOSITION DES PERSONNE INTERESSEES.

THE AUTHOR RETAINS OWNERSHIP OF THE COPYRIGHT IN HIS/HER THESIS. NEITHER THE THESIS NOR SUBSTANTIAL EXTRACTS FROM IT MAY BE PRINTED OR OTHERWISE REPRODUCED WITHOUT HIS/HER PERMISSION.

L'AUTEUR CONSERVE LA PROPRIETE DU DROIT D'AUTEUR QUI PROTEGE SA THESE. NI LA THESE NI DES EXTRAITS SUBSTANTIELS DE CELLE-CI NE DOIVENT ETRE IMPRIMES OU AUTREMENT REPRODUITS SANS SON AUTORISATION.

ISBN 0-612-05236-2

Canada

Name Kevin Thuvide

Dissertation Abstracts International is arranged by broad, general subject categories. Please select the one subject which most nearly describes the content of your dissertation. Enter the corresponding four-digit code in the spaces provided.

Analytical Chemistry  
SUBJECT TERM

0486  
SUBJECT CODE

U·M·I

**Subject Categories**

**THE HUMANITIES AND SOCIAL SCIENCES**

**COMMUNICATIONS AND THE ARTS**

Architecture 0729  
Art History 0377  
Cinema 0900  
Dance 0378  
Fine Arts 0357  
Information Science 0723  
Journalism 0391  
Library Science 0399  
Mass Communications 0708  
Music 0413  
Speech Communication 0459  
Theater 0465

**EDUCATION**

General 0515  
Administration 0514  
Adult and Continuing 0516  
Agricultural 0517  
Art 0273  
Bilingual and Multicultural 0282  
Business 0688  
Community College 0275  
Curriculum and Instruction 0727  
Early Childhood 0518  
Elementary 0524  
Finance 0277  
Guidance and Counseling 0519  
Health 0680  
Higher 0745  
History of 0520  
Home Economics 0278  
Industrial 0521  
Language and Literature 0279  
Mathematics 0280  
Music 0522  
Philosophy of 0998  
Physical 0523

Psychology 0525  
Reading 0535  
Religious 0527  
Sciences 0714  
Secondary 0533  
Social Sciences 0534  
Sociology of 0340  
Special 0529  
Teacher Training 0530  
Technology 0710  
Tests and Measurements 0288  
Vocational 0747

**LANGUAGE, LITERATURE AND LINGUISTICS**

Language  
General 0679  
Ancient 0289  
Linguistics 0290  
Modern 0291  
Literature  
General 0401  
Classical 0294  
Comparative 0295  
Medieval 0297  
Modern 0298  
African 0316  
American 0591  
Asian 0305  
Canadian (English) 0352  
Canadian (French) 0355  
English 0593  
Germanic 0311  
Latin American 0312  
Middle Eastern 0315  
Romance 0313  
Slavic and East European 0314

**PHILOSOPHY, RELIGION AND THEOLOGY**

Philosophy 0422  
Religion  
General 0318  
Biblical Studies 0321  
Clergy 0319  
History of 0320  
Philosophy of 0322  
Theology 0469

**SOCIAL SCIENCES**

American Studies 0323  
Anthropology  
Archaeology 0324  
Cultural 0326  
Physical 0327  
Business Administration  
General 0310  
Accounting 0272  
Banking 0770  
Management 0454  
Marketing 0338  
Canadian Studies 0385  
Economics  
General 0501  
Agricultural 0503  
Commerce-Business 0505  
Finance 0508  
History 0509  
Labor 0510  
Theory 0511  
Folklore 0358  
Geography 0366  
Geontology 0351  
History  
General 0578

Ancient 0579  
Medieval 0581  
Modern 0582  
Black 0328  
African 0331  
Asia, Australia and Oceania 0332  
Canadian 0334  
History of Science 0585  
Law 0398  
Political Science  
General 0615  
International Law and Relations 0616  
Public Administration 0617  
Recreation 0814  
Social Work 0452  
Sociology  
General 0626  
Criminology and Penology 0627  
Demography 0938  
Ethnic and Racial Studies 0631  
Individual and Family Studies 0628  
Industrial and Labor Relations 0629  
Public and Social Welfare 0630  
Social Structure and Development 0700  
Women's Studies 0433

**THE SCIENCES AND ENGINEERING**

**BIOLOGICAL SCIENCES**

Agriculture  
General 0473  
Agronomy 0285  
Animal Culture and Nutrition 0475  
Animal Pathology 0476  
Food Science and Technology 0359  
Forestry and Wildlife 0478  
Plant Culture 0479  
Plant Pathology 0480  
Plant Physiology 0477

Biology  
General 0306  
Anatomy 0287  
Biostatistics 0308  
Botany 0309  
Cell 0379  
Ecology 0329  
Entomology 0353  
Genetics 0369  
Limnology 0793  
Microbiology 0410  
Molecular 0307

Biophysics  
General 0786  
Medical 0760

**EARTH SCIENCES**  
Biogeochemistry 0425  
Geochemistry 0996

Geodesy 0370  
Geology 0372  
Geophysics 0373  
Hydrology 0388  
Mineralogy 0411  
Paleobotany 0345  
Paleoecology 0426  
Paleontology 0418  
Paleozoology 0985  
Palynology 0427  
Physical Geography 0368  
Physical Oceanography 0415

**HEALTH AND ENVIRONMENTAL SCIENCES**

Environmental Sciences 0768  
Health Sciences  
General 0566  
Audiology 0300  
Chemotherapy 0992  
Dentistry 0567  
Education 0350  
Hospital Management 0769  
Human Development 0758  
Immunology 0982  
Medicine and Surgery 0564  
Mental Health 0347  
Nursing 0569  
Nutrition 0570  
Obstetrics and Gynecology 0380  
Occupational Health and Therapy 0354  
Ophthalmology 0381  
Pathology 0571  
Pharmacology 0419  
Pharmacy 0572  
Physical Therapy 0382  
Public Health 0573  
Radiology 0574  
Recreation 0575

Speech Pathology 0460  
Toxicology 0383  
Home Economics 0386

**PHYSICAL SCIENCES**

**Pure Sciences**  
Chemistry  
General 0485  
Agricultural 0749  
Analytical 0486  
Biochemistry 0487  
Inorganic 0488  
Nuclear 0738  
Organic 0490  
Pharmaceutical 0491  
Physical 0494  
Polymer 0495  
Radiation 0754  
Mathematics 0405  
Physics  
General 0605  
Acoustics 0986  
Astronomy and Astrophysics 0606  
Electronics and Electricity 0607  
Elementary Particles and High Energy 0798  
Fluid and Plasma 0759  
Molecular 0609  
Nuclear 0610  
Optics 0752  
Radiation 0756  
Solid State 0611  
Statistics 0463  
**Applied Sciences**  
Applied Mechanics 0346  
Computer Science 0984

Engineering  
General 0537  
Aerospace 0538  
Agricultural 0539  
Automotive 0540  
Electronics and Electrical 0544  
Heat and Thermodynamics 0348  
Hydraulic 0545  
Industrial 0546  
Marine 0547  
Materials Science 0794  
Nuclear 0532  
Packaging 0549  
Petroleum 0745  
Geotechnology 0426  
796  
795  
994

**PSYCHOLOGY**  
General 0421  
Developmental 0620  
Experimental 0623  
Industrial 0624  
Personality 0625  
Physiological 0989  
Psychobiology 0349  
Psychometrics 0632  
Social 0451



**TO MY FAMILY**

## TABLE OF CONTENTS

	Page
<b>TABLE OF CONTENTS</b>	v
<b>LIST OF FIGURES</b>	viii
<b>LIST OF TABLES</b>	x
<b>ABSTRACT</b>	xi
<b>LIST OF ABBREVIATIONS</b>	xii
<b>ACKNOWLEDGEMENTS</b>	xiv

### 1. INTRODUCTION

1.1 Essentials Of A Flame Photometric Detector	3
Phosphorus	4
Sulfur	5
1.2 Quenching Effects	7
1.3 Properties Of The Flame And Burner	9
Adaptations	12
1.4 Motivations For The Present Research	15
The Fuel-Rich Reactor: A Macro Scale FPD	16

### 2. EXPERIMENTAL

2.1 The Flame Photometric Reactor	18
The Burner	18
Gas Inlet Chamber	21
Reaction Housing Unit	22
Upper Sample Introduction Tube	23
Related Pieces	25

Gases And Reagents	25
Sample Delivery And Collection	26
Gas Chromatography Of Reactor Samples	27
2.2 The Reactive Flow Detector (RFD)	28
Spectra	29
Quenching Studies	29
Flame Ionization Adaptations	31
The Singing Flame Detector	32
<b>3. THE FLAME PHOTOMETRIC REACTOR</b>	
3.1 Burner Dynamics	33
Addition Of Nitrogen	38
3.2 A Test Compound In The Flame	41
3.3 Defining And Evaluating The Experiment	45
Percent Recovery	45
Collection Efficiency	47
3.4 Into The Fire: A Survival Study Of Quenchers	49
Product Discovery	50
Analyte Recovery	53
<b>4. THE REACTIVE FLOW DETECTOR</b>	
4.1 Introduction	60
4.2 Creation Of A Reactive Flow	62
4.3 Analytical Applications Of The RFD	65
Other Elements	75
Characterizing The Reactive Flow	76

<b>5. QUENCHING FREE REACTIVE FLOW PHOTOMETRY</b>	
5.1 Introduction	86
5.2 Evaluation Of Quenching In The RFD	88
<b>6. REACTIVE FLOW - FLAME IONIZATION DETECTION</b>	
6.1 Introduction	98
6.2 Evaluating The (RFD)FID	104
Optimizing FID vs. RFD	104
Single And Double Flames vs. The Reactive Flow	108
Response Correlations	113
Response Linearity And Detection Limits	119
<b>7.A FINAL NOTE: THE SINGING FLAME DETECTOR</b>	
7.1 Singing In The Flame	123
7.2 Characterization	126
7.3 The Singing Flame Detector	131
<b>8. CONCLUSION</b>	136
<b>REFERENCES</b>	138

## LIST OF FIGURES

	Page
1. The Flame Photometric Reactor Design	19
2. The Burner Capillary Assembly	20
3. Schematic Of The RFD Prototype	30
4. Reactor Flame Stability Chart	35
5. Flame Shape And Luminescence Relative To The Burner Design	39
6. Chromatogram Of Benzene Reactor Sample	43
7. Illustration Of Analyte Recovery From The Reactor	54
8. Percent Recovery Of n-Alkanes In The Reactor Diffusion Flame	56
9. Percent Recovery Of n-Alkanes From Both A Diffusion And A Premixed Reactor Flame	58
10. Creation Of A Reactive Flow	65
11. Optimization Of Sulfur And Phosphorus Response In The RFD	66
12. RFD Calibration Curves Of Phosphorus, Sulfur, And Carbon	68
13. Phosphorus And Sulfur Peaks Near Their Detection Limit In The RFD	69
14. RFD Calibration Curve Of Sulfur And Carbon Through A 405nm Interference Filter	72
15. RFD Calibration Curve Of Phosphorus And Carbon Through A 524nm Interference Filter	73

16.	RFD Calibration Curve Of "Linear" Sulfur	74
17.	Spectrum Of Background Luminescence In The RFD	77
18.	Spectrum Of t-Butyldisulfide In The RFD	79
19.	Spectrum Of Triethylphosphite In The RFD	80
20.	Spectrum Of Hydrocarbons In The RFD	81
21.	Spectrum Of Tetra-n-butyltin In The RFD	82
22.	Spectrum Of MMT In The RFD	83
23.	Quenching Profile Of Different Emitters In The RFD	90
24.	RFD Response Of A Sulfur Peak On And Off The Solvent Tail	92
25.	(RFD)FID vs. FID Response Optimization	106
26.	(RFD)FID Response vs. Premixed Air	111
27.	(RFD)FID vs. FID Response Of Various Elements	116
28.	Response Linearity Of The (RFD)FID vs. FID	121
29.	Typical Microphone Output From The Singing Flame	127
30.	Calibration Curve Of n-Dodecane In The Singing Flame Detector	132

## LIST OF TABLES

	Page
1. Combined Reactor Gas Flows	41
2. Survey Of Analyte Decomposition In The Reactor	51
3. RFD Sensitivities For Phosphorus, Sulfur, And Carbon	69
4. Detection Limits Of Various Elements In The Reactive Flow	76
5. (RFD)FID, FID, And RFD Response Of Various Elements	114

## ABSTRACT

For almost thirty years, gas chromatographers (GC) have praised the Flame Photometric Detector (FPD) for being a sensitive and selective analytical tool, and condemned it for suffering from response quenching in the presence of hydrocarbons. This study describes the construction and characterization of a large, low-temperature, fuel-rich flame reactor designed for studying the survival rates of organic compounds in the flame and the assumedly related quenching processes in the FPD. Results show that the traditional diffusion flame discriminates, in terms of decomposition, against the carbon number of a series of introduced n-alkanes, while a premixed flame does not. As well, a diffusion flame decomposes heterocyclic organic compounds much more than their pure hydrocarbon equivalents.

Subsequent studies of premixed hydrogen and air flames, in small glass jets, led to the discovery of an elongated "glow", previously unknown, and presently referred to as a "reactive flow". Current research qualifies this phenomenon for analytical use as a new GC sensor: the Reactive Flow Detector (RFD). The RFD demonstrates elemental sensitivity that is about as good as, or better than, the FPD. As well, it operates under a single set of conditions and does **not** suffer from response quenching. The detector can also be modified for in-series Flame Ionization Detection (FID), whose sensitivity is only a factor of two lower than that of a comparable FID. The burner also gives rise to a singing flame which changes pitch in response to the chromatographic concentration profile of  $\mu\text{g}$  quantities of organic compounds.

Thus, by performing several simultaneous roles, the Reactive Flow Detector offers GC a new method of analysis, which avoids the various impediments that have hampered the FPD's application and performance in the past.

## LIST OF ABBREVIATIONS

AED:	Atomic Emission Detector
cf:	[L <i>confer</i> ] compare with
cm:	centimeter
ECN:	effective carbon number
e.g.:	[L <i>exempli gratia</i> ] for example
et al.:	[L <i>et alii</i> ] and others
FID:	Flame Ionization Detector(or Detection)
FPD:	Flame Photometric Detector(or Detection)
g:	gram
GC:	Gas Chromatography(or Chromatographic)
HAFID:	Hydrogen Atmosphere Flame Ionization Detector
Hz:	Hertz (cycles per second)
i.d.:	inside diameter
i.e.:	[L <i>id est</i> ] that is
LRS:	lit reactor sample
m:	meter
mC/gC:	millicoulombs per gram of carbon
MHz:	megaHertz
ml/min:	milliliters per minute
mm:	millimeter
ng:	nanogram
nm:	nanometer
o.d.:	outside diameter
pg:	picogram

PMT: photomultiplier tube  
RFD: reactive flow detector  
s: second  
SCD: sulfur chemiluminescence detector  
SNR: signal to noise ratio (S/N)  
 $\mu\text{g}/\mu\text{l}$ : micrograms per microliter  
ULRS: unlit reactor sample

## **ACKNOWLEDGEMENTS**

An unpayable debt of gratitude is owed to my supervisor, Dr. Walter Aue, for his patience, understanding, extraordinary intuition, and friendship. Thank-you for teaching me the art of science.

Special thanks also go to Dr. R. Stephens, Dr. S. Grossert, Dr. P. Wentzell, and Dr. X-Y. Sun for their various forms of input and assistance during my years at Dalhousie.

Much appreciation is extended to Jürgen Müller, Master Glassblower, for his excellent craftsmanship and prompt, courteous service. Thanks also go to the machine shop for the fine work in building several parts for these detectors.

Finally I would like to acknowledge the financial support of the Dalhousie Graduate Fellowship, and thank my family, in Calgary, who has always understood for so many years.

My thesis supervisor, Dr. Walter A. Aue, has the unrestricted right to use any or all of this thesis, and its technical and descriptive content, in whatever way he deems appropriate.

-----

Author's Signature

-----

Date

## **1. INTRODUCTION**

The co-dependence that exists between separation and detection dictates that one is only as good as the other; that is, at least with reference to their combined analytical viability. In the case of gas chromatography (GC) employing flame photometric detection (FPD), it is the detector which now seems poised for advancement.

The flame photometric detector (FPD) has long been established as a selective and sensitive tool in the analysis of hetero-organic compounds<sup>[1-19]</sup>. Since its first combination with gas chromatography (GC) for the purpose of determining sulfur and phosphorus containing eluents<sup>[20]</sup>, GC-FPD has been extended to a great variety of elements including halogens<sup>[21,22,23]</sup>, boron<sup>[24]</sup>, chromium<sup>[25,26]</sup>, tin and germanium<sup>[27-31]</sup>, selenium and tellurium<sup>[32,33]</sup>, and several others<sup>[34-39]</sup>.

Its rugged design, ease of operation, cost effectiveness, and good response towards several elements have all reinforced the FPD as an attractive technique for a number of applications. These have included sulfur and phosphorus determination in pesticides<sup>[20,40-43]</sup>, analysis of oil and gas samples<sup>[38,44-49]</sup>, air pollution studies<sup>[50-54]</sup>, and the monitoring of food and health related samples<sup>[25,55-58]</sup>, to name just a few. However, while some efforts continue to develop the FPD's performance towards greater sensitivity and "infinite selectivity"<sup>[59-61]</sup>, some inherent difficulties associated with FPD analyses have caused a significant portion of the

attention, initially focussed on this detector, to be re-directed towards other methods suitable for similar assays.

For instance, the sulfur chemiluminescence detector (SCD) has received much notoriety in recent years [7,11,62], and has been applied to the analysis of petroleum products<sup>[63]</sup>, as well as adapted for the detection of tellurium and selenium compounds<sup>[64]</sup>. Also worthy of mention in this category is the atomic emission detector (AED)<sup>[7,11,12]</sup>, which has also found recognition in the petrochemical industry<sup>[63]</sup> and is suited for multi-elemental analysis.

While both of these methods boast significant improvements over the FPD, they are still afflicted, to some degree, by the same fundamental impediments that occur in the traditional FPD. More importantly, these techniques are expensive, delicate, and require highly skilled analysts in order to obtain reliable information, thus limiting their practicality and hindering their usage in production laboratories and process instruments<sup>[63,65]</sup>.

Despite the ailments that impede the FPD's performance, it still continues to be one of the most commonly used systems in its field. Considering the agricultural, environmental, and industrial issues that reside within the capabilities of this small, inexpensive analyzer (relative to some other tandem GC alternatives) it seems that the further development of the flame photometric detector as a chromatographic sensor remains a considerably appealing solution to both an economic and

scientific problem.

The work presented here is aimed towards characterizing some of the mystery surrounding the FPD, and employing this information to further advance the usefulness of an already quite versatile detector. It will therefore be helpful to begin by reviewing the situation at hand.

### 1.1 Essentials Of A Flame Photometric Detector

The FPD evolved from an observation made by Salet in the 1800's, as described by Gilbert<sup>[66]</sup>. At the time, Salet noted the strong blue emission that occurred when a low-temperature, hydrogen-rich flame was placed near the surface of a relatively cool object (containing sulfur). Almost a century elapsed before Brody and Chaney capitalized on this chemiluminescence with the introduction of the flame photometric detector<sup>[20]</sup>. Although since that time there has been much modification and developmental work done on the detector, today's commercial FPD contains all of the same essential components as that which was originally presented.

This can be schematized as follows: the GC column effluent is swept into a hydrogen/air diffusion flame, entrained in a fuel-rich atmosphere. Analytes exposed to these conditions emit light which is monitored by a photomultiplier tube (PMT) mounted orthogonally to the flame burner. Separating the PMT from the flame and its gases is a quartz window. This is often accompanied by an optical filter that

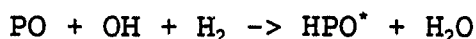
allows a particular wavelength(s) to be isolated.

In order to fully appreciate the reputation of the FPD and accurately evaluate the alterations that it has undergone, it is first necessary to understand more about its analytical performance. While today some twenty elements give rise to an FPD response, those of phosphorus and sulfur, for which the detector was originally hailed, have been extensively studied and provide a good representation of the system.

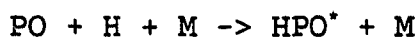
### **Phosphorus**

The green emission owing to phosphorus compounds in a fuel rich hydrogen/oxygen flame has a spectrum which extends from 490 nm to 600 nm. The emitter, identified as the excited HPO species<sup>[67]</sup>, displays maxima at 510, 526 and 560 nm, the second of which is commonly used in phosphorus determination due to its relative intensity.

The phosphorus compound is believed to first decompose to PO upon entry into the flame and then form the light-emitting HPO species via chemiluminescent reactions. The mechanism proposed by Gilbert<sup>[66]</sup> suggests that HPO is produced as follows:



whereas Syty and Dean<sup>[68]</sup> propose a third body (M) mechanism:



The FPD shows both a very good sensitivity and linearity towards phosphorus containing compounds. The minimum detectable limit is on the order of  $1-5 \times 10^{-13}$  g P/s along

with a linear response over 4 or 5 orders of magnitude. Selectivity over hydrocarbons is  $10^4$  and up.

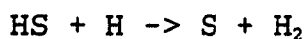
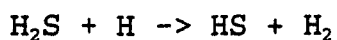
### **Sulfur**

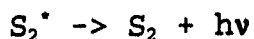
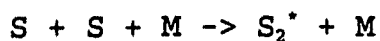
The luminescence of sulfur in a fuel-rich hydrogen/air flame exhibits response mechanisms and characteristics that are considerably different than those of phosphorus, and has come to serve as somewhat of a legacy for FPD analysts.

The spectrum of sulfur emission consists of a series of sharp bands from 300 nm to 600 nm. This extensive range has been shown to cause interference with the phosphorus channel, at 526 nm, during simultaneous sulfur and phosphorus analyses<sup>[69]</sup>. The most intense bands lie approximately between 360 to 410 nm and consequently a 394 nm interference filter is commonly used in FPD sulfur analyses.

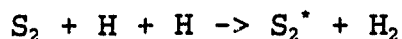
The species believed accountable for the blue emission is the excited  $S_2$  molecule<sup>[20]</sup>. In recent years, the belief that  $S_2$  is the sole sulfur emitter in the FPD has been subject to some scrutiny<sup>[15]</sup>. However, despite attempts to explain the phenomenon better, exclusive  $S_2^*$  emission remains the simplest and most practical model for sulfur response in the FPD.

In 1973, Sugiyama et al. proposed a third body excitation mechanism<sup>[70]</sup> to follow the formation of sulfur, from its compounds, described by:

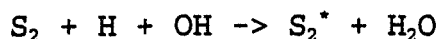




Earlier, however, H.G. Crone, in a letter to Gaydon and Whittingham<sup>[71]</sup>, suggested  $S_2$  excitation to result from a recombination reaction:



just as Sugden and Demerdache<sup>[72]</sup> similarly did in a later report:



Perhaps the most perplexing features of FPD sulfur detection surround its quadratic response<sup>[20]</sup>. The signal generated by a sulfur compound is approximately proportional to the square of its concentration inside the detector. Reports indicate the exponential factor to vary between 1 and 2 with experimental conditions<sup>[16,73-75]</sup>, and despite attempts to linearize the response, the inconsistency of this factor renders these methods to have very limited effectiveness.

Generally, the minimum detectable amount of sulfur which the FPD will sense is approximately  $10^{-11}$  g S/s. A linear range over 2 orders of magnitude may be obtained when operating with a constant background of sulfur emission<sup>[33]</sup>. Sulfur's selectivity relative to hydrocarbons is concentration dependent due to its quadratic nature, and may vary from  $10^3$  g C/g S at low levels to  $10^6$  g C/g S at higher amounts. Obviously, a varying exponential factor and a rather limited linear range seriously hamper sulfur's flame photometric

detection.

Recently, Aue and Sun happened upon a linear sulfur emitter in the region of 600 nm that displayed very promising analytical utility<sup>[76]</sup>. This species (believed to be HSO) sports a linear range over 4 orders of magnitude, while its sensitivity and selectivity suffer only minorly in comparison to the customary quadratic response. Given its preliminary nature, this new sulfur mode holds much potential of becoming even more competitive with conventional techniques than it already appears.

With relief in sight, by way of a linear sulfur response, the flame photometric detector is still not free of burdens. Even though this major impediment from its past has been appreciably removed, response quenching, quite probably the FPD's most fierce adversary, has yet to be eliminated.

### **1.2 Quenching Effects**

The fate of sulfur's FPD response is greatly influenced by the simultaneous presence of organics in the flame which have been shown to quench the  $S_2^*$  luminescence<sup>[77,78]</sup>. The Sugiyama group explains the phenomenon as the deactivation of the excited  $S_2$  species by its combination or collision with an organic compound and/or the degradation products of the latter<sup>[79]</sup>. While some contradiction and general confusion exist in the literature addressing itself to the problem<sup>[15]</sup>, the effects of hydrocarbon quenching have been reviewed and

revised<sup>[80]</sup>, and common conclusions were drawn from the work:

(a) A certain level of carbon flow is necessary before the hydrocarbons will cause a significant reduction in the sulfur response.

(b) Relative quenching is only slightly dependent on the amount of the sulfur compound present.

(c) The prerequisite for accurate quantitation is the complete separation of the sulfur compounds from any main hydrocarbon component of the sample.

Attempts to overcome the quenching interference due to co-eluting hydrocarbons have employed high resolution capillary columns<sup>[53]</sup>, however, this failed to be consistently successful.

Rupprecht and Phillips noted the considerably smaller quenching effect produced by carbon dioxide relative to hydrocarbons<sup>[78]</sup>, and correspondingly, a dual-flame arrangement was proposed to reduce quenching. In such a system, the analytes are first decomposed in an oxygen-rich flame, and are then allowed to luminesce in a second, hydrogen-rich flame. A comparative study of single and dual-flame analyses under identical experimental conditions has shown the dual-flame method to provide a more uniform sulfur response that is less dependent on sample composition, and hence, the need for the high resolution capillary columns previously mentioned<sup>[81]</sup>.

However, the method proved to be less sensitive and was still susceptible to response quenching at larger (though never quantified) levels of organic effluent. Patterson et al. attribute some of the upper response limit, at high sample concentrations in the dual-flame apparatus, to self-absorption effects in the emitting flame<sup>[82]</sup>.

Although a sizeable amount of work has been dedicated to the problem of response quenching, it is surprisingly easy for the accounts to mislead one into assuming that this affliction is unique to sulfur. Many elements respond in the FPD, and even though mention of their observed quenching is sparse at best, it cannot be dismissed.

In a recent paper by Aue and Sun, response quenching of elements in addition to sulfur were investigated<sup>[83]</sup>. In the report, they conclude that several elements are quenched by co-eluting hydrocarbons, even carbon itself. Furthermore, the elements are not unique amongst each other in the manner that they are observed to be quenched. This led them to affirm the possibility that hydrocarbons quench the exciting flame as opposed to the excited analyte, which in turn suggests a common or related excitation process.

### **1.3 Properties of the Flame and Burner**

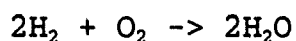
The standard hydrogen/air diffusion flame burner, found in an FPD, is usually constructed such that the air is delivered to the flame base through a central orifice and the

hydrogen enters peripherally about the center of the base.

Initially, column effluents were introduced to the flame through the air inlet (air and/or oxygen have been used in different cases). However, when large quantities of sample solvent would ascend into the burner, they would momentarily starve the flame of oxygen and thereby extinguish it<sup>[20]</sup>. This caused the need for a post-solvent re-ignition in the early models, and made applications such as automatic analysis difficult. The work that challenged this complication is summarized<sup>[16]</sup>, and basically charts the success of different gas/effluent arrangements going into the flame jet.

The most effective and widely used method for eliminating this problem was proposed by Goode<sup>[84]</sup>, and, in a related endeavour, by Burgètt and Green<sup>[85]</sup>. In their reports, they simply combined the column effluent with the hydrogen line, and found that this arrangement could withstand normal, and elevated solvent injection amounts while supporting a flame. Although it has been suggested that this change in sample delivery may cause the FPD to be subject to more background hydrocarbon interference, no experimental data accompanied this claim<sup>[82]</sup>.

The stoichiometric flame may be represented by the equation:



which should be interpreted as the overall reaction. Many intermediate products can be formed during the process which

greatly affect the chemistry of compounds entering the flame. As well, these intermediates are, in turn, dependent on the flame stoichiometry ( i.e. hydrogen-rich, oxygen-rich, etc.).

The Sugiyama group has demonstrated a dramatic decrease in  $S_2^*$  emission intensity with increasing air flow rates<sup>[70]</sup>. As well, regarding fuel-rich operation of the flame, Patterson<sup>[82]</sup> illustrates the dependencies of sulfur and phosphorus response on the concentration of  $H_2$ , based on the mechanisms cited earlier.

Tang investigated the behaviour of response quenching in the hydrogen/air diffusion flame<sup>[86]</sup>, by comparing a "hydrocarbon doping ring" above the flame, to conventional sample introduction methods through incoming gas lines. Results of the study confirmed that the more hydrogen-rich the chemical atmosphere and/or the lower the temperature, the more prominent the observed quenching effect will be. He also noted that the degree of quenching showed little dependence on the structure of the quenching molecule.

From the effort, Tang concluded that dual-burning FPD systems were reasonable to use, and expanded on the explanation put forth by Dressler<sup>[5]</sup>, which attributes lower quenching in hot/oxygen-rich flames to more complete sample decomposition and the sizeable quenching in cool/fuel-rich flames to incomplete sample decomposition and oxidation. His interpretation proposed that decomposition in fuel-rich flames would still occur but that the fragments would be more

hydrogenated than oxidized, and would thus exhibit more quenching. Variations in sample structure would not greatly affect the quenching ability, as most of the quenchers would be hydrogenation products of similar fragments from different larger molecules. Unfortunately, no data were available to support the hypothesis.

It is interesting, but perhaps not surprising due to their demanding nature, that premixed flames have been primarily overlooked in favour of their diffusion counterpart. Aside from Moye's premixed version<sup>[87]</sup>, designed in an attempt to solve the early flame-out problem, there is little mention of premixing burners being used in flame photometric detectors. They are, however, used in a variety of constructions in other modes of spectroscopy<sup>[88]</sup>.

A more unusual approach has recently adopted the use of a combustible gas mixture that is unable to sustain a continuous flame, at the flow rates by which it is supplied<sup>[89,90]</sup>. This method, dubbed "pulsed" FPD by the authors, claims improved detection limits for sulfur and phosphorus (relative to the FPD), and has a unique feature of simultaneous temporal information that is gained during an analysis. Although the system requires a more elaborate assembly and is still subject to response quenching, its novelty is preserving.

### **Adaptations**

The original FPD was built on the foundation where a

flame ionization detector (FID) once stood; in fact they shared the same burner<sup>[20]</sup>. Although the FPD was still earning its place as a sensitive and *selective* detector, the FID was already known to be a very sensitive *universal* detector.

The flame ionization detector is renowned as probably the most widely used detector in gas chromatography<sup>[91,92]</sup>. It exhibits excellent linearity and sensitivity towards organic compounds, and its response mechanisms have been a great source of interest<sup>[93]</sup>. For many analysts, it has become an indispensable laboratory technique.

Given that the FPD and FID deliver valuable information from the same type of burner, it is inevitable that scientists would attempt to have them reside in the same housing. Examples of in-situ<sup>[94-96]</sup>, and parallel<sup>[97]</sup> FPD/FID arrangements can be found in the literature, and as an added feature for some FPD manufacturers. Unfortunately, the different flame properties that promote optimum response for each detector, make this attractive pairing incompatible. The FID requires an air-rich flame and the FPD prefers a fuel-rich atmosphere, hence, conventional chemiluminescence in the former is low or non-existent, while ionization in the latter is accompanied by a large, noisy background that yields a poor detection limit. There are certain cases, however, where beneficial FID performance occurs in a hydrogen-rich atmosphere.

Hill and Aue introduced a hydrogen atmosphere flame ionization detector (HAFID) that, when operated within

parameters different from those of a common FID, displayed considerably selective organometallic response relative to hydrocarbons<sup>[98]</sup>. They also described a minor interference, due to a background oscillation, which could be removed by increasing the flow of hydrogen, without significant loss in response. A somewhat related, but more severe oscillating phenomenon was put to use by Graiff in a "singing" flame ionization detector, where 2-3 times the sensitivity of a normal FID was reportedly obtained<sup>[99]</sup>.

The flame photometric detector has, however, been successfully coupled to other techniques. Recent accomplishments of note include supercritical fluid chromatography-FPD<sup>[100]</sup>, and capillary electrophoresis-FPD<sup>[101]</sup>. Another dimension has also been added to GC-FPD with the acquisition of "on-line" spectral information, obtained by means of a rotating variable interference filter, from a single chromatographic peak<sup>[102]</sup>.

Much of the chemistry involved with the flame photometric detector remains unclear, and has sparked many debates attempting to explain the sometimes unusual response characteristics that it displays. The hydrogen-rich diffusion flame, which sustains these processes, appears to be the culprit. Oddly, it exhibits a dual role, where in one aspect, it supports the luminescence of an element, and in another, it provides the conditions which quench its response.

Several studies have been carried out to investigate the

effects of quenching, and the various factors involved. This has subsequently spawned a few theories of the phenomenon that are repeatedly referenced by researchers, probably in the absence of a better description, and partially, perhaps, due to a weariness of the discussion. This is unfortunate because, even though this problem has been monitored over the FPD's lifespan, none of the works has succeeded in establishing the reactions, products, and/or intermediates of the quenching process. In fact, there exists no clear knowledge of how these quenching molecules behave in the FPD at all; knowledge that would at least advance the present conceptions of the chemistry inside the flame photometric detector, and possibly provide information that could relieve the trouble that has frustrated GC analysts for almost three decades.

This information can only be found in the heart of this detector: the flame.

#### **1.4 Motivations for the Present Research**

The work described in this report is mainly targeted towards illuminating the nature of quenching, and related molecules in the flame photometric detector. The most direct method of achieving this goal, we believe, begins with the collection and analysis of post-flame products from the FPD. Perhaps then their chemistry can be further elucidated by trailing it backwards into the burner.

The first and most troublesome problem in doing the

experiments is one of quantity. There is obviously no guarantee that 100% of the products, generated from compounds introduced to the flame, can always be collected. Furthermore, the amounts needed for easy analysis are considerably larger than the small quantities that the FPD can process in one peak. However, if larger quantities could be produced under very similar conditions, then sampling and analysis would become much easier and the concern for 100% recovery could be eliminated. As part of the current study, a useful route around this obstacle is offered for consideration.

#### **The Fuel-Rich Reactor: A Macro-Scale FPD**

Assume, for a moment, that one could multiply the size of an average flame photometric detector several times and not alter the experimental flame conditions to which normal GC effluents are subjected. Such a device could serve as a very useful tool in the accumulation and identification of combustion products contained within an ordinary FPD, during a given analysis. Although this exact scenario is not possible, much the same effect may be realized with the combination of more than one FPD.

The average burner in an FPD contains an air nozzle approximately 1mm in diameter, surrounded by hydrogen, and upon which a stable flame is supported. It seems logical, then, with that being the essence of the FPD's operation, that a burner could be constructed out of several tiny air nozzles, each enveloped in a hydrogen-rich atmosphere. It further

reasons that if an even gas flow is obtained across the burner head, that a uniform flame, displaying size and temperature similar, or even equivalent, to that of a singular FPD burner, could believably exist. Therefore, combustion products collected from compounds entering the flame, can sensibly be assumed to have formed under conditions representative of an average FPD. The construction of an apparatus of this type, is one of the primary goals of the present work.

To create the desired reactor, the employment of a capillary burner would seem fitting. Capillary burners have been used in the past for a variety of purposes including spectrometry of premixed flames<sup>[103,104]</sup>, diffusion flames<sup>[105]</sup>, and 'separated' flames<sup>[106]</sup> in which corrugated steel strips were used in place of capillaries. They offer a relatively simple means of establishing a very even gas flow over an entire burner head.

Once assembled, the burner can be placed in a closed housing, with an atmosphere rich in hydrogen. From there, species contained within the flame gases may be cooled and collected, in a cold trap, and then analyzed.

The results of the analysis will provide the groundwork for the other primary goal of this research: using the information, if viable, to construct a new, or modify the existing, flame photometric detector, with the hopes of removing some of the barriers that have bordered this method since its inception.

## **2. EXPERIMENTAL**

### **2.1 The Flame Photometric Reactor**

An assembled view of the reactor is depicted in Figure 1. It stands approximately 13" in height and at its widest point it occupies a diameter of about 2.5". It consists mainly of a burner, a gas inlet chamber, a reaction housing unit, and an upper sample introduction tube. The following provides a brief description of each.

#### **The Burner**

Two pieces, the head and the body, combine to make the burner. The head is made out of 1/16" o.d. x 0.030" i.d., type 316, stainless steel capillary tubing purchased from Chromatographic Specialties Limited.

It was put together by layering rows of 2" long capillaries, between rows of 2" and 5" long capillaries in a hexagonal close packing arrangement. The design ensured that the 5" capillaries were evenly spaced, and each was surrounded by 2" capillaries (Figure 2). All met flush at the end to be the burner head.

Holding the tubes together was Duralco 4525, acquired from the McMaster-Carr Supply Company. This high temperature epoxy is ideally suited for potting applications, can withstand up to 260°C, and cures at room temperature.

Epoxy was poured over the capillaries between each layer, and was kept within a 1" area centered about the middle of the small capillaries to prevent interference with the openings.

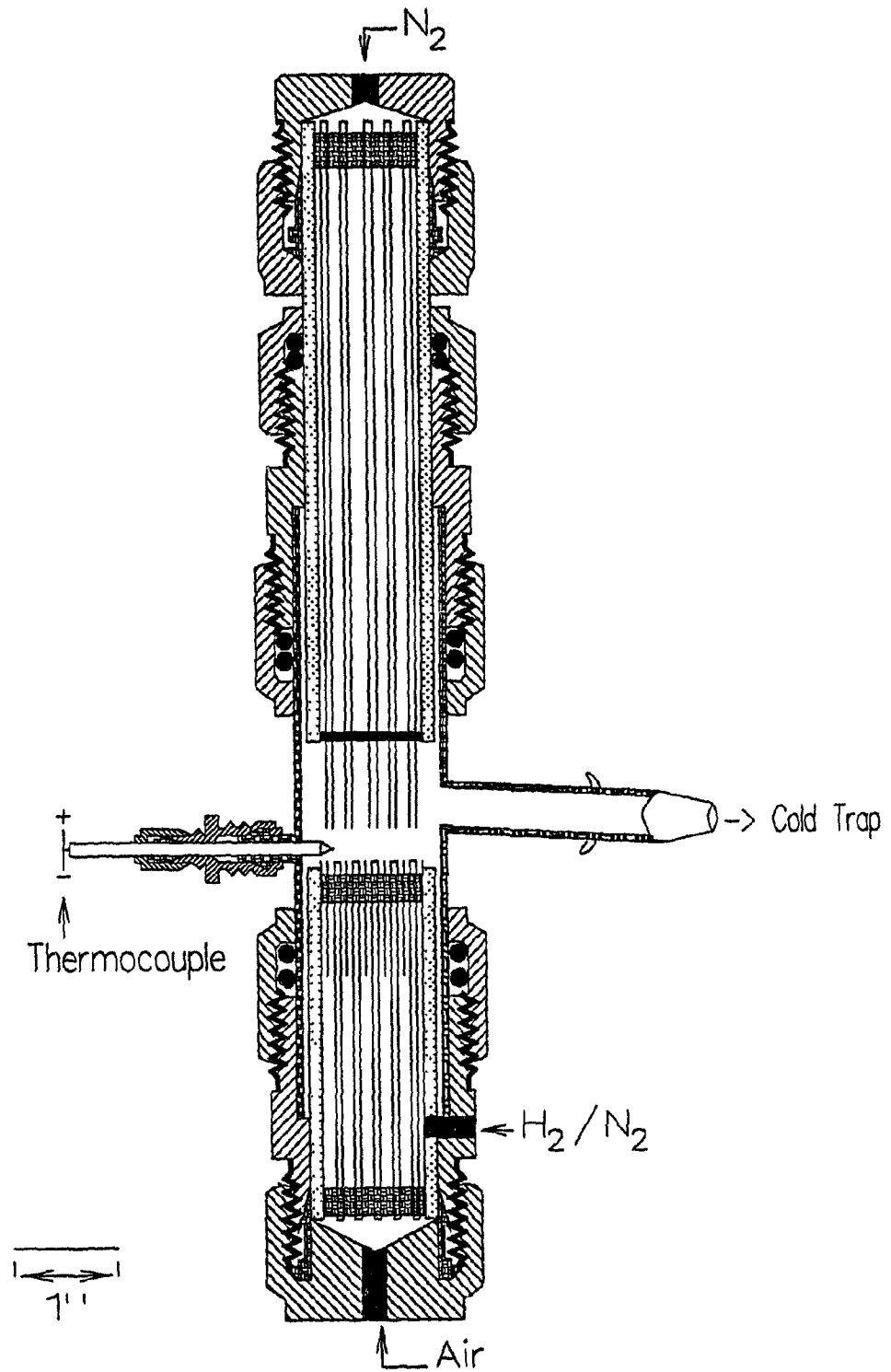


**Figure 1:** The Flame Photometric Reactor design.

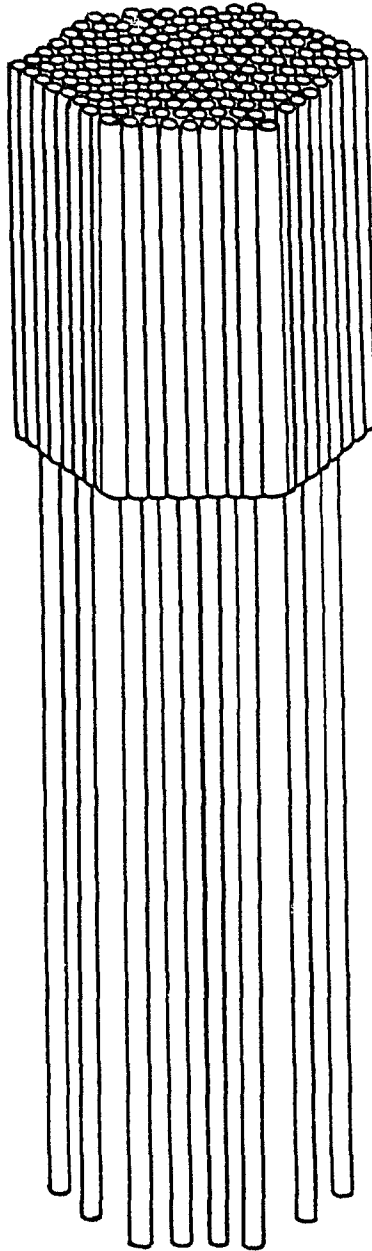


**Figure 2:** The capillary assembly.

Half the head was constructed and left to cure, so that it could be turned over and built upon to completion. Once assembled, the burner end was ground off to an even flat surface, hexagonal in shape, and measuring about 1" across at its widest point.

The burner body was made from a seamless stainless steel pipe cut to a length of 4", and bored down to 1.25" o.d. with a 1/8" wall thickness. A 1/8" hole, located where the gas line was to enter, was also drilled through the side.

The burner head was placed level inside the body and positioned about 6mm above its edge, as recommended by Aldous et al.<sup>[103]</sup>, in order to prevent overheating. The unit was sealed into place by a 1/2-3/4" layer of epoxy. What remained of the 5" tubes, projecting out the other end, were also secured in about a 3/4" layer of epoxy, and then ground flush with the body upon curing. Caution was exercised, when using the epoxy, so as to prevent it from entering the capillaries and plugging them.

#### **Gas Inlet Chamber**

Flame gases are conducted to the burner by way of the gas inlet chamber. It should be gas tight and adaptable to the reaction housing unit. For this purpose, Swageloks were deemed to be the most appropriate item.

All Swageloks were stainless steel and purchased from Atlantic Valve and Fitting Limited. The chamber was made from a 1.5" - 1.25" reducing union. This size union was not

available from the company, and so it had to be manufactured from the bisection of a 1.5" and a 1.25" union.

The two halves had their inner shoulders bored out and were banked together by a stainless steel weld. An 1/8" hole was tapped through the side, in line with the burner hole, and a 1/8" reducer-tube stub, again with its inner shoulder bored out, was silver soldered in its place.

The 1.25" nut was modified to accommodate a stainless steel cap. Holes were threaded into it, and a cap was made to fit. The cap was furnished with a 1/8" reducer-tube stub centered on it, with silver solder, and made gas tight with the use of a silicone rubber seal.

The burner, now essentially a porous tube, can be placed into the Swagelok, swaged gas tight, and have the gas lines connected. This assembled unit affords the introduction of hydrogen and air into the large burner body, while preventing any premixing of the fuel and oxidant. Air is delivered up through the body in the long capillaries, and hydrogen is conveyed directly into the body, in between the two layers of epoxy, and amongst all of the air tubes. The hole, around the hydrogen line, was sealed with silicone rubber caulking to help prevent gas from escaping.

#### **Reaction Housing Unit**

The requirements of the reaction housing unit are that it be (a) gas tight, (b) adaptable to the burner, upper sample introduction tube, and the cold trap, (c) inert to its

environment, and (d) able to perform under elevated temperatures. Glass was chosen for the above reasons as well as for allowing the flame to be visually monitored.

A glass tube, 7" in height, 1.5" in outside diameter, and 1/16" in wall thickness, was constructed. Three ports were built off of it. One, 1/2" long x 1/4" O.D., another, 3/8" long x 7/16" O.D., and a third, 2.5" long x 1/2" O.D. at an angle 3° below the perpendicular to the burner body, and fitted with a 14/20 clear fit joint. These openings were placed for devices to measure the reactor temperature, ignite the flame, and collect products from the housing unit, respectively.

In order to swage the reaction housing unit into the Swageloks without doing it damage, flexible, high-temperature, silicone rubber o-rings were used in place of the standard stainless steel front and back ferrule assembly provided.

#### **Upper Sample Introduction Tube**

This component of the reactor is meant to sit atop the flame and introduce compounds downward into it. Therefore, it needs simply to be gas tight and able to convey a steady flow of sample into the flame.

The tube, 7" long, was constructed in the same manner as the burner body. As well, half of the inside wall, on one end, was bored down an 1/8" to create a shoulder on which a cap could rest.

A cap, 1.25" in diameter and 1/4" thick, was crafted from

stainless steel. An  $1/8$ " was ground from its thickness,  $1/16$ " from the edge, all the way around it, so it could rest upon the inner shoulder of the tube. A 3x3 matrix of  $1/16$ " holes were drilled about the center of the cap, 8mm apart from one another.

9" capillaries, of the same type used to make the burner head, were fitted into the holes, left extending 1.25" out the flat end of the cap, and silver soldered into place from the other side. This piece was then placed into the tube, so that the raised cap and the tube shoulder met flush against each other, and was silver soldered from the outside, along the seam.

This unit was then insulated uniformly around the capillaries with glass wool, aluminum foil, and finally MN-silica gel N (Sigma Chemicals) so that a final, gas tight layer of the epoxy, approximately  $3/4$ " thick, could be applied. Once the epoxy cured, the capillaries jutting from it were ground level with the tube.

Next the tube was placed into a 1.25" Swagelok cap, fitted with an  $1/8$ " reducer-tube stub silver soldered in the center, and swaged tightly.

The assembly was held into place and fitted to the reaction housing unit by a 1.5"-1.25" reducing union fabricated from the bisection of two unions, as mentioned above. Again, to protect the glass tube, and also for ease of movement, the stainless steel ferrules were replaced by

silicone rubber o-rings.

#### **Related Pieces**

The entire reactor was supported vertically, by clamps, on a large ring stand which was counter-balanced by weights. For safety reasons, it was operated within a fume hood and was shielded behind a sheet of plexi-glass and the fume hood cover. All gas and power lines were run underneath the front guard of the hood.

An igniter was provided by attaching a thin wire to the plug leads from a variac, and applying a current sufficient enough to cause it to glow. The leads were left extending from a stainless steel tube, 1/4" o.d., filled with silicone rubber caulking. The igniter was made to fit gas tight in the reaction housing unit with the help of silicone rubber o-rings. This arrangement allowed a replaceable glow plug, of any length, to be used at will.

Temperature measurements were conducted by an Omega DH-1-24-J-12 (iron-constantan) thermocouple and output was displayed on a Fisher 32-JG voltmeter. The thermocouple was fixed to the reaction housing unit by a 1/4"-1/8" Swagelok reducing union, with its inner shoulder bored out, using nylon ferrules in place of those made from stainless steel. The unit was calibrated against a chromatographic oven before being used.

#### **Gases and Reagents**

Gases employed in the experiments were reagent grade

nitrogen, prepurified hydrogen, extra dry air, prepurified argon, and high purity oxygen, purchased from Linde, along with high purity helium obtained from Matheson. They were conveyed to the reactor through Brooks flow meters (float ball type) and managed by Nupro flow controllers. All meters were calibrated with a soap bubble/stop watch apparatus.

Reagents and solvents were purchased mostly from Aldrich (some from Fisher Scientific) and were of at least 95% purity.

#### **Sample Delivery and Collection**

A bypass was created on the nitrogen line, such that a controlled flow of nitrogen could be passed through a glass tube on its way to the flame. Therefore, when samples were placed in the tube, a regulated amount of the compound could be introduced to the flame. Entry to the flame could be either with the fuel, denoted as "conventional introduction" from Tang's work<sup>[86]</sup>, down through the upper sample introduction tube, or both. Samples were delivered at a rate just below that which corresponds to their maximum luminescence in the flame, which was determined visually.

All diffusion flames, used in the collection experiments, were supplied with 1000 ml/min hydrogen, 550 ml/min air, and ~150 ml/min nitrogen (depending on the compound being delivered). Premixed flame experiments used 1400 ml/min hydrogen, 1000 ml/min air, and 500 ml/min nitrogen in addition to the doping vessel flow. In comparison experiments, the

diffusion flame used the exact same flows as the premixed flame.

Species contained within the flame gases were collected in a cold trap. Two traps, both made from glass and fitted with 14/20 clear fit joints, were set, tandemly, in dewars filled with ice. They were connected to each other, and to the reaction housing unit, by springs looped around glass hooks furnished on each piece. The first cold trap was empty while the second cold trap forced flame gases to be bubbled through a suitable organic liquid. The exhaust was then run through plastic tubing directly into the fume hood vent. After the reactor was shut down, both traps would be rinsed with the organic liquid. This portion was then used for analysis.

#### **Gas Chromatography of Reactor Samples**

All samples were analyzed by a Tracor model 550 gas chromatograph equipped with a flame ionization detector (FID). The glass column used for separation was 2 m x 1.8 mm i.d. and packed with 10% Apiezon L on Chromosorb W 45/60 mesh. GC accessories were obtained from Chromatographic Specialties Ltd. Reactor analyses were subjected to a temperature program from 25°C to 240°C at a rate of 10°C/min. The usual flow of the carrier gas, nitrogen, was approximately 12 ml/min depending on conditions. Flow rates into the commercial FID were 70 ml/min hydrogen and 150 ml/min air. All other parameters varied with the analysis.

## 2.2 The Reactive Flow Detector (RFD)

The metal jet of the FID on the Tracor GC, mentioned above, was replaced by a borosilicate capillary. The capillary had an inner diameter of 1.8 mm and a restriction of 1 mm i.d. about 3.5 cm from the top. (These dimensions are typical and, for the most part, not crucial. Quartz capillaries also worked well). When present in excess, background luminescence was suppressed with large injections of tetraethyllead <sup>[102]</sup>; deposits were removed with injections of Freon-113 [c.f. 31]. (Usually these tricks work, occasionally they don't).

For initial experiments, the outside of the capillary was painted with high-temperature black paint - of the type used on car exhausts - leaving a ca. 0.5 cm broad ring untouched (painting the capillary later turned out to be unnecessary). A 6" long, 1/4" o.d. glass image conduit (item # 38307, Edmund Scientific Co.), shielded from light by a protective metal pipe, was inserted through the detector wall and moved against (the transparent section of) the capillary. The other end of this optical feed-through terminated just in front of the photocathode of a Hamamatsu 268 or 374 photomultiplier tube (with nominal wavelength ranges of 300 to 650, and 300 to 850 nm, respectively), leaving a gap wide enough to insert an optical filter if desired. The PMT housing could be easily opened, giving the operator the chance to observe the reactive flow through the image conduit. The detector housing was reconstructed to prevent ambient light from entering, but no

effort was made to change the Tracor detector base and FID-type design. Figure 3 offers to-scale schematics of the RFD prototype.

The signal from the Tracor electrometer was routed through a departmentally-made 3-pole filter set at an RC = 0.5 second time constant, before being displayed on a Linear strip-chart recorder. Other props and procedures were conventional as well; where important they will be described in the text or in the captions to the figures.

### **Spectra**

Spectra were obtained from either a Jarrell-Ash model 82-415 quarter-meter monochromator with a 1180 grooves/mm grating blazed for 500 nm, or an Oriel model 7155 filter monochromator, as specified in the figures. Slits used ranged from 0.5 mm to 4 mm, and the image conduit mentioned above was occasionally replaced by a quartz rod of equal or slightly tapered dimensions. Analytes were repeatedly injected while the wavelength drive was manually advanced, or, when appropriate, a constant flow of compound (through the doping vessel from the reactor experiments) was introduced and the wavelength drive was automatically forwarded. A Hamamatsu R1104 PMT (180-850 nm) was usually employed for acquiring spectra.

### **Quenching Studies**

The quenching experiments were carried out by finding a hydrocarbon that would co-elute with a standard analyte

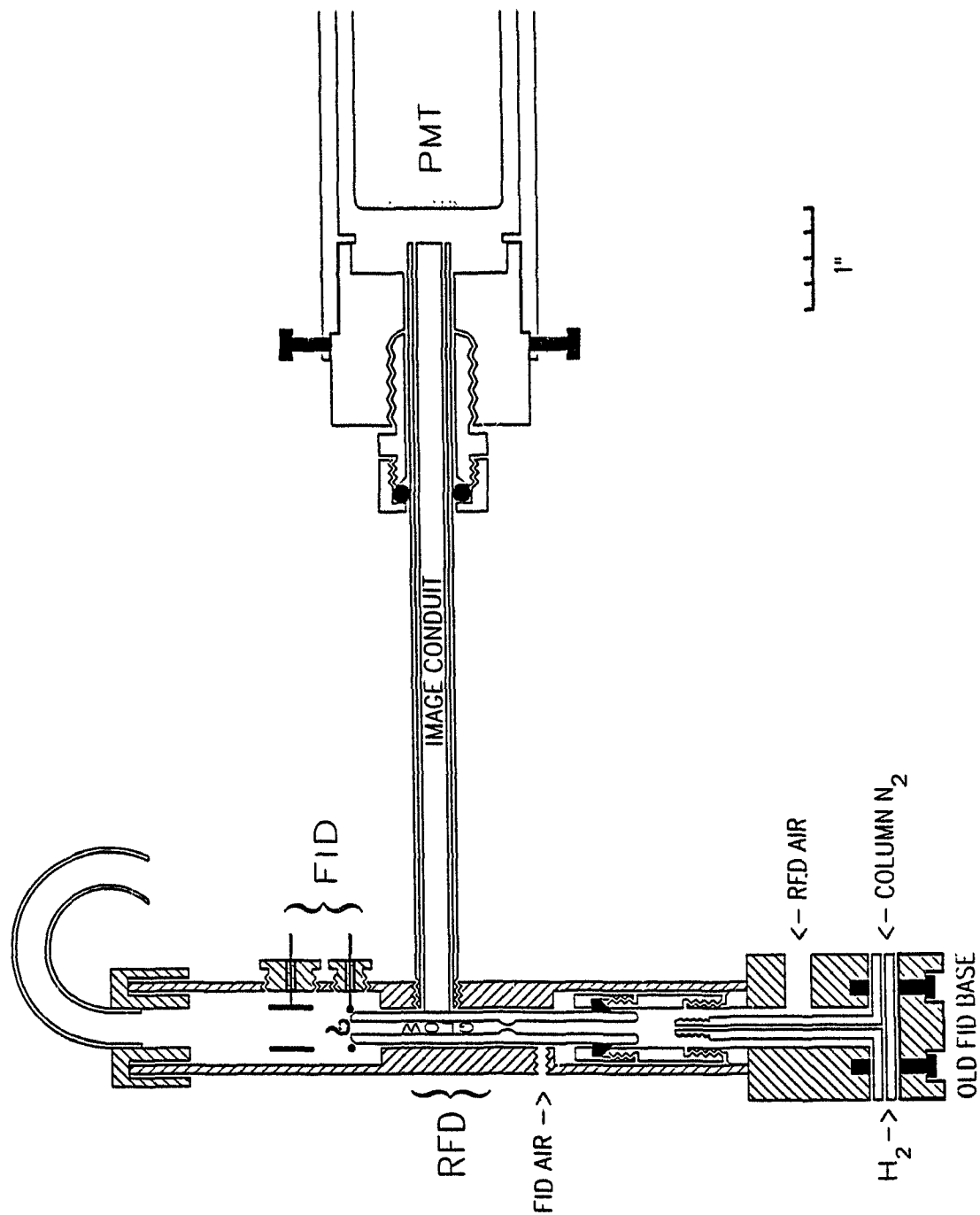


Figure 3: Schematic of The Reactive Flow Detector prototype.

containing S, P, Sn or Mn. The concentration of the hydrocarbon quencher was varied from zero to the point where it overloaded the reactive flow (see chapter 4).

#### **Flame Ionization Adaptations**

The FID arrangement looks very similar to the original Tracor commercial model, except for the light guide piercing its side and peering at its reactive flow. For this study, the "run-along" RFD channel is monitored by the Hamamatsu R-268 PMT. The dual detector assembly is also depicted in Figure 3 above.

To test the FID properties of the flame that burns the excess hydrogen on top of the RFD glass capillary, the reactive flow below it is switched on and off, back and forth, as the test compounds are repeatedly injected. This procedure is considered preferable to comparing the output of a separate, conventional FID, since FID response depends very strongly on various constructional and operational details - not just for overall performance but, much more disturbingly, for the relative responses between differently structured compounds [e.g. 92 and references cited therein].

Some of the test solutions were, however, also injected into the conventional Tracor FID model to ensure the absence of any pronounced discrepancy between the two types of FID flames and, equally important, to reveal any possibly exploitable effects. However, none of the latter was found.

Unless stated otherwise, in the FID experiments, 40

ml/min hydrogen and 60 ml/min air are added to the column effluent before the mixture enters the RFD capillary. The auxiliary air flow (for the FID flame) is kept around 150 ml/min.

#### **The Singing Flame**

For these preliminary experiments, capillaries of varying inner diameter were fed by different combinations of gases and, where important, these parameters are stated in the text.

The sound of the flame was monitored by removing the cap from the RFD and placing an inexpensive microphone (Realistic model 33-986B) diagonally close to its mouth. The signal was fed through a Brüel and Kjaer model 2638 amplifier and displayed on a Tektronix 2232 100 MHz digital storage oscilloscope.

A simultaneous FID was run, and the apex of the hydrocarbon peaks it displayed, were used as the point at which oscilloscope measurements were made for the singing flame.

### 3. THE FLAME PHOTOMETRIC REACTOR

#### 3.1 Burner Dynamics

Initial attempts to ignite the burner were done at flow rates of approximately 50-150 ml/min hydrogen and 50-400 ml/min air. The lowest possible flow rate for which a stable flame was ignited, occurred at 100 ml/min hydrogen and 250 ml/min air. Henceforth, the term "stable flame" is intended to characterize a flame that was not observed to be extinguished and that exhibited a reasonably constant temperature reading (approximately within +/- 20°C).

Because the aim was for the burner to be operated hydrogen-rich, safety precautions had to be adhered to when igniting the flame. The most successful method used, was to begin with a steady air flow and slowly add hydrogen, at an increasing rate, while the glow plug was on. Once ignition was achieved, the hydrogen flow could be slowly elevated to the desired level. Furthermore, for extremely hydrogen-rich operation of the flame, the most effective way in which to ignite it was by starting with a large air flow, 800 ml/min in most cases, and glowing the plug while ascending to the chosen amount of hydrogen, until it was lit. Then, the air flow could be carefully turned down to the required amount. Both these techniques allow for the creation of a hydrogen-rich flame, while preventing ignition in the presence of an excess of fuel.

The product of a hydrogen/air flame is water, and, in

this case, large quantities of it. Routine usage of the reactor generated an abundance of water condensing on the glass reaction housing unit, and occasionally dripping, from the top, down onto the flame. The runoff from this condensation would collect in the bottom of the gas inlet chamber, around the base of the burner. To help remove this interference, a heating tape was wrapped around the reactor and held at a temperature around 100°C, hopefully persuading species from the flame to remain in the vapour phase. Subsequent operations showed this solution to work well.

Figure 4 shows the regions in which a stable flame was observed, at various hydrogen and air flow rates. In general, the average air flow rate needed for a stable flame was about 400 ml/min, with the exception of a few air-rich zones which occasionally supported a flame with as low as 250 ml/min of air. The amount of hydrogen required for stability was commonly around 150 ml/min. Merging from one stable area into another could be done without extinguishing the flame.

The fuel-rich area of interest was located at hydrogen flows of 1000 ml/min or greater, accompanied by air flows increasing from 400 to 800 ml/min. The flames within this region are quite steady, and, if necessary, flow rates beyond the substantial 1500 ml/min hydrogen, that have already been realized, may be achieved. In fact the reactor has been operated with hydrogen flows as large as, approximately, ten litres per minute.

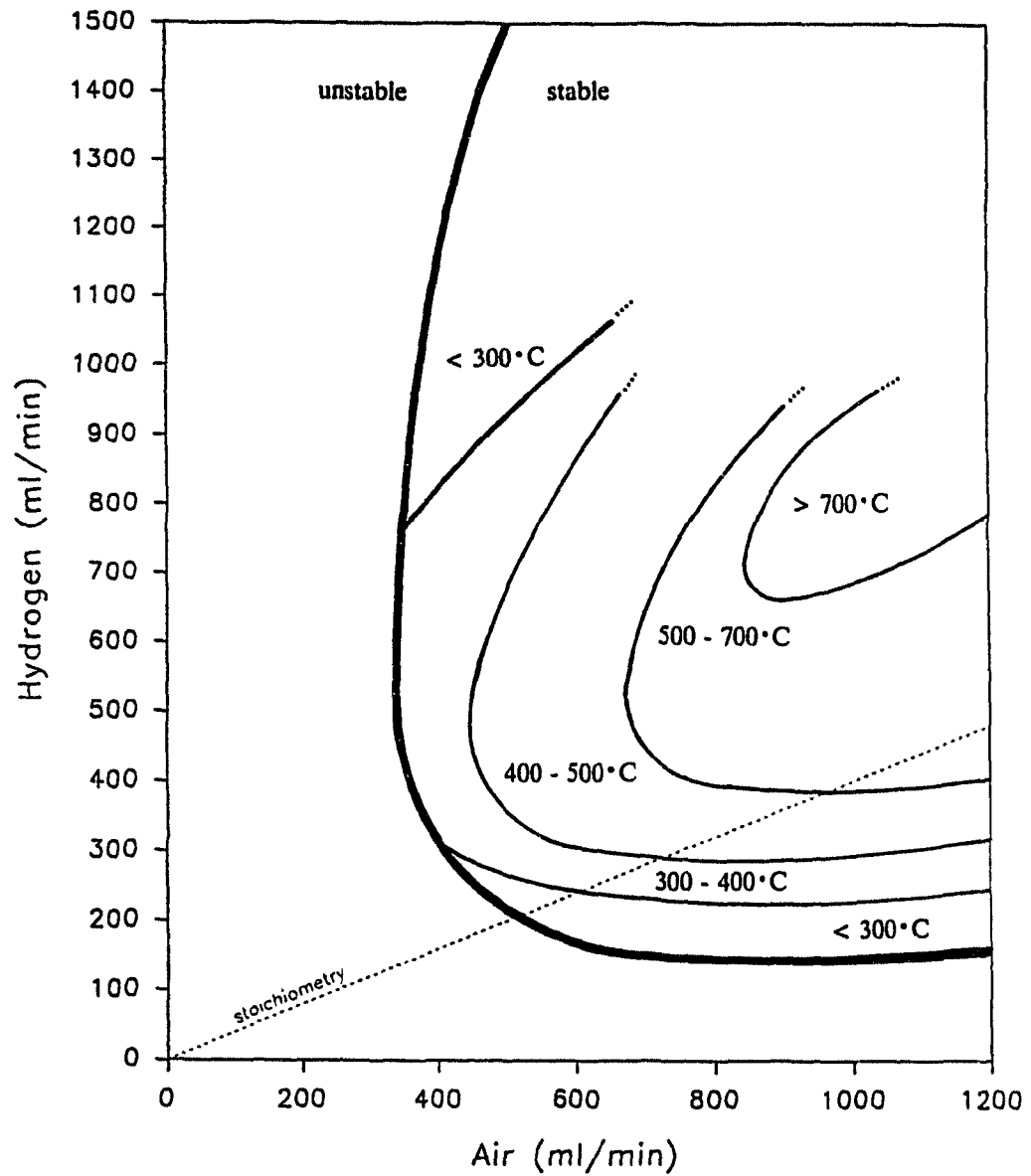


**Figure 4:** Flame stability chart for various combinations of hydrogen and oxygen. Temperatures represent those at the point of measurement and are only approximate.

Figure 4 also displays a very rough overview of the different temperatures observed, at the point of measurement, for various combinations of hydrogen and air. Although this forecast is coarse, it still serves as a useful guide to the gas flows that provide flames conducive to further study, and particularly those that should be avoided. For example, it immediately reveals which gas flows, relative to the same point of measurement, produce a hydrogen-rich flame of the lowest temperature. As well, it demonstrates the areas which are dangerous to venture into, where the highest temperatures, relative to the same point of measurement, were observed. Incidentally, this area, 900 ml/min hydrogen and 1000 ml/min air, is deemed to be dangerous because, while exploring it, the epoxy began to break down and, if it had melted through, an explosion could have possibly occurred. The greatest temperature observed in this region, at the point of measurement, was 800°C, and the heat that it conveyed to the burner was more than the epoxy could withstand. As a result, temperatures greater than or equal to 650°C at the point of measurement were no longer studied, and this was treated as the upper limit of the burner.

When the epoxy overheats and loses its tensile strength, two concerns arise. First, has the burner's shape or structure been distorted, and secondly, have any of the capillaries been plugged by the melted epoxy? After the above temperature zone was investigated, the burner retained its initial construction

specifications, however, two of the hydrogen tubes were deeply blocked. Although the usual procedure for clearing the epoxy was to drill through it with a fine bit, none was long enough to reach the clog. Finally, the obstruction was successfully removed with a piano wire sharpened at one end. This simple application subsequently provided a fine, yet tough, drill bit of any length, that easily bored through the epoxy.

Although the line of stoichiometry in figure 4 appears to be offset, this impression is misleading. Deceptively, the flame temperature seems to increase as the gas flows become more fuel rich. Initial reasoning questioned whether or not the flows coming from the meters were actually representative of those streaming from the reactor. However, this explanation was deemed to be unsatisfactory as the experimental comparison indicated that there was little difference between the two flows, for all gases employed (with the exception of air which, at larger flows, gave only slightly smaller readings coming from the reactor than what the meter had suggested). In spite of this, the position of the stoichiometry line may be rationalized when one considers what the temperatures actually represent. The measurements are merely an indication of the reactor temperature at the fixed location of the thermocouple inside the housing unit. They are not related to a particular point of reference within a given flame. Therefore, because the flame's shape and volume changes with gas flows, any temperatures quoted can only be interpreted as stemming from

the particular position within the reactor from which the measurement was taken and are not necessarily indicative of the actual flame temperature.

The shape of the flames, supported on the burner head, was visualized by doping carbon disulfide into the nitrogen gas stream, and monitoring the resultant "classic" blue sulfur emission. Figure 5 depicts how, during hydrogen-rich operation, the flames were arranged and also how the luminescent area above the burner head appeared. As mentioned in the experimental section, each air tube, 37 in total, was surrounded by 6 hydrogen tubes, 147 in total (also shown in figure 5) and this is reflected exactly in the ignited burner's surface. 37 tiny flame cones, approximately 1-3 mm in height, appeared in a magnificent array atop the air tubes (reminiscent of city street lights at night). The intensely luminescent sea of blue above the burner head was about 3-5 mm tall, and lay uniformly over the entire capillary face. These observations demonstrate that the burner was indeed successful in obtaining the initially desired, even, fuel-rich reaction zone, from the assembly of several small FPD-like burners, with, it is hoped, a comparable flame chemistry.

#### **Addition of Nitrogen**

Nitrogen was added to the hydrogen flow in order to gain some idea as to how much of it the flame could tolerate, before being extinguished. This information becomes useful when compounds are to be introduced to the reactor (i.e. via

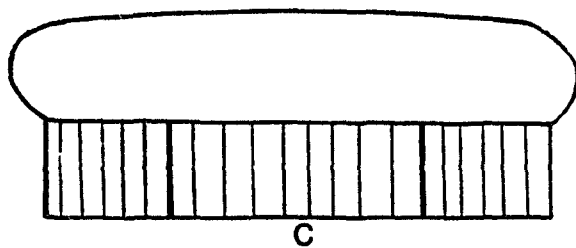
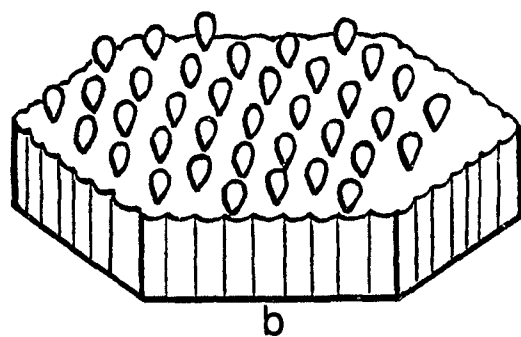
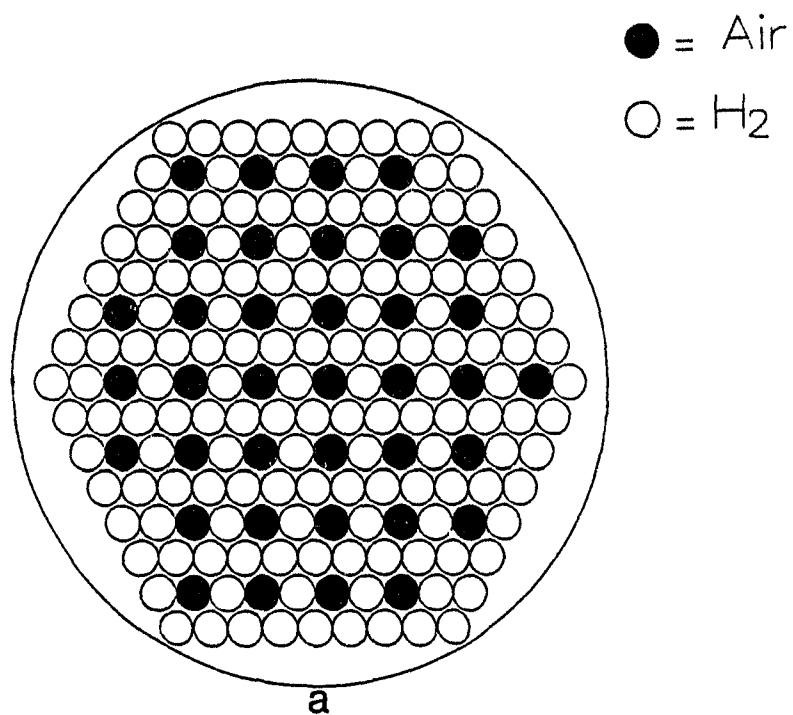


**Figure 5:** Overhead view of the burner (a), appearance of individual flames (b) and the luminescent area above them (c).

nitrogen). It was found that fuel-rich flames could endure nitrogen flows of up to ~4000 ml/min before being extinguished, whereas air-rich flames could withstand ~2000 ml/min of nitrogen while supporting a flame. A stoichiometric flame showed little change in stationary thermocouple response and flame stability towards the presence of nitrogen, checked up to ~2000 ml/min. As a matter of comparison another carrier gas, helium, was utilized in place of nitrogen; however, much the same results were obtained.

This investigation spawned another query as to whether or not the combined hydrogen/nitrogen input line was restricting the respective flow of each gas. Also, what flows could the flame withstand, before being extinguished, if the nitrogen line was spliced with the air line, and hydrogen was delivered directly?

The question of changing gas inputs was pursued by, obviously, switching the lines to hydrogen and air/nitrogen. With this change, the effect of nitrogen flows on the flame were inspected again. For the same fuel-rich, stoichiometric, and air-rich flames, as above, the flow of nitrogen required to extinguish the flame was approximately 150, 1000, and 1200 ml/min respectively.

To discover if the combined flows of hydrogen and nitrogen were restricting one another, the gas lines were changed back to their original arrangement. A test was performed to see if their individual flows combined to deliver

the overall additive flow. The results have been arranged in Table 1.

**Table 1: Combined Gas Flows (ml/min)**

Nitrogen Flow	45	99	174	201
Air Flow	50	103	183	600
Expected Output	95	202	357	801
Observed Output	94	200	343	750
Nitrogen Flow	45	99	174	201
Hydrogen Flow	100	210	375	923
Expected Output	145	309	549	1124
Observed Output	141	308	522	1000

The combination of air and nitrogen was first investigated, in order to have some basis of comparison; then the merging of hydrogen and nitrogen was checked. It was found, in both cases, that the combined flows were additive and therefore did not restrict each other. The hydrogen/nitrogen and air delivery method was employed in all subsequent studies.

### 3.2 A Test Compound in the Flame

After obtaining preliminary temperature and flow information from the reactor, the introduction of compounds into the flame, along with the collection and analysis of any corresponding output gases, was initiated.

Samples were delivered via the conventional introduction method so as to determine what flow of nitrogen (through the

doping vessel) produced the maximum luminescence of the compound in the flame. Any "processing" of analytes by the flame is thought to be greater at this rate of introduction, and thus, hopefully, the burner would be used to its full capacity, without being overloaded.

The first test compound chosen for study in the flame was benzene; a commonly encountered organic molecule. Testing showed that its maximum luminescence in the flame corresponded to a nitrogen flow of 108 ml/min, and this was used for its introduction into the flame. This figure indicates a benzene flow, per flame jet, of  $\sim 5 \times 10^{-6}$  g/s, which is in agreement with an average individual FPD burner (upper limit to linear range  $\sim 10^{-6}$  to  $10^{-5}$  g/s). While this evidence is hardly considered concrete, it is interesting to note as a possible attestation to the desired similarity between the new reactor and the FPD flame.

The reactor was supplied with a fuel-rich flame, 1000 ml/min hydrogen and 550 ml/min air, and a thermocouple response equivalent to roughly 325°C was observed. Benzene was delivered for an arbitrarily chosen running time of about 15 minutes. The flame gases were collected as explained in the experimental section, and 40 ml of "hexanes" were used for organic washings.

Chromatographic analysis of the reactor sample and a benzene standard ( $\sim 6 \mu\text{g}/\mu\text{l}$ ) used for comparison, are reproduced in Figure 6. Benzene was identified in the mixture

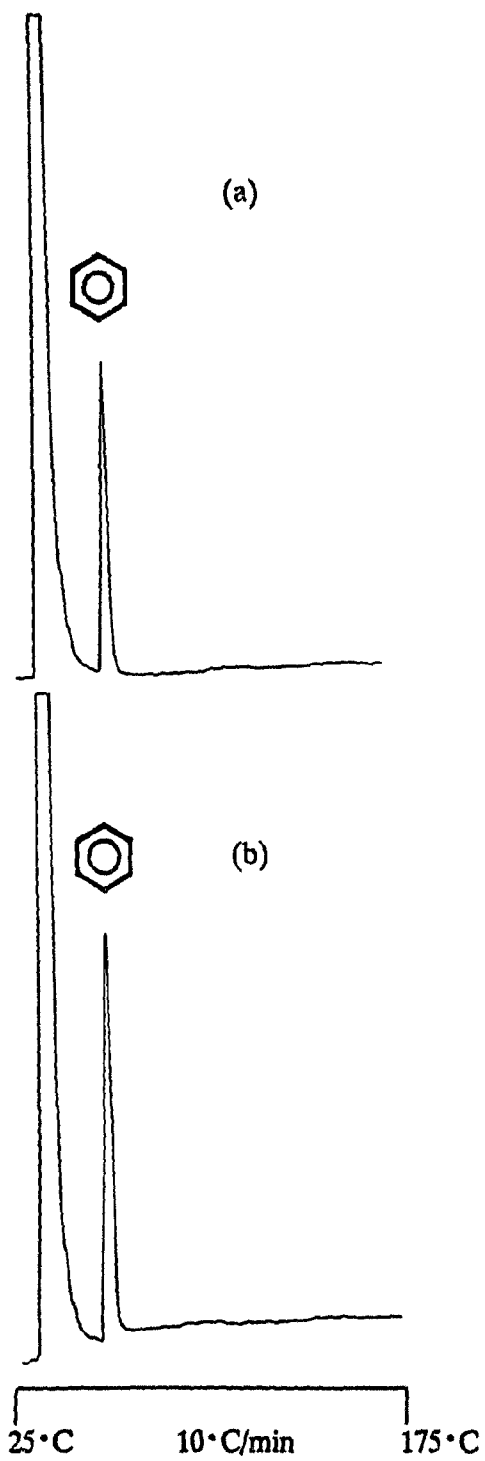


**Figure 6:** Chromatograms of a benzene standard (a) and a reactor sample (b).

by retention times.

Under the same conditions, benzene was again conveyed to the flame, only this time through the upper sample introduction tube as well as via the conventional introduction route. The same result, i.e. similar chromatograms, was realized again.

The fact that GC analysis exhibited no recognizable difference between the sample and standard implies that benzene's presence in the hydrogen-rich reactor flame produced no new species (at least not in sizeable amounts). That different products were not obtained, is neither totally unexpected, nor without implications of its own. The result actually demonstrates a more important feature: some benzene was able to survive the flame. This is significant when one considers that FPD literature commonly assumes organic compounds to be oxidized and/or decomposed by the flame. It is, of course, reasonable that some degradation and possibly some product formation did occur, however it is apparent that an appreciable amount of benzene traversed the flame intact. This also adds more fuel to the conviction that a "mild" environment has been achieved within this reactor which displays seemingly comparable qualities relative to an FPD burner.

In general, it is quite promising that the system appears to work. Different reactor atmospheres can be achieved, particularly the low temperature, fuel-rich environment

modeled after the FPD. In addition to this, the method of collecting a compound for analysis appears to work well. These initial findings suggest that reactor experiments involving molecules of varying size, structure, and composition may be conducted, and that the chemical environment of this unit may be reasonably assimilated to a scaled-up version of an individual flame photometric detector. They also pose new questions.

For example, if benzene survived the flame intact, then could other molecules also accomplish this, and if so, to what degree? Also, what amount of products, if any, could be formed from these compounds? First, however, an assessment of the experimental method will be useful in perhaps applying interpretation to later findings.

### **3.3 Defining and Evaluating the Experiment**

Considering that benzene was retrieved after travelling through the flame, it is interesting, and necessary, to know how much of the compound actually endures the reactor conditions without being destroyed. To adequately monitor this, some experimental criteria were established and inspected prior to further studies.

#### **Percent Recovery**

The primary basis for comparing compounds in the reactor, is the extent to which the flame consumes them. This is termed *percent recovery* and can be defined as "the percentage of a

compound that is regained after being delivered through the flame (at a constant rate and for a specified amount of time), compared to that which is collected, from an equivalent experiment, when the flame is not ignited". In short, it represents the difference in recovery with the reactor flame on and off. This parameter was used to gauge a compound's decomposition in the reactor, and, from the chromatographic data, was calculated as follows:

$$\%Recovery = \frac{\text{lit reactor sample (LRS) response}}{\text{unlit reactor sample (ULRS) response}} \times 100$$

Two factors linked to the "equality" between trials of a sample, are the amount of analyte delivered, and evaporation of the collection solvent.

To ensure that comparable amounts of analyte were delivered in both the LRS and ULRS, the doping vessel was weighed before and after each run. This performed as an easy indicator for any disproportions between the samples, and was also more accurate than head space calculations. The latter are blind to such errors and differ considerably from the actual amount of compound delivered, at higher flows through the vessel.

In blowing the reactor gases through the collection solvent, some evaporation was occasionally witnessed. To be sure that the sample runs were again comparable, the cold trap

was graduated and monitored at the beginning and end of each trial. In all studies performed with the reactor, any evaporation of the collection solvent was the same for the lit and unlit flame runs.

To gain some further understanding how percent recovery was affected by experimental conditions, further tests were performed with regard to both analyte and hydrogen flow into the reactor.

Analyte flows, over a wide range, were examined for their respective percentage recoveries from the reactor. The recoveries were found to be approximately the same at moderate flows where experiments were being performed, but at much greater flows, where the capacity of the flame was exceeded, they were significantly larger (by as much as 25%).

The effect of the fuel-rich atmosphere on percent recovery was also investigated. Results showed that as the environment became about three times more hydrogen-rich, approximately 30% more analyte was recovered. Small variations in the hydrogen flow, however, showed little or no effect.

#### **Collection Efficiency**

Another concern arose as to how much of the delivered compound was being collected by the solvent. This was determined by analyzing the unlit reactor sample, and comparing it to the sample that would exist if all of the delivered analyte was held in the volume of solvent that remained after the experiment. This was termed the *collection*

*efficiency* and it to served as an indicator for experimental problems.

For instance, if samples were depositing in the gas lines or on the walls of the reactor, then results could become distorted. This was responded to by flushing the lines and heating the unit, after a regular ULRS trial had been run, and observing the collection efficiencies. No discrepancies were witnessed in their analysis, and it is believed that samples travel the unignited system non-adhesively.

A related, minor query concerned the lit sample and questioned if perhaps exhaust gases from the flame (largely water) could affect a compound's transport through the collection solvent. By introducing the sample with the output gases (i.e. after the flame) and comparing the results with those obtained from a normal unlit sample trial, it was found that flame gases had no effect on the compound's collection.

Collection efficiencies are also useful in determining if a leak has occurred in the system over the course of its use. This is usually done by rechecking a past result to find if it was reproducible.

As very small collection efficiencies are undesirable, it is helpful to have some knowledge of how they are affected by different experimental variables. For example, with regard to increasing analyte flow, the collection efficiency was found to decrease moderately, but did not vary greatly with small changes.

Certain things do, however, have a more acute affect on the collection efficiency. Experiments showed that different solvents increased the overall collection of an analyte, and that solvent in both Dewars also provided a noticeable improvement, but to a lesser extent. As well, if glass balls were placed in the cold trap, with the solvent, and the gases were forced to percolate through, this divided the bubbles and, again, improved the collection efficiency.

While it is comforting to know that the collection of a compound from the flame gases can be increased, to an extent, it is important to realize that none of these methods had any bearing on the resultant percentage recovery.

Although acquiring this understanding of the flame photometric reactor is cumbersome, its establishment is vital to any progress that is to be made in characterizing the conduct of quenchers in the flame. Only now that this knowledge has been attained, can it be reasoned with certainty that any decomposition and/or product formation associated with a compound, occurred as a result of the flame and not due to some artifact of the system or method.

### **3.4 Into the Fire: A Survival Study of Quenchers**

Without any question, the variety of organic molecules that may be surveyed in a study of this nature is enormous, and this certainly has been the undertaking of some other works, probing different systems<sup>[107,108]</sup>. However, in order to

meet the aims of the present research, a comprehensive examination of innumerable chemical structures is not entirely necessary, or practical.

More appropriate, is a condensed overview of some model compounds familiar to the flame photometric detector. By systematically altering the framework, size, and composition of these analytes, a coarse, yet suitable representation of how such variations play upon a quencher's performance in the FPD, should unfold. At the very least, it would lend some clue as to where further reactor experiments should be directed. A series of worthy candidates were offered to the reactor and subsequently analyzed for their degree of decomposition and the presence of any products derived from them. The results are displayed in table 2.

A quick glance shows that the behavior of these molecules is quite varied. While the absolute values hold no meaning, they do warrant consideration relative to one another, and hence, a more detailed examination will be useful.

#### **Product Discovery**

For most of the compounds surveyed, new species were not found in the analysis of the lit reactor samples relative to the unlit reactor samples. Furthermore, of the products that did turn up in analyses, none were present in tremendous amounts compared to the primary analyte of interest. This is illustrated in the observation that, of the hydrocarbons listed, only the hexane isomers revealed products; and they

**Table 2: Survey of Analyte Decomposition in the Reactor**

---

<u>Analyte</u>	<u>Percent Recovery</u>	<u>Products Noted</u>
n-pentane	82	-
n-hexane	79	yes
2-methylpentane	74	yes
3-methylpentane	80	yes
n-heptane	58	-
n-octane	32	-
1,7-octadiene	18	-
1-octyne	13	-
n-nonane	23	-
n-butylether	5	-
n-decane	2	-
n-butylbenzene	3	-
iso-butylbenzene	7	-
sec-butylbenzene	6	-
tert-butylbenzene	11	-
benzene	73	-
cyclohexane	74	-
cyclopentane	76	-
tetrahydrothiophene	7	yes
pyridine	10	yes
piperidine	9	yes

---

existed in quantities of less than 2% of the parent compound. With heterocyclic molecules, however, it became obvious that something more substantial was occurring.

Following the introduction of piperidine, a brown tar, smelling of smoke, was observed on the walls of the heated glass housing unit. Subsequently, two new peaks were observed in the chromatogram of the LRS, and eluted just after the original compound, each comprising approximately 8% of its response. The deposit was easily wiped from the glass. A similar tar and odor occurred with pyridine, although new species were not disclosed in the analysis and the substance was more difficult to remove. On the other hand, tetrahydrothiophene produced a white film on the glass, this time emitting a stench of burnt rubber, but also failed to unveil any new peaks in the chromatogram of the LRS.

Although these results do not clearly establish any definite models regarding new species being formed from the original molecule, in the flame, the existence of products is apparent. As well, it is not unreasonable to presume that more products were actually present than were able to be captured or detected. For now, though, the insinuated transformations observed for the heterocyclic compounds are interesting to note, but would require much further work (GC-MS, NMR, etc.) for complete analysis. These findings do acquire more foundation, however, when they are coupled with the sample decomposition data.

### **Analyte Recovery**

As table 2 is scanned, percentage recoveries are seen to range from 2% to as high as 82%. To gain more perspective on how the results relate to one another, they have been re-assembled in figure 7. Although these trends are not based on entirely thorough examinations, their rudimentary implications are appreciably convincing.

For the short series of hexane isomers and the cyclic-acyclic hexane/pentane group, there appears to be no real difference in their percent recoveries. This also seems true of aromaticity, at least for cyclohexane/benzene and further down for piperidine/pyridine. Alone, these features do not display any distinction in the flame, but when placed together in a structure, a significant difference is observed, as can be seen for the side chains of benzene. When a butyl isomer is joined with the phenyl group, a marked increase in decomposition occurs. Note also, that no products (i.e. benzene or toluene) were discovered in the analysis of these largely degraded molecules.

Another short set of structures exhibit a notable decrease in percentage recovery as multiple bonds are added. Increasing decomposition is observed respectively for n-octane, 1,7-octadiene, and 1-octyne. This stands in contrast to the aromatic systems examined.

In view of the product discovery information, it is probably no surprise that the group of molecules containing

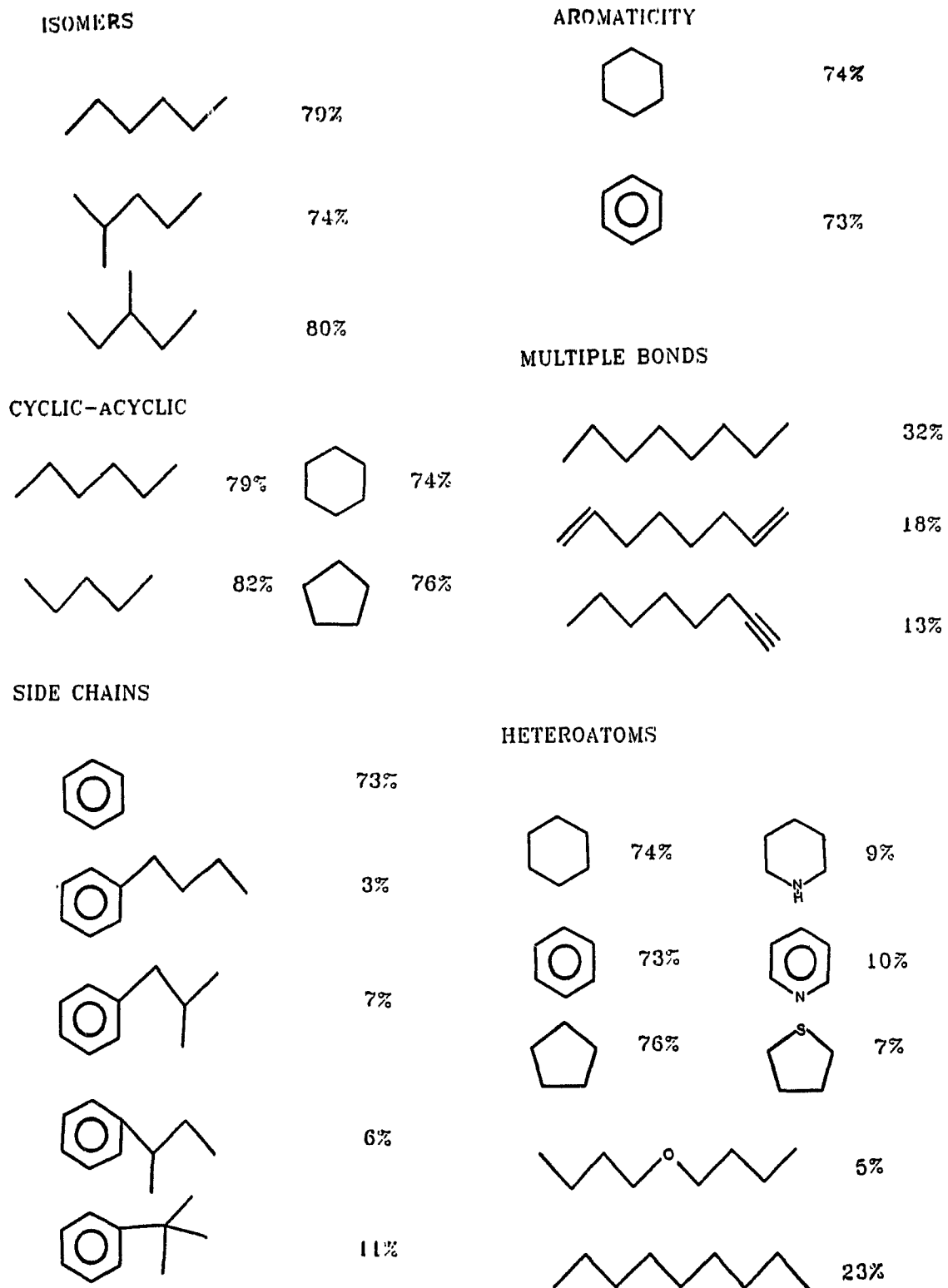


**Figure 7:** Illustration of analyte recoveries from the reactor.

heteroatoms displayed greater decomposition than those used for analogy. Piperidine, pyridine, and tetrahydrothiophene all show remarkable decreases in percentage recovery relative to their respective comparators. This is perhaps predictable, considering that the FPD is presumed to disassemble such analytes, however, quantifying this presumption helps to lend foundation to the available theories. n-Butylether also displayed a smaller recovery compared to n-nonane, but the difference was not as great as the other hetero-organics. This is better understood by another observation.

Probably the most interesting feature of table 2 lies in the series of n-alkanes, and is plotted in figure 8. As can be seen, hydrocarbon decomposition increases with the carbon number of the alkane. This is somewhat surprising that the flame would discriminate against these compounds given their common structure and *presumed* associated FPD responses and quenching abilities. The immediate question posed by this information inquired whether it was the molecule's character or the flame itself that instigated this pattern. The best way to answer this, was to change the nature of the flame from diffusion to premixed.

Various premixing caps were fitted for the reactor and tested for flame stability. All of them made it difficult to keep a stable flame, particularly with sample introduction, and so this method was abandoned in favor of changing the gas line arrangement.

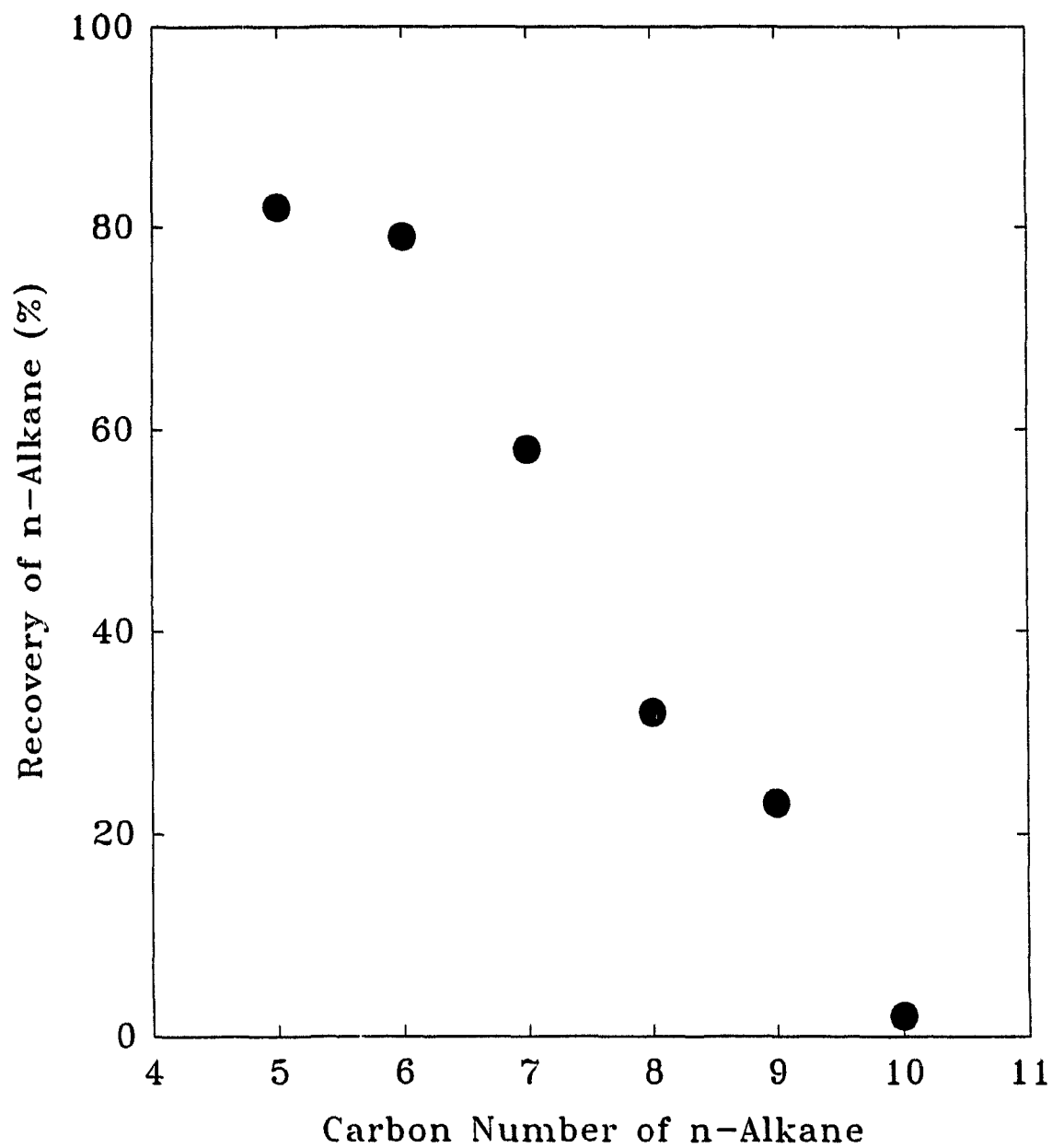


**Figure 8:** Percent recovery of n-alkanes from a diffusion flame.

By premixing the air and hydrogen in the burner body, a stable flame could be established on the normal capillary surface. Although larger flows (see experimental) were required to maintain flame steadiness and temperature, both experiments (i.e. diffusion and premixed flames) could be run with identical gas flows but with different introduction methods. As well, analyte could flow through this system without concern of the flame extinguishing. Employing this technique, a series of n-alkanes were again studied, only now under a direct comparison between a diffusion and a premixed flame. The result is plotted in figure 9.

The trace for the diffusion flame experiment in figure 9, seems to have the same shape as before (c.f. figure 8), only at overall lower recoveries. This implies that the plateau at lower carbon numbers is "real" in the sense that it is not just approaching 100% recovery in figure 8.

Conversely, the premixed flame yields the lowest overall recoveries, and, most importantly, appears to be indiscriminate toward the alkanes. Oddly, n-pentane does not follow this behavior, although its recovery is lower in the premixed than in the diffusion flame. No products were discovered in the premixed flame analysis of these samples.

At this point, it is uncertain why premixed flames do not recognize the carbon number of alkanes in the same way that diffusion flames do. It is plausible that the greater blending of flame species in the premixed arrangement forces more of

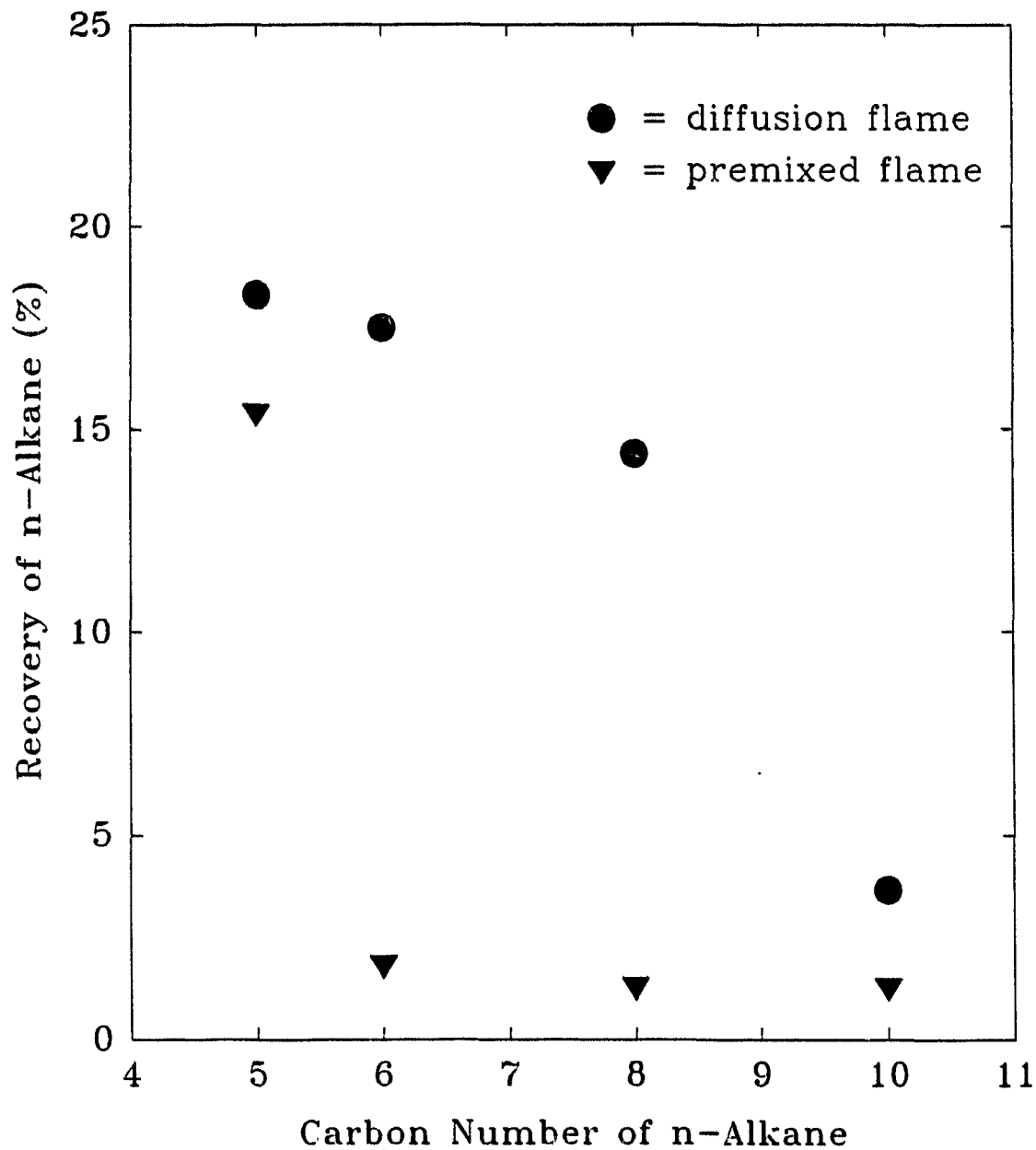


**Figure 9:** n-Alkane recovery from both a diffusion and a premixed flame.

the analyte through the primary reaction zone, and that this would occur to a lesser degree in the diffusion flame.

The data on isomers and related structures show that, while potentially helpful, theories based solely on bond dissociation energies cannot fully explain this complex system. Chemical action, such as hydrogen cracking (see chapter 6), may also play a major role. However, time constraints did not allow this, and many other interesting, related topics to be followed up.

Theories aside for the moment, the inverse nature of the curves in figure 9 is a significant finding and may share some relationship with the quenching behavior of n-alkanes and perhaps many more hydrocarbons. Therefore, as a result of these, and other preliminary reactor experiments, it may be possible to use the information regarding compound decomposition in the flame photometric reactor to study slightly different system models. Perhaps a novel design can incorporate some of these ideals and then be evaluated for its performance relative to the FPD. For this task, it is worthwhile to scale down, back to the typical dimensions of a regular flame photometric detector, and observe the processes of a smaller burner.

## 4. THE REACTIVE FLOW DETECTOR

### 4.1 Introduction

This study describes a new detector for gas chromatography, which mimics some of the properties of the FPD and other well-established GC detectors. Its concept hails from the general study of survival/transformation rates of organic molecules in the multi-capillary, high-capacity flame photometric reactor. From the information gathered, it became clear that a premixed flame showed significant differences, in terms of hydrocarbon consumption, from the traditional diffusion flame of the FPD.

To gain further insight into the stability of these premixed flames at their capillary orifices, single jets were also used. These jets were made of glass. Glass jets in open and encased versions could be produced fast, cheap, and in-house; they were relatively inert; and they could reveal the location of flames by the orange atomic emission of traces of sodium emanating from their hot surfaces. Owing to the great general importance of combustion processes and various forms of spectroscopy, tomes are available on the physical behaviour, optical characterization, and analytical use of multifarious flames<sup>[c.f. 66, 108, 109]</sup>.

While working with capillary glass jets, it was noticed that premixed gases would often form elongated glows; glows that were situated beneath (and were dependent on the presence of) stable flames burning on top. Typically, such glows would

extend over 1 to 4 cm in capillaries of 1.5 to 3 mm i.d., and would fill the available volume between the upper rim of the capillary and some lower restriction. If, however, a true flame (as judged by shape and heat, i.e. by the attendant sodium emission) would establish itself at the restriction, the glow above it would vanish.

The latter situation (though not used in, and of no direct relevance to, the current study) calls to mind the "separated" flame described by Smithells and Ingle<sup>[110]</sup> more than a century ago. A similarly configured hydrogen-flame burner, cooled to enhance the Salet effect of the divorced  $S_2$  and HPO emissions, has in fact been put to good spectral and analytical use<sup>[66]</sup>. The brilliant colors prompted the author to suggest that the device might also provide a lovely alternative to a table candle. Presenting some imagination, its design might also have served as forerunner of today's dual FPD flames<sup>[78,81]</sup>. Yet, to our knowledge, a "glow" (as described here) was never found in such devices - not surprisingly so if one considers the dual-flame design - as well as the dimensions, materials and operating conditions - of the Smithells separator.

The glow in this study used a hydrogen-rich premixture, and therefore typical premixed flames should be considered as potential points of reference. Premixed low-temperature hydrogen flames have indeed been used for molecular luminescence, but they proved less efficient than diffusion

flames<sup>[111]</sup>. Another device that used flame gases premixed (though not premixed with the column effluent), was the welder's torch FPD design of Moye<sup>[87]</sup>. Any remaining references to similarly employed arrangements are sparse at best.

Thus we are not aware of any case where glows similar to the ones described here have been observed; much less where, containing analyte, they have been used to analytical ends. However, the range of interests that may have produced such glows is very large indeed, and a presumption of absolute novelty is not withstanding correction. For instance, typical plasma afterglows, pre-ignition glows, cool flames, etc., may have some relevance to the ambient-pressure premixed hydrogen/air glows encountered here, but there does not appear to have existed any kindred device that observed them.

#### **4.2 Creation of a Reactive Flow**

The observed glows, which developed easily inside the capillary carrying an FID-type flame on top, would turn brilliantly blue in the presence of small amounts of sulfur. Their visual appearance was certainly unlike that of any conventional flame - difficult however it may be to define what does and what does not constitute a "flame"<sup>[109]</sup> - but of something that, for lack of a better term, is referred to as a "reactive flow".

This reactive flow is not self-sustaining: it requires continuous access to a stable flame. A somewhat premature

description of the phenomenon may assert that steady-state free-radical reactions are initiated and supported by the stable flame at the upper border of the reactive flow, and extend downward through the capillary to the lower border formed by the nearest stabilizing restriction; in a process that is sustained by the counter-reactionary mass movement of the premixed, excited gases.

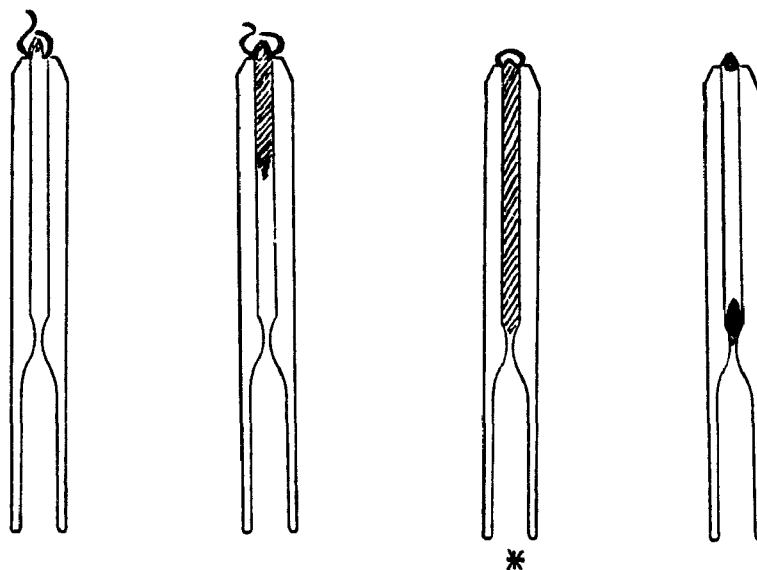
As mentioned before, the reactive flow can give birth to a second flame at the restriction ( if presented a suitable composition and supply rate of the hydrogen/air mixture). Yet if it does, the reactive flow is simultaneously terminated.

However, the reactive flow does need a flame above it. If the flame atop the reactive flow is slowly suffocated - i.e. by carefully diminishing the auxiliary air supply - the reactive flow dies with it. The reactive flow may also succumb to, say, a sudden influx of solvent. But this is merely a temporary expulsion: As the injection solvent enters, the reactive flow appears to burst out of the capillary into the upper flame, which in turn becomes large and bright. Then, with the solvent gone, the flame shrinks and dulls again, sending the reactive flow back into the capillary. The extreme stages of this process are often accompanied by characteristic sounds. Such events, however, occur only under extreme, i.e. gas supply boundary or analyte overload conditions. The typical reactive flow was silent and did not visibly fluctuate (as judged by the operator, and the

oscilloscopic trace from a PMT); as well it was tolerant of considerable variation in flow conditions and was stable in time.

Reactive flows are also capable of being formed with pure hydrogen/oxygen mixtures, although they are anything but tame in nature. This feature does, however, allow for the creation of reactive flows within capillaries of much smaller inside diameter (note that with hydrogen/air mixtures, the flame would not retreat into the capillary). Argon and helium could also replace the nitrogen, if necessary, without greatly disturbing the system. However, although several combinations of these gases were tested (with various capillaries), the hydrogen/air/nitrogen combination, originally employed, clearly outperformed all others. Figure 10 is offered to give the reader some conception of how a typical reactive flow is perceived by the operator. Although it can be viewed on its own, it is more easily traced by the introduction of a sulfur compound.

The unexpected brightness of the blue  $S_2$  bands in the reactive flow (though in part due to visual compression by the capillary) suggested that the RFD's analytical potential be explored with organosulfur and, because of its striking similarity with the FPD, with organophosphorus compounds as well.



steady hydrogen flow



increasing air flow

**Figure 10:** Creation of a reactive flow.\*

#### 4.3 Analytical Applications of the RFD

Figure 11 shows the typical gas supply range for a reactive flow, as judged by the resulting signal/noise ratio (SNR) for test compounds of sulfur and phosphorus. Clearly, reactive flows could be established at quite a variety of conditions. In the upper portions of the curve, the hydrogen input was about two thirds in excess of stoichiometric. (Note that a certain excess of hydrogen was necessary to support the top flame and thereby provide radical sustenance to the

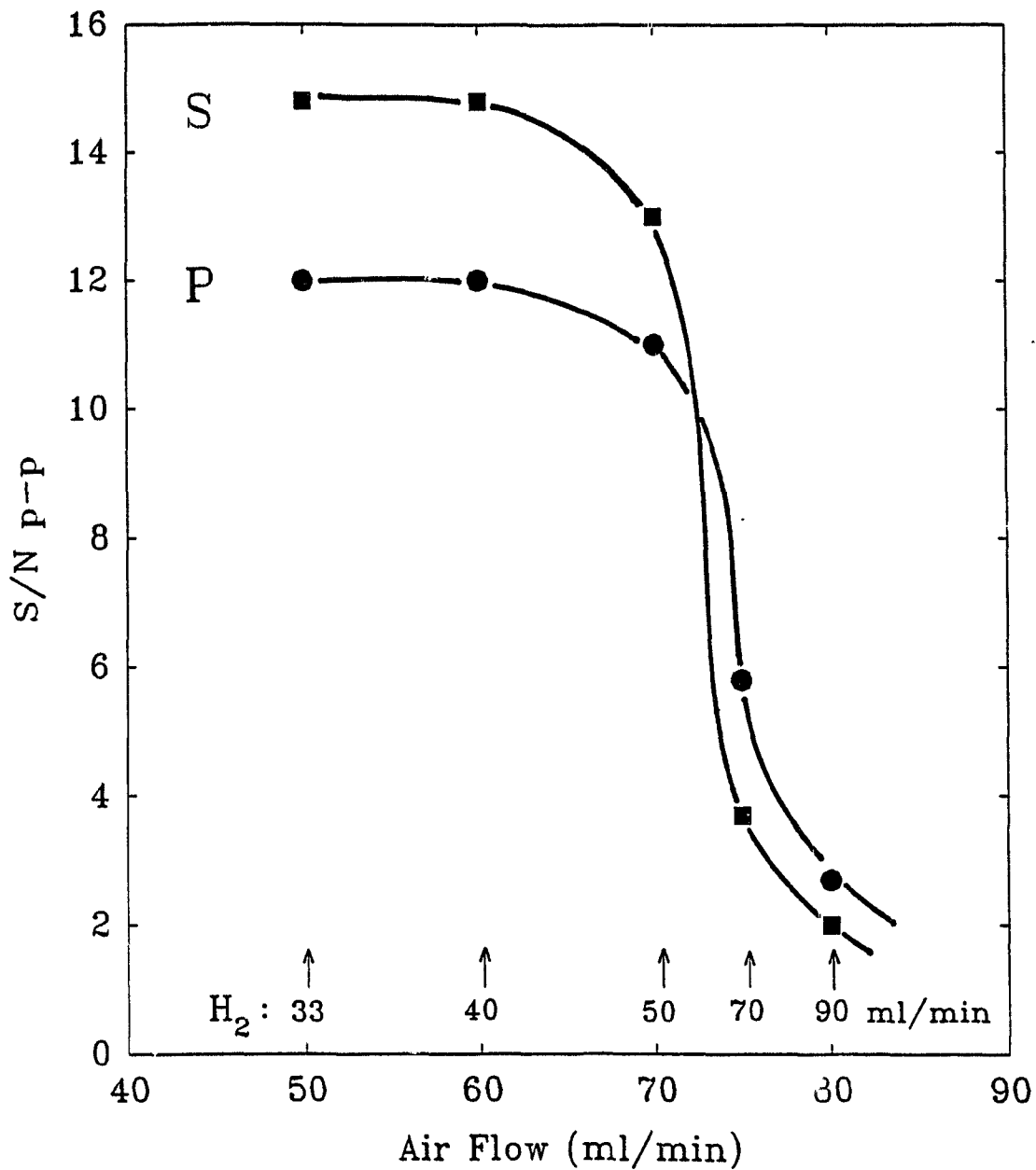


**Figure 11:** Response of sulfur(S) and phosphorus (P) containing analytes in reactive flows of different gas velocity and composition. No optical filter, R-268 PMT.

reactive flow.) The thermocouple temperatures at four different flows of Figure 11 were all in the 200 to 230 °C range. (These measurements were done with the detector housing removed, the thermocouple tip touching the reactive flow, and only minor heat emanating from the detector base.)

The most important criterion for setting gas supply rates was the creation of the reactive flow itself. Changing gas rates within its stability band (region of existence) contributed but little to its relative sensitivity for sulfur and phosphorus. If this should be confirmed as a characteristic trait of the RFD in broader-based future investigations, the detector could be used at one and the same condition for all elements to which it responds. That would greatly simplify analytical methodology, albeit at some cost in selectivity. (Note that, with the possible exception of Joonson and Loog's dual-chamber model<sup>[112]</sup>, most flame photometric detectors use distinctively different gas supply rates for sulfur and phosphorus determinations<sup>[5]</sup>.)

Figure 12 shows calibration curves of sulfur and phosphorus analytes, and allows their comparison with aliphatic and aromatic hydrocarbons, in the "open", i.e. filterless mode. The straight-line portions of these log/log calibration curves are deliberately drawn at slopes of precisely 1 (for P and C) or 2 (for S).  $N_{p-p}$  is the peak-to-peak noise of the baseline, with spikes and drift excluded, and S is the signal (peak height).

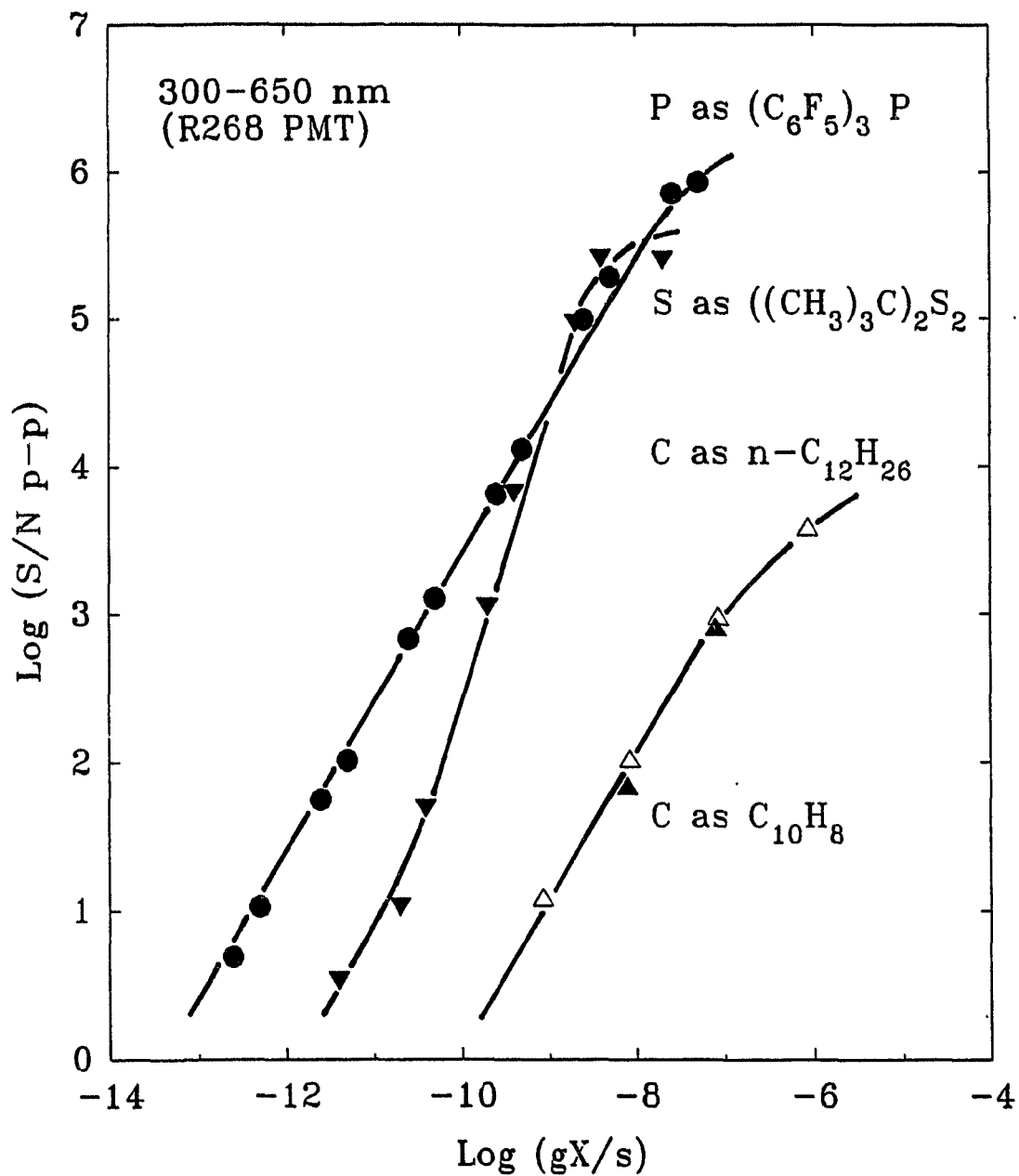


**Figure 12:** Calibration curves of phosphorus, sulfur and carbon (X=P,S,C respectively) analytes without optical filter. Gas flows: hydrogen 40, air 60, column nitrogen 12 ml/min.

Graphically, the calibration curves end at the common chromatographic detection limit of  $S/N_{p-p} = 2$ . Table 3 charts these limits and, of more original appeal, Figure 13 pictures them as peaks of sulfur and phosphorus rising out of the baseline noise.

**Table 3: RFD Sensitivities From Figure 12**

<u>Compound</u>	<u>Detection Limit (<math>\alpha</math> X/s)</u>
t-butyldisulfide	$2 \times 10^{-12}$
tris(pentafluorophenyl)phosphine	$8 \times 10^{-14}$
naphthalene & n-dodecane	$2 \times 10^{-10}$

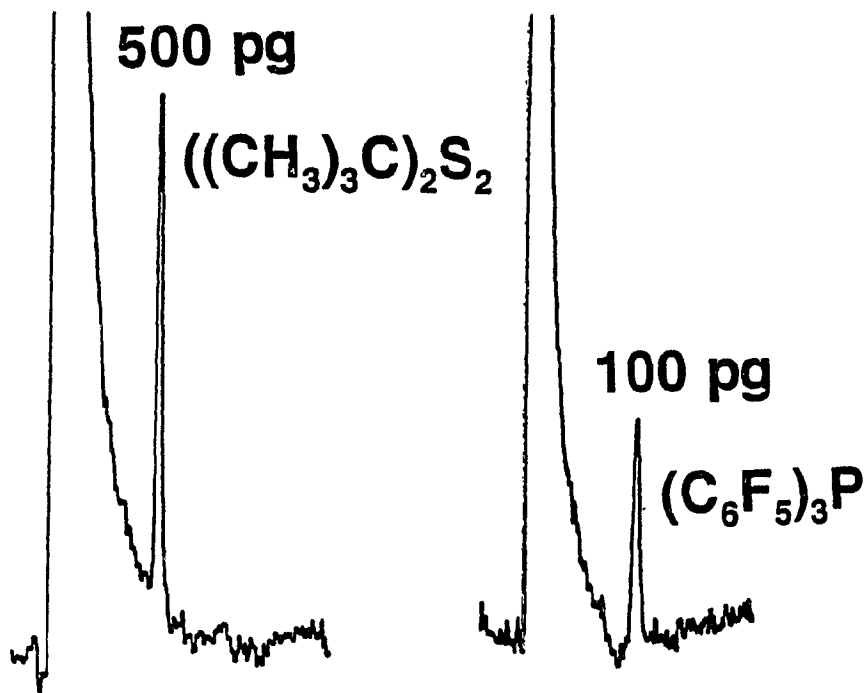


**Figure 13:** Peaks of phosphorus and sulfur analytes near their detection limit. Conditions as in Figure 12.

The most interesting aspect of the results shown in Figure 12 and Table 3 emerges from their comparison with the characteristic performance of the flame photometric detector. Dressler states in his monograph<sup>(5)</sup> that "the minimum detectable mass rate ranges from about  $1 \times 10^{-13}$  g/s to  $2 \times 10^{-12}$  g/s of P for phosphorus compounds and from about  $2 \times 10^{-12}$  g/s to  $5 \times 10^{-11}$  g/s of S for sulphur compounds". In other words, the minimum detectable amounts in the RFD are equal to or better than those of the FPD. They are, however, notably worse than those of the "pulsed-flame photometer", the "atomic emission detector", or the "sulfur chemiluminescence detector" (see Introduction).

It may be noted that, at present, the RFD remains a simple prototype, designed to evaluate analytical potential in the shortest possible time and with the least instrumental effort. For instance, the type of inexpensive light conduit it uses restricts the optical range to the visible (whereas some of the strongest  $S_2$  bands lie in the UV). It also samples only a fraction of the light generated by the reactive flow.

The shapes of the RFD phosphorus and sulfur calibration curves typically match those of the FPD (i.e the signature bend-off to a first-order slope at the bottom of the sulfur curve). Also as in the FPD, temperature programming causes only minor, if indeed any, baseline drift. The few data points for n-dodecane and naphthalene were added to figure 12 as an

afterthought, just to indicate how strongly (or weakly) matrix hydrocarbons might show up in the RFD. As is well known, aromatics respond in the FPD stronger (and with a different spectrum<sup>[39]</sup>) than aliphatics. This seems not to be the case here. While that matter is of only minor interest under the present circumstances, it may well warrant careful study in a future context, considering the measurements of hydrocarbon survival with the flame photometric reactor (Ch.3). Indeed, much more work would need to be done on such systems before clear connections between the large-volume reactor experiments, the typical performance of the FPD, and the still largely unexplored behavior of the RFD could be established. Given the existing parallels, however, the work does seem promising.

In analytical practice, sulfur and phosphorus luminescences in the FPD are monitored through interference filters. Included, therefore, are calibration curves for two popular wavelengths in figures 14 and 15. No unexpected features appear to be present. The minimum detectable amounts are slightly worse than under filterless conditions, as one would expect.

Also included, via Figure 16, is the calibration curve for "linear sulfur"<sup>[76]</sup>. Increasing the relative response of the red HSO vs. the blue S<sub>2</sub> bands through the use of different hydrogen/air ratios, while helpful in the flame, proved of only limited value in the glow. Instead, the RFD was operated

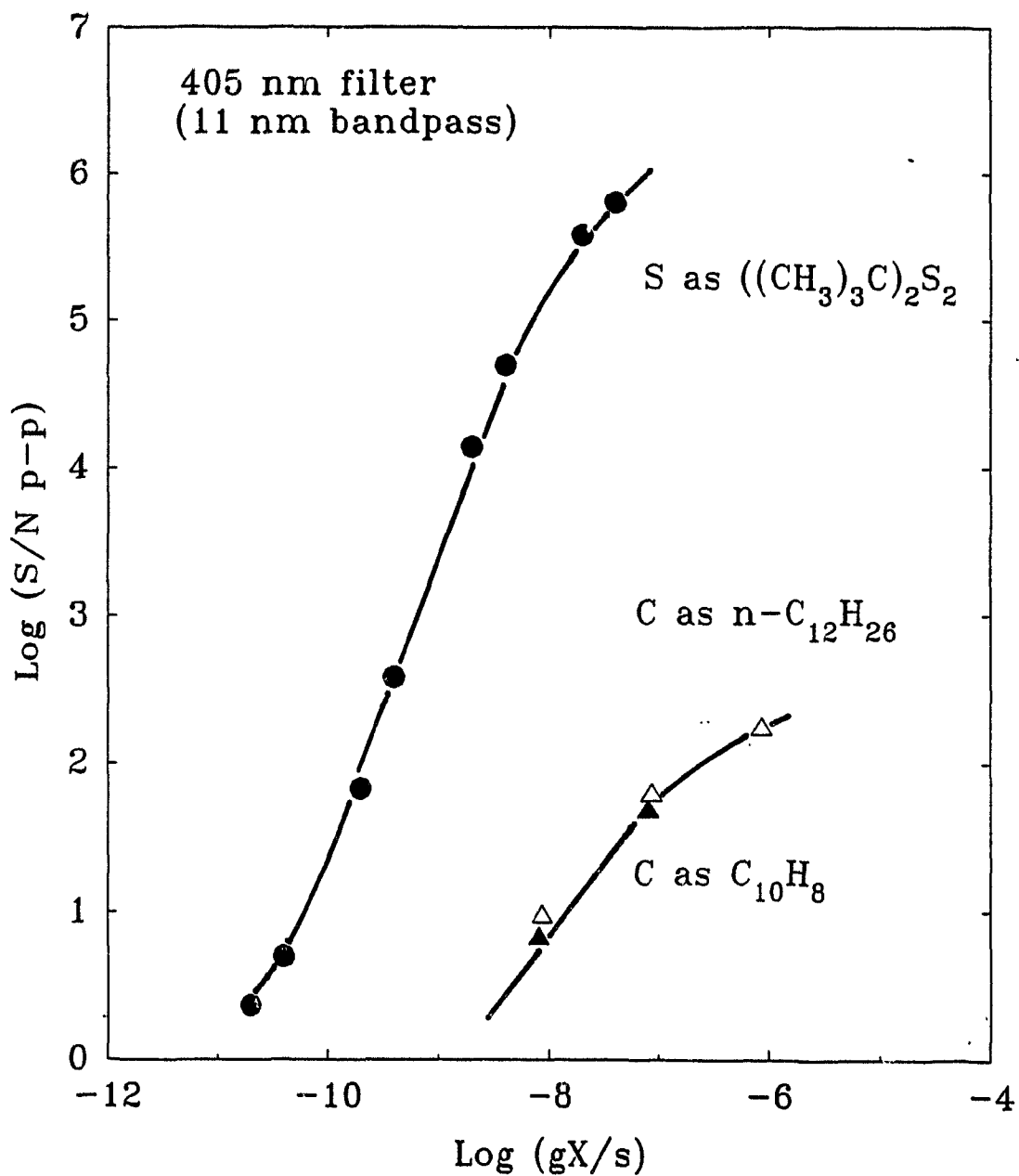


**Figure 14:** Calibration curves for sulfur and carbon analytes through a 405nm interference filter. Other conditions as in figure 12.

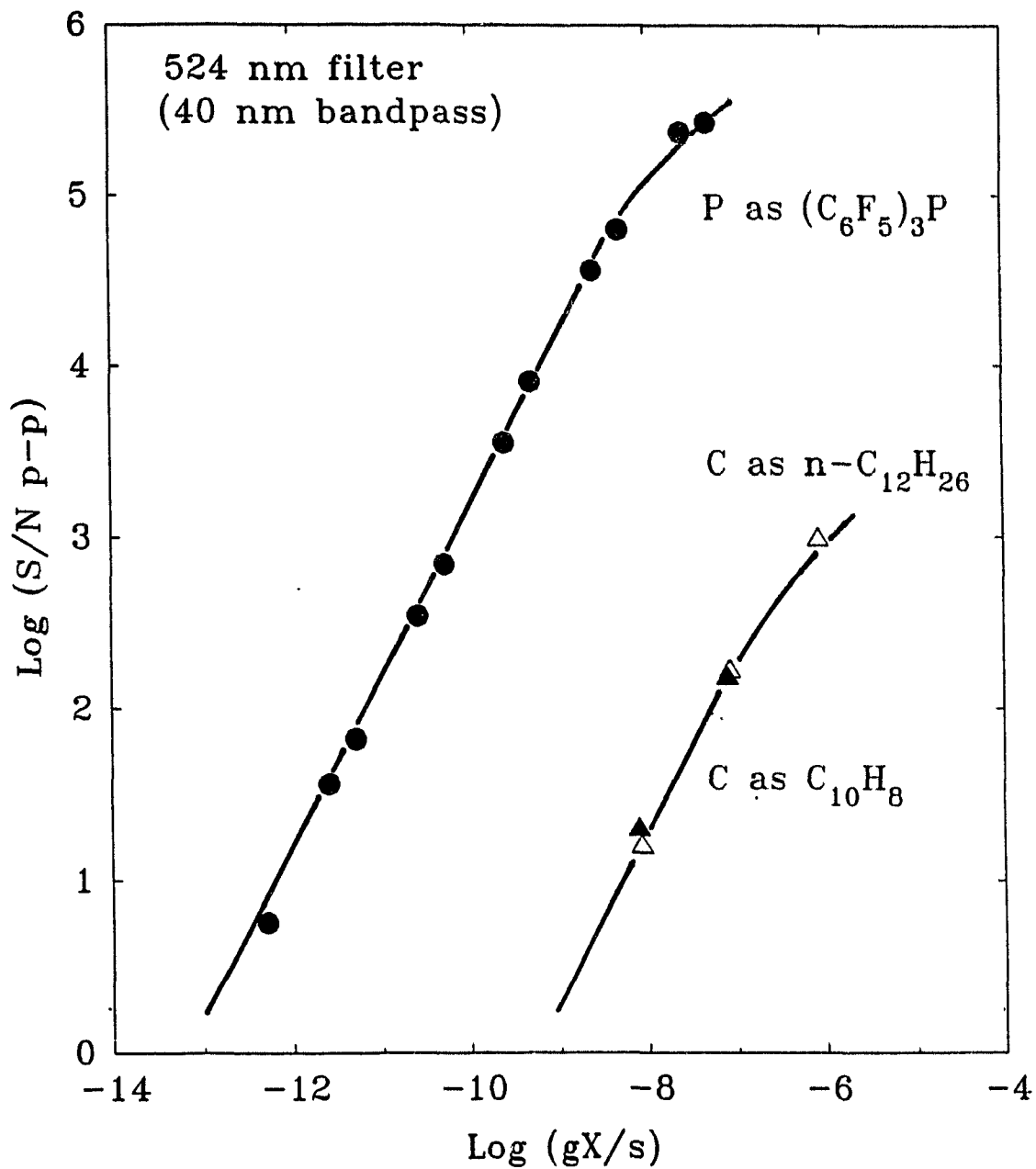


**Figure 15:** Calibration curves for phosphorus and carbon analytes through a 524nm interference filter. Other conditions as in figure 12.

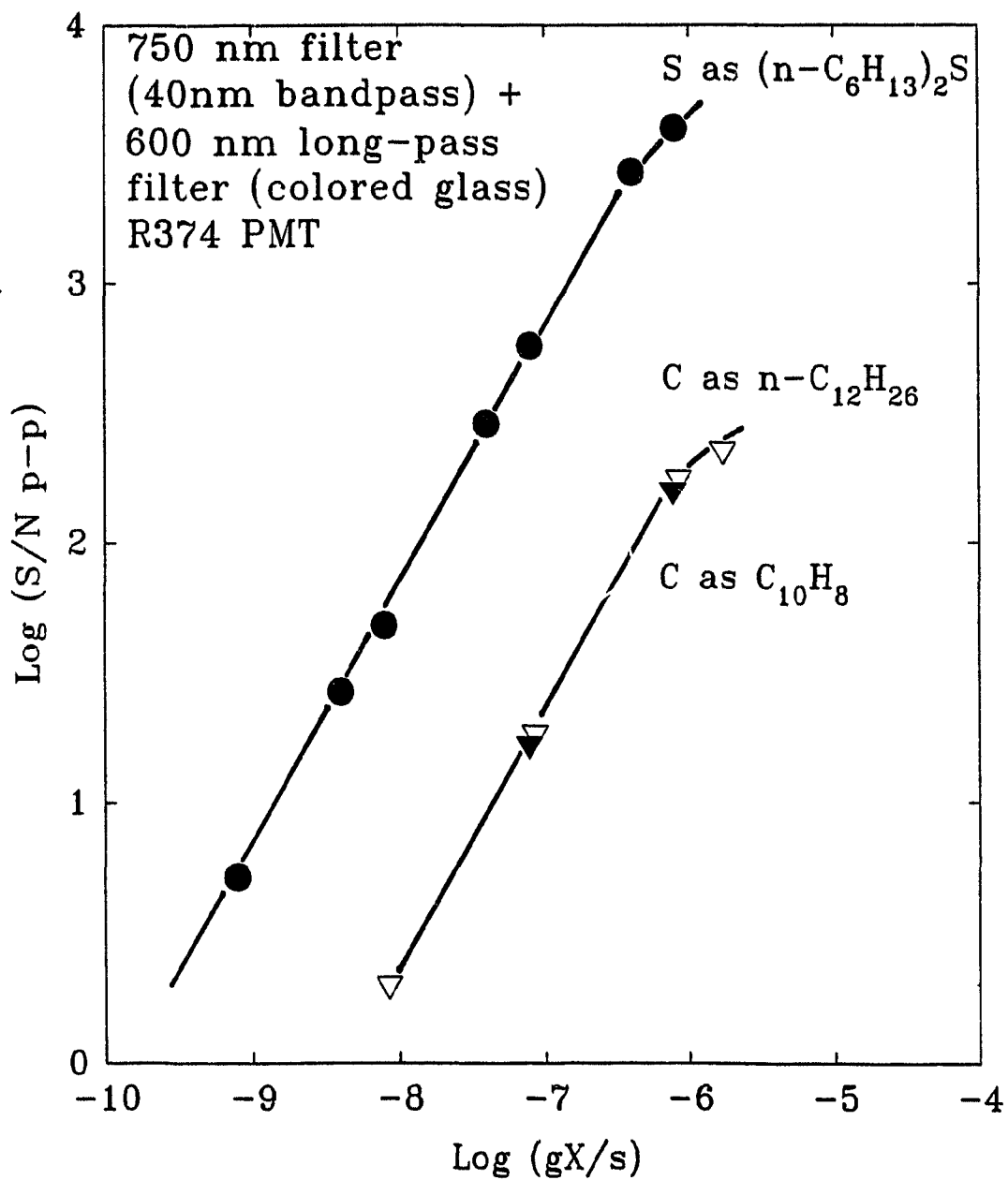


**Figure 16:** Calibration curves of sulfur and carbon analytes. Hydrogen 100, air 85 mL/min. Both lines are drawn at exactly unity slope.

at an overall larger supply rate of reactant gases; an approach that appeared to depress  $S_2$  slightly more than HSO. Also, a red-sensitive PMT was used and two optical filters restricted the light input to the 750nm band of HSO. The HSO luminescence was not as strong in the glow as it had been in the FPD flame; also, its selectivity against carbon was lower. It is interesting to note in this context that, in the RFD, carbon compounds give rise to conventional peaks, while in the FPD they usually produce negative peaks (decreases in baseline luminescence) at wavelengths above, very roughly, 600 nm.

#### **Other Elements**

As mentioned above, the optimized responses for both sulfur and phosphorus in the RFD occur at the same gas flows. Given this analytical tidbit, several other elements (known to respond in the FPD) were randomly chosen and roughly investigated for their minimum detectable limits in the RFD; at the optimum gas flows from figure 11 (hydrogen 40, air 60 ml/min). The noteworthy results are displayed in Table 4.

The most obvious fact derived from table 4 is that the RFD responds to several other elements aside from sulfur and phosphorus. The implication, however unrefined at this point, is that most, perhaps all, of the elements that give rise to a response in the FPD, respond just as well (possibly better in some cases) in the RFD. The single most important difference between the two, is that the RFD does it under one set of conditions. While this is not a comprehensive study of

**Table 4: Detection Limits of Other Elements in the RFD**

<u>Element</u>	<u>RFD -log(mole/s)</u>	<u>FPD -log(mole/s)</u>
Ru	15.4	15.0
Sn	17.6	17.3
Pb	12.3	12.5
Os	14.2	12.8
Fe	14.0	13.3
Re	11.7	12.2
N	11.1	11.6
As	12.7	13.5
Sb	12.2	11.9
Mn	13.0	13.3
Se	12.4	12.7

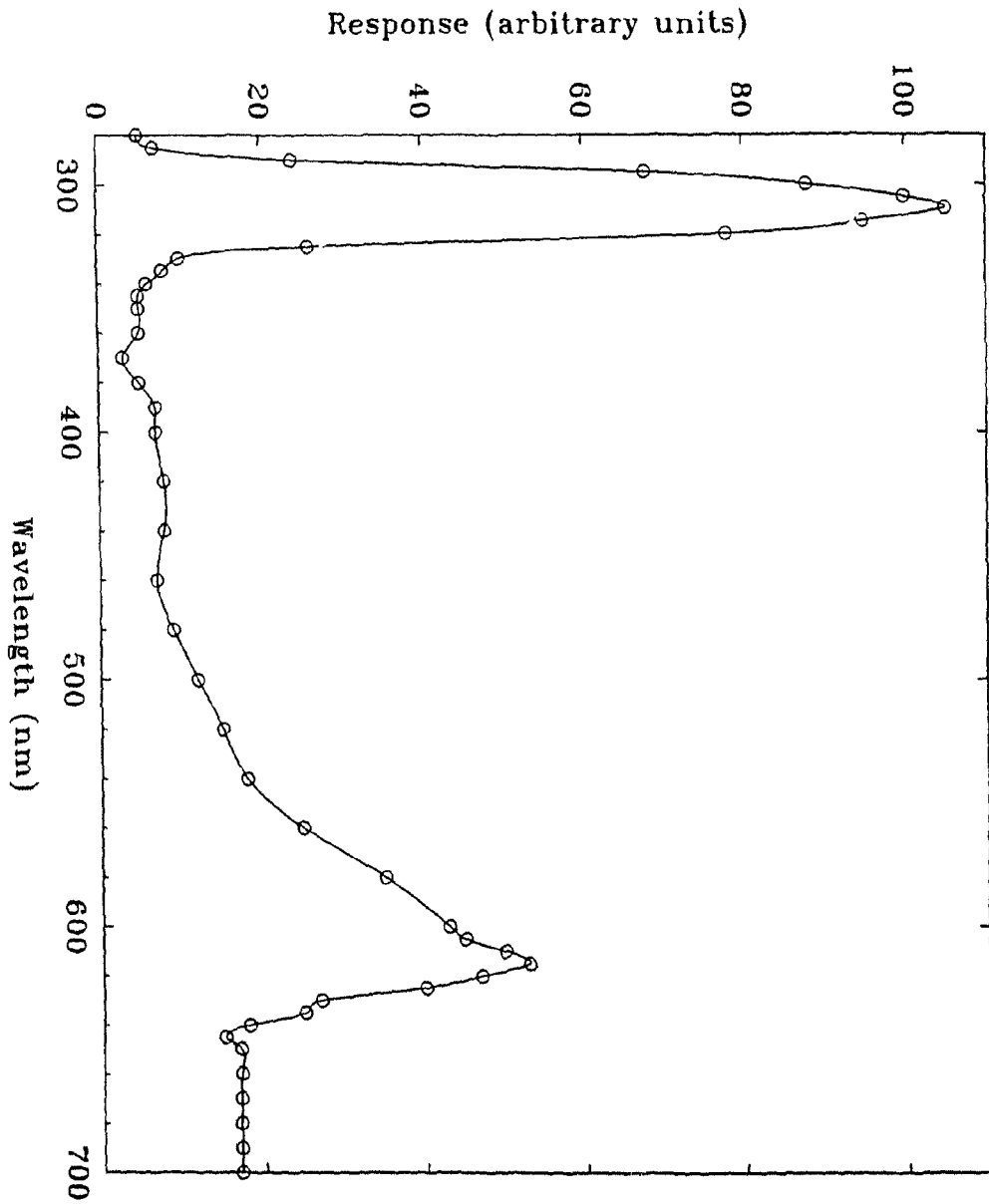
the RFD's sensitivity (i.e. optimizations have not been performed for all elements), it holds much promise for analysts to conduct multi-elemental assays in these systems, using the same gas flows, and obtain performance that is, at the very least, comparable to the FPD.

#### **Characterizing the Reactive Flow**

In working with these reactive flows, it was wondered if the apparent analogies that were sketched between them and the FPD flame, could be substantiated by the RFD's spectral behavior. Consequently, some representative spectra were taken in order to help characterize the reactive flow.

Figure 17 shows the background spectrum obtained for the reactive flow. The most prominent feature therein, is the band that occurs at around 305 nm, and is believed to be that of OH<sup>[66]</sup>. Its presence is common in hydrogen/air flames, and is

Figure 17: Spectrum of the reactive flow. Gas flows as in Figure 12. Grating monochromator bandpass: 30 nm; R-1104 PMT



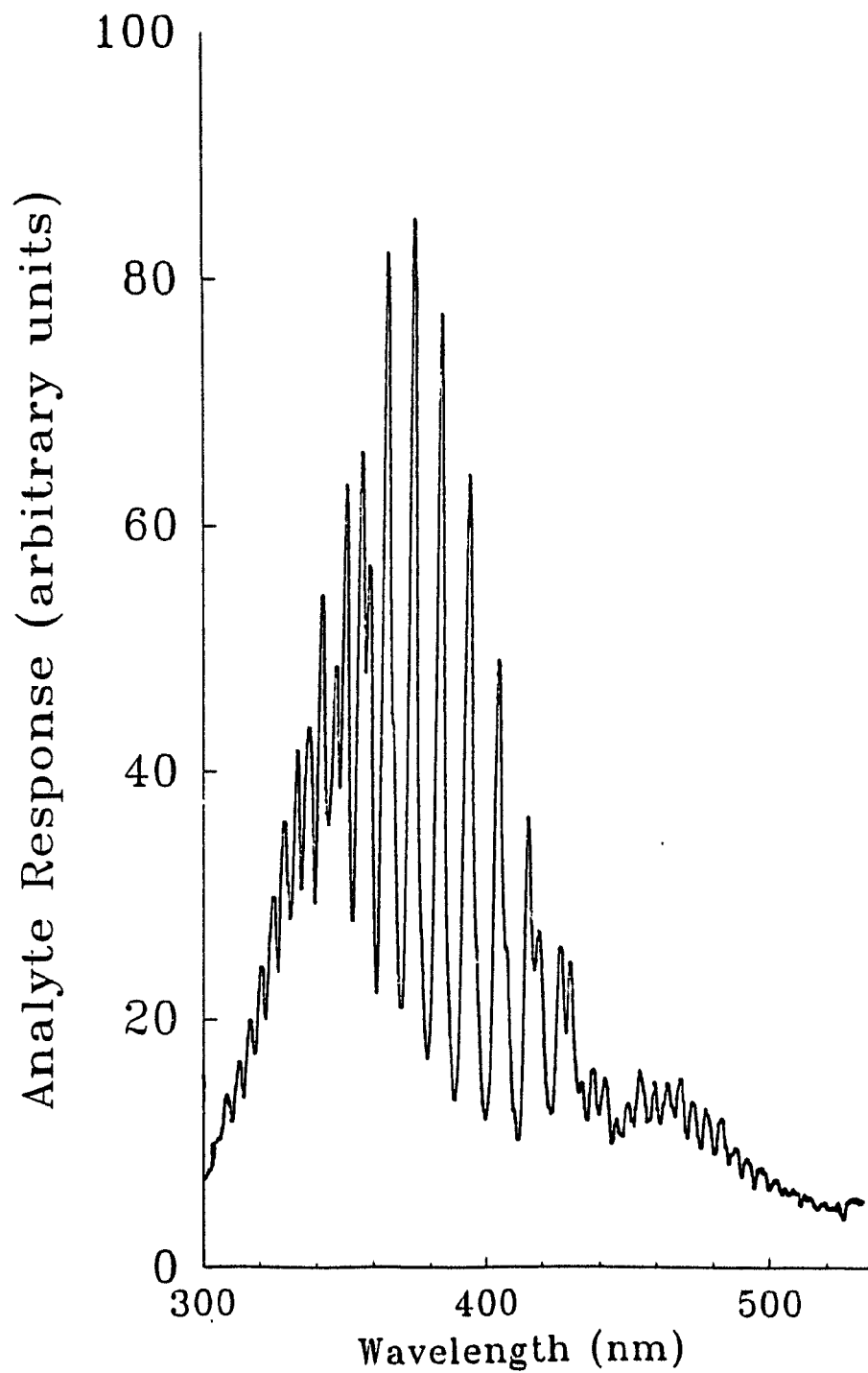
a conceivable constituent of the reactive flow.

Sulfur and phosphorus in the reactive flow are represented in figures 18 and 19 respectively. These spectra show, very convincingly, the character of the  $S_2$  (figure 18) and the HPO (figure 19) emitters observed in the past<sup>[5]</sup>.

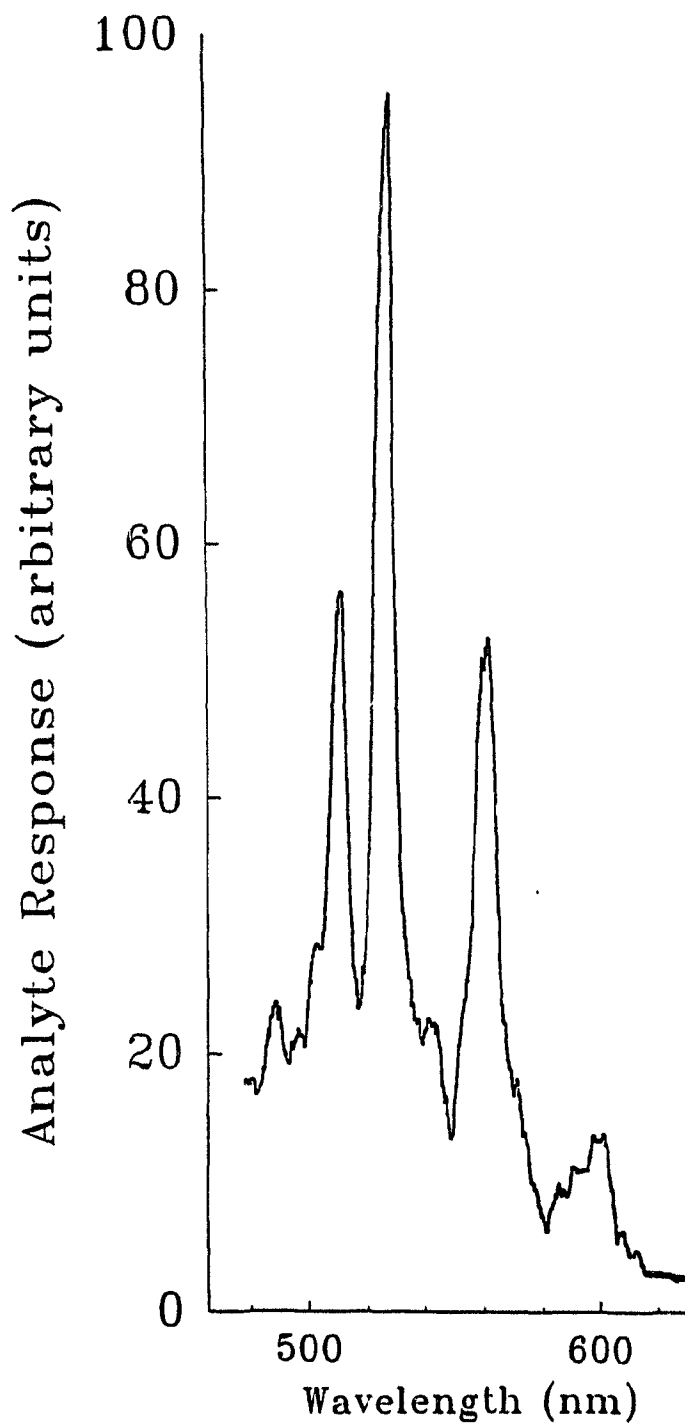
Of more interest, were the spectra of carbon as both n-dodecane and naphthalene, and how they relate to one another in the reactive flow. Figure 20 illustrates this. The spectrum of each of these compounds appear to be the same in the reactive flow, both displaying maxima at about 431 nm (believed to represent CH), but differ from their behavior in the FPD<sup>[39]</sup>. This helps to explain the equivalent response for aliphatics and aromatics in the RFD, and also may have some relation to the indiscrimination of carbon compounds in the premixed flame photometric reactor (Ch.3). As yet, however, this is inconclusive.

Given the multi-elemental response in the RFD, two remaining rough spectra were obtained for tin and manganese, and are shown in figures 21 and 22 respectively. While any fine structure in these spectra is certainly questionable, their coarse features seem quite reasonably close to that of the corresponding FPD spectra<sup>[31,38]</sup>.

Taken together, the RFD behavior for sulfur, phosphorus, carbon, and others, suggests that the glow responds frequently, though not always, in a manner similar to that of the FPD. But why? It could be argued, of course, that the

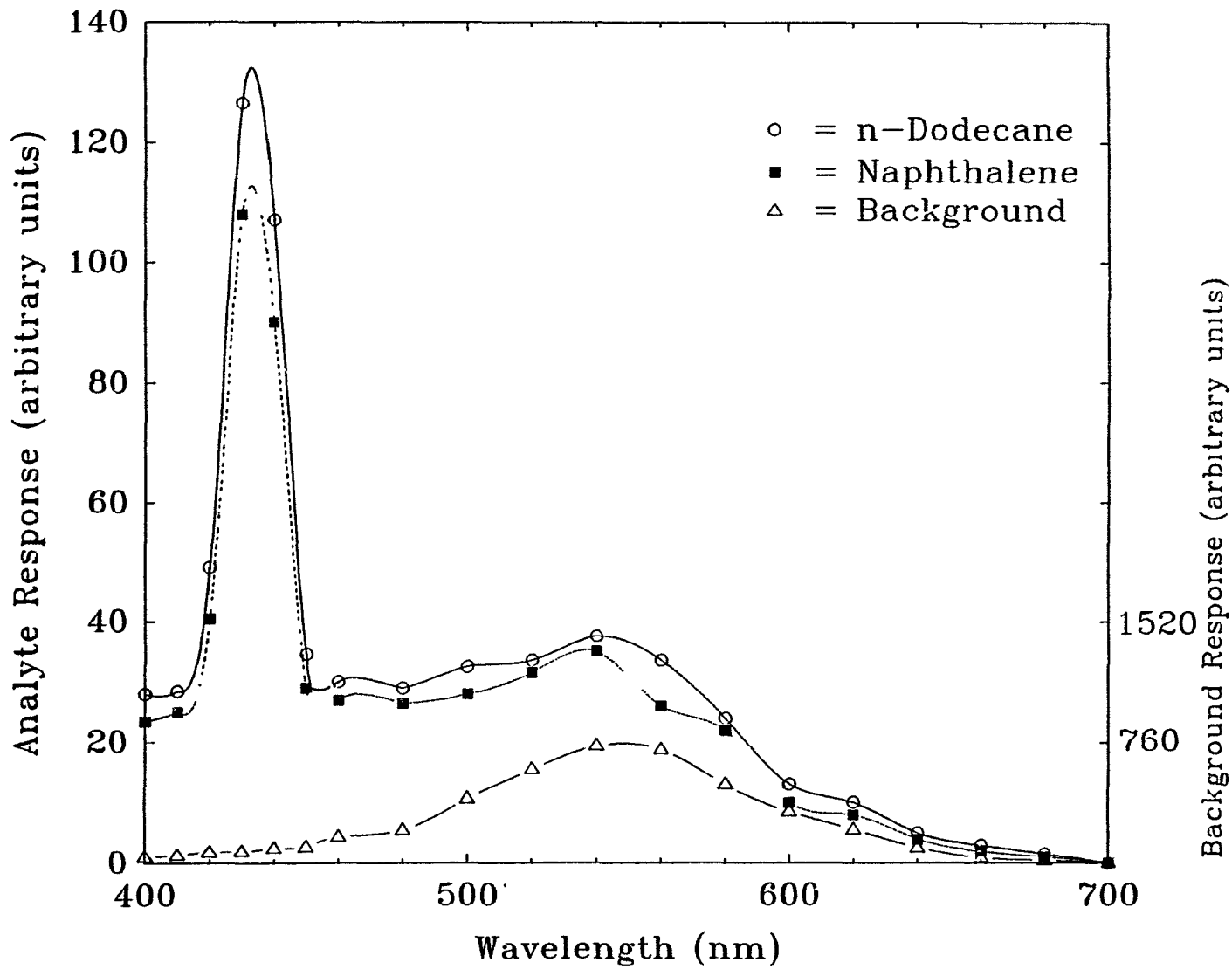


**Figure 18:** Spectrum of t-butyl disulfide in the reactive flow. Gas flows as in figure 12. Grating monochromator bandpass: 2nm; R-1104 PMT.



**Figure 19:** Spectrum of triethylphosphite in the reactive flow. Gas flows as in figure 12. Grating monochromator bandpass: 2nm; R-1104 PMT.

**Figure 20:** Spectrum of carbon in the reactive flow. Gas flows as in figure 12. Filter monochromator bandpass: 25nm; R-268 PMT.



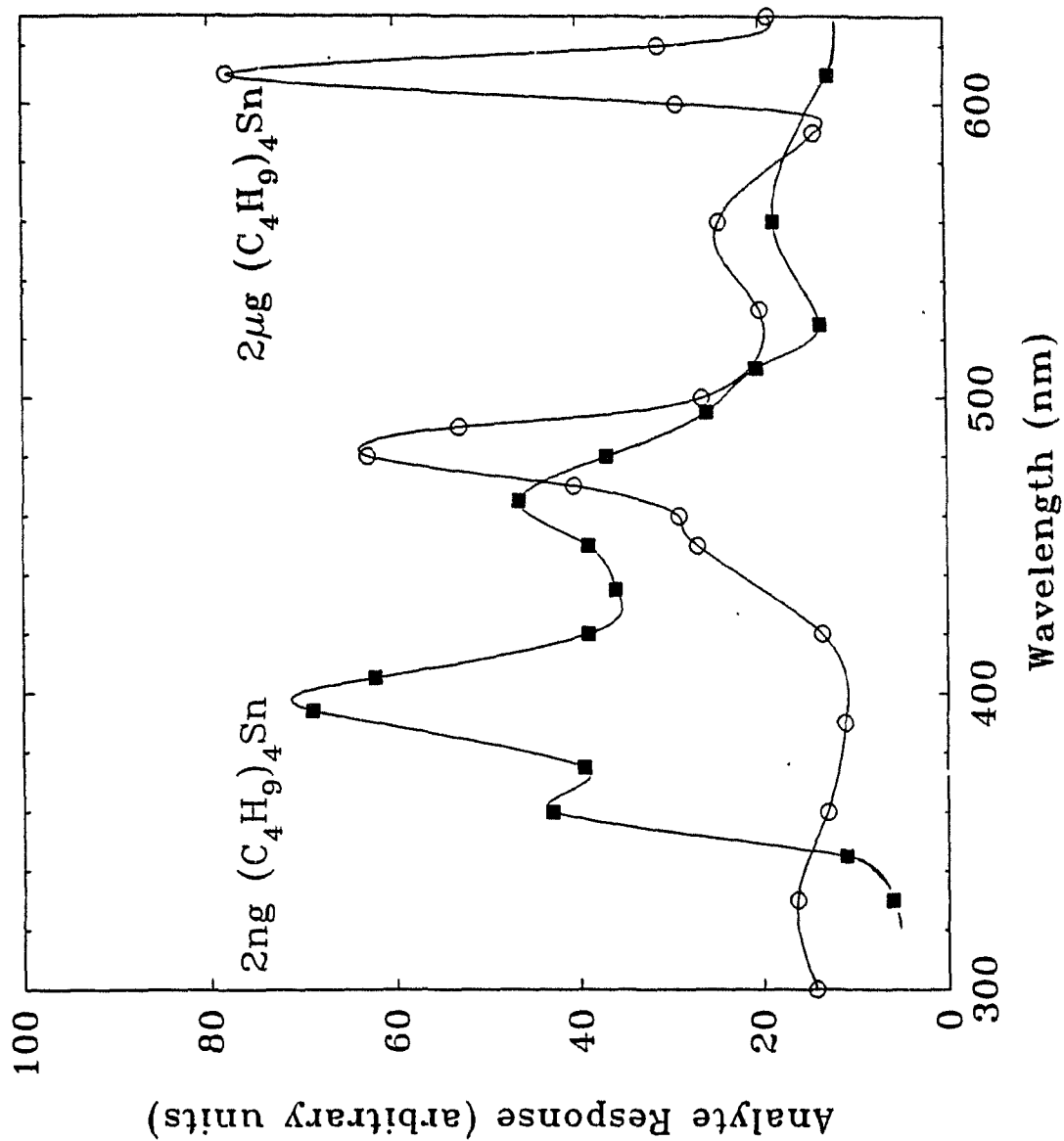


**Figure 21:** Spectrum of tetra-n-butyltin in the reactive flow. Gas flows as in figure 12. Grating monochromator bandpass: 30nm; R-374 PMT.

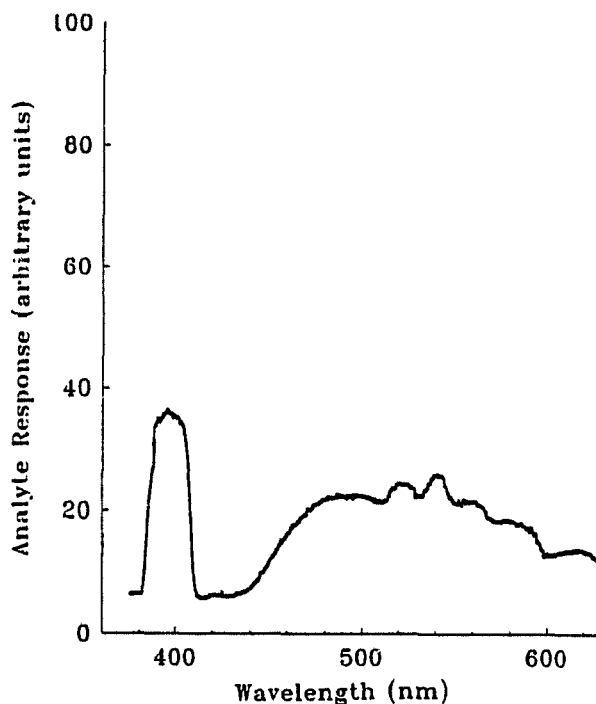


**Figure 22:** Spectrum of methylcyclopentadienyl manganese tricarbonyl in the reactive flow. Gas flows as in figure 12. Grating monochromator bandpass: 30nm; R-1104 PMT.

FPD flame should contain a region similar in composition to the reactive flow. Yet the existence of such a region is neither a necessary nor, obviously, a sufficient criterion for observing luminescence. When, in an unrelated earlier study, sulfur compounds were introduced into an FPD from the top, strong sulfur response could still be obtained<sup>[86]</sup>. Since both the point of introduction and the luminescent region were situated clearly above the (visible) flame region in those

early experiments, the inevitable conclusion is that high-energy species - e.g. hydrogen atoms - had to transcend the visible flame in large enough numbers to excise a significant fraction of sulfur atoms from the analyte molecules above. By general principle as well as optical analogy, such free radicals (H, OH, peroxy-type structures, etc.) are likely present in reactive flows.

The suggested excision scenario is also in general agreement with the measured survival rates of various hetero-organics (containing N, O or S) en route through the flame photometric reactor: their survival rates are much lower than those of the pure hydrocarbons (Ch.3). It is also possible to introduce test compounds above the flame of the reactor (in fact, that's what the reactor was in part designed for). However, no thorough study of analyte survival under such conditions has yet been carried out.

Nor, indeed, have the contents of typical reactive flows been collected and analyzed for residual molecules of, or products from, hydrocarbons and hetero-organics of interest. These analytes/reagents are easily added as vapors - via a continuous doping stream or as chromatographic peaks - to the premixed hydrogen/air supply gas. Such an "RFR" (a reactive-flow reactor) may indeed appeal to some areas of spectral, kinetic, or even synthetic interests.

That would certainly be helpful: the RFD is in dire need of basic understanding (a need not unlike that of the FPD;

never mind the latter's much longer history). Similar to many other chromatographic detectors that appear to represent simplicity itself - and certainly similar to the FPD - the RFD may yet turn out to be much appreciated before it is much understood.

## 5. QUENCHING FREE REACTIVE FLOW PHOTOMETRY

### 5.1 Introduction

The properties of the RFD, as far as investigated, suggest that it is closely paralleled - in performance if not in principle - to the FPD. For example, this is certainly true of its response to S and P, in particular in terms of minimum detectable amounts and shapes of calibration curves. One clear difference found so far between the RFD and the FPD relates to their behavior regarding two test hydrocarbons: The RFD responded equally well (or badly) to naphthalene and n-dodecane; the FPD, as is well known, strongly favours the former.

A second possible difference, also relating to carbon behavior, may have occurred in the determination of detection limits: sulfur and phosphorus peaks were allowed to ride up on the solvent tail (figure 13). In the conventional FPD this would have been foolish: the solvent tail could have seriously quenched the response of the analytes.

Recall from chapter 1 that quenching by co-eluting hydrocarbons is a - if not the - major drawback of the FPD. Given the prominence and importance of this detector, it is not surprising that many attempts should have been made to explain and, more importantly, to expunge its quenching behavior. Not all such efforts have been entirely successful. Perhaps this was not solely the fault of the FPD: quenching effects are known to affect even high-energy, thermal emission

sources - although less so than they plague the low-energy, chemiluminescent FPD system. The quenching effect, of carbon on phosphorus for instance, has been known for more than a century: in the words of P. T. Gilbert, E. Mulder found in the 1860's "that a single drop of ether in the hydrogen generator quenches the green spectrum"<sup>[66]</sup>.

Clearly, if the RFD is to have any chance of serving the analytical community, it must be less, not more, susceptible to quenching than the FPD. The FPD has so far been shown to respond in an analytically interesting manner to several elements, and, as previously mentioned in chapter 1, it has been suggested "that hydrocarbons may quench the exciting flame rather than the excited analyte"<sup>[83]</sup>.

Presuming, perhaps wrongly so, that hydrocarbonaceous quenching mechanisms are similar or identical<sup>[83]</sup> for most or all of the FPD-active elements, it was decided to test only a few in the RFD. The choice of which to test was influenced by a desire to acknowledge analytical relevance and, at the same time, achieve a suitable representation of different types of emitting species.

Sulfur and phosphorus are obvious candidates owing to their spectroscopic and instrumental history, as well as their industrial, environmental and biochemical importance. Both are prominent analytes in present-day analytical labs and produce molecular emitters. The green  $\text{HPO}^*$  conforms to a linear calibration curve; the blue  $\text{S}_2^*$  to a roughly quadratic

one<sup>[5]</sup>. Sulfur response can also be linear if the red  $\text{HSO}^*$ <sup>[76]</sup> is sampled. Tin, a main-group metal, is the most sensitive element in the FPD in the form of its blue surface luminescence, i.e. a continuum of spectroscopically unknown origin<sup>[31]</sup>; its weaker emitters are the greenish  $\text{SnOH}^*$  and the red  $\text{SnH}^*$ . Industrially, organotins are also often monitored by the FPD. The transition metal manganese produces, in addition to a somewhat less prominent continuum, strong atomic  $\text{Mn}^*$  emission. Its FPD response can be used, for instance, in the determination of a common gasoline antiknock additive<sup>[38]</sup>.

The four elements S, P, Sn and Mn thus represent a good cross-section of chemically important, spectrally varied, and analytically representative test species. To check separately for each one of their known emitters would have been a daunting task. However, this turned out not to be necessary. If the usual FPD interference filter is removed, all emissions within photomultiplier range are recorded, and the quenching of any emitting species is registered. Since, as will be demonstrated later, none ever was, it can safely be assumed that all emitting species of each particular element are immune to quenching within the range of RFD operating conditions.

### 5.2 Evaluation of Quenching in the RFD

By fortunate circumstance, overlapping pairs of analyte and quencher were easily found for the Apiezon-L packed column

used in these experiments (Ch.2). (Its low resolution represented, in this case, a definite advantage.) The pairs were thianaphthene and naphthalene for sulfur, tris(pentafluorophenyl)phosphine and n-hexadecane for phosphorus, tetra-n-butylstannane and n-hexadecane for tin, and methylcyclopentadienylmanganese tricarbonyl (MMT) and n-dodecane for manganese. Figure 23 shows the consistently pleasing results, expressed as fractional analyte response versus the (logarithmic amount) of quencher. Clearly, the co-eluting quencher exerts no influence on the analyte's response in any of the four cases.

Experimentally, the quenchers were also chromatographed by themselves, serving as background checks for when they co-eluted with the analyte peaks. This was done to ascertain that the peak of the quencher (i.e. the quencher's own luminescence) was indeed small enough not to interfere with the measurement of the "quenched" peak of the analyte. (For one data point of Figure 23, the quencher peak turned out a bit too large and had to be deducted.) Quencher amounts between 10 and 100 ug - and above, of course - cause the luminescent column of the reactive flow to temporarily abandon the capillary: this defines the upper limit of the RFD's operational range.

It would be surprising if the clear result of Figure 23 - no quenching anywhere in the RFD - were not to hold for other elements and quenchers as well. Therefore, the series of

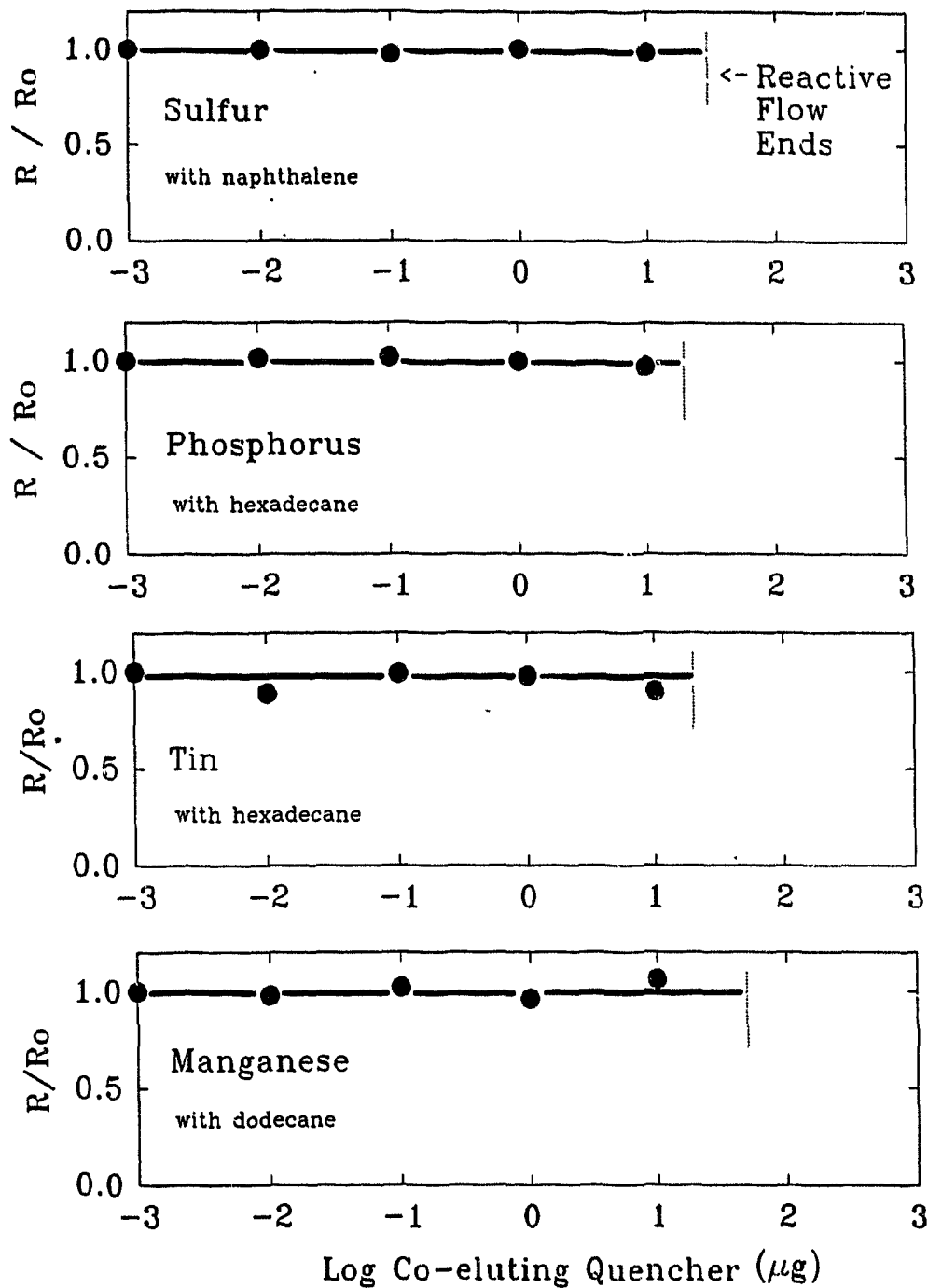


**Figure 23:** RFD response in the presence of co-eluting hydrocarbons as indicated. Analytes: 50ng thianaphthene, 500ng tris(pentafluorophenyl) phosphine, 1ng tetra-n-butyltin, and 500ng MMT.

tested elements was not extended beyond the prominent FPD foursome of S, P, Sn and Mn.

Yet there remains one aspect that, while subject to easy prediction, still begs experimental verification. It concerns the analyte concentration. The four analytes, whose behavior is depicted in Figure 23, were for obvious reasons injected in large and constant amounts. By analogy with the FPD, the fact that these amounts were large and constant should not make a difference: fractional quenching in the FPD depends primarily on the concentration of the quencher, and barely at all on the concentration of the analyte (Ch.1). However, since the RFD has shown itself to be so different from the FPD in quenching behavior, similarity in regard to analyte concentration should perhaps not be presumed.

Experimentally that suggests an investigation of the "quenching" of small amounts of analyte. This is difficult to do in the framework of Figure 23, since the peak of the quencher is likely to tower over the peak of the analyte. For this reason a type of experiment - often carried out unwittingly, rarely carried out deliberately<sup>[81]</sup> - in which a small analyte peak rides on the tail of a large quencher (solvent) peak, was employed. Obviously, the more prominent the tail the more pronounced the quenching in the FPD.

Figure 24 shows one typical experiment from a series of tests that comprised various elements (i.e. the above mentioned foursome along with others) but produced invariably

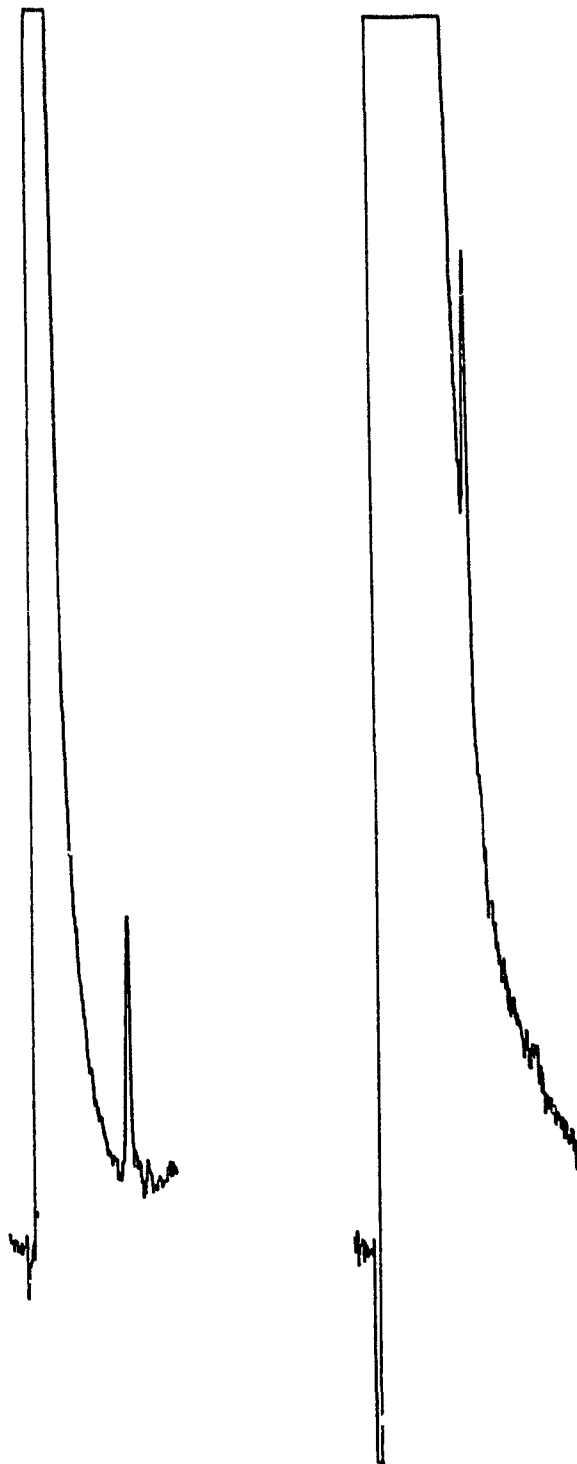


**Figure 24:** RFD response of a trace sulfur peak on and off the solvent tail. The amount of injected analyte (1ng thianaphthene) is the same; however the amount of solvent (acetone) has been increased 12 times for the second chromatogram by drawing additional acetone into the syringe prior to injection.

the same result. The amount of analyte is now much closer to the detection limit, and, as suggested by Figure 23, the quencher (the solvent tail in this case) exerts no visible influence on the analyte's peak height; it remains reassuringly the same. It is found therefore that quenching does not occur to any significant extent in the RFD, regardless of analyte (or quencher) concentration.

From an analytical viewpoint that is a welcome find indeed. Quenching has been a major problem for the FPD, particularly since this detector is often used to determine trace analytes contained in hydrocarbonaceous matrices. The most typical cases might involve sulfur compounds in natural gas and oil; but thiophosphate pesticides, and a variety of other interesting species found in environmental systems have been proven important as well (Ch.1).

While the RFD does not appear to be subject to quenching, it should be noted that its operating range is shorter than that of the FPD: A large amount of hydrocarbon, just like the usual solvent peak, will temporarily extinguish the reactive flow. This occurs in the prototype RFD with amounts in excess of 10 to 100  $\mu\text{g}$  (and above). Whether different flow rates, different glowing-column dimensions, etc. would extend the upper operating limit has not been investigated. On the other hand, this much of a quencher influx hardly if ever occurs from capillary columns; if contained in a single peak it would represent about a 1 to 10% component of a 1  $\mu\text{L}$  injection.

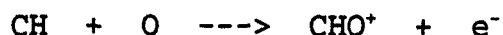
A direct comparison with the FPD is difficult because its quenching effects are dependent on detector construction and operation. Farwell and Barinaga's review mentions that "several tens of nanograms of carbon per second are necessary before hydrocarbons will produce significant reduction in the sulfur response"<sup>[15]</sup>. In our own laboratory GC-FPD, quenching effects (by a constant stream of methane) became noticeable at roughly 1  $\mu\text{g C/s}$ <sup>[83]</sup>.

From a mechanistic viewpoint, the fact that quenching does not occur in the reactive flow is certainly interesting. For the sake of opening a discussion, a scenario is offered as a plausible cause for the phenomenon. It should be understood, however, that this kind of proposal represents, at such an early age of the RFD, imagination with no experimental basis as yet.

The reactive flow regime may be compositionally related to the well-studied region between the second and third explosion limits of hydrogen-oxygen mixtures, where peroxide chemistry plays a decisive role<sup>[108,109]</sup>. If so, it is possible that a radical like the oxygen atom, whose characteristic function is chain-branching, could be near absent in the RFD.

Let it now be assumed that quenching in the FPD is indeed a quenching "of the exciting flame rather than of the excited analyte"<sup>[83]</sup>, and that such quenching occurs via the reaction (or reactions) of the oxygen atom and a simple carbon species (or a pool of simple carbon species) - say reactions not

unlike the chemiionization usually considered responsible for FID<sup>[91]</sup> response:



Such reactions would tend to diminish chain branching, i.e. reduce the concentration of those free radicals (H, OH) whose recombination is believed to provide the energy for many of the chemiluminescent processes monitored in the FPD<sup>[66,109]</sup>. Hydrocarbons introduced into the FPD flame have been observed to quench the radical-driven OH emission (experimentally the bands at 306-309 nm); and there also appears to exist some correlation between the quenching of the OH bands and the quenching of several FPD-active elements in the same, methane-doped flame<sup>[113]</sup>. In contrast, the 306 nm OH emission from the RFD showed little or no quenching by  $\mu\text{g}$  amounts of typical quenchers and analytes.

A variety of reactions have been considered responsible for the appearance of the OH bands under various conditions<sup>[109]</sup>, for example



and



and it is thus possible to attribute the quenching of FPD

response by hydrocarbons to a quenching of the radical chain mechanism operating the hydrogen-air flame. Whether it is indeed the oxygen atom that serves as the primary target of carbon species is, of course, open to debate: too little is known about the FPD flame and the RFD glow.

But assume now - for sake of a sample argument - that it does. It then becomes clear why the presence of hydrocarbons should have little influence on the reactive flow. The RFD must have a different chemistry: if it had a rate of oxygen atom formation comparable to that of the FPD, and used it for propagation, it likely could no longer remain a glowing column but would revert to a hydrogen-rich, small flame burning at the bottom of the capillary (just as the one that is produced by changing the composition of the gas supply, thereafter causing the glow above it to vanish [Ch.4]).

It is also possible to use speculation of quite a different nature. For instance, a reactive flow may be less destructive toward hydrocarbon molecules than a regular flame (although the RFD's response to various elements, including carbon, clearly indicates that it is chemically corrosive). In this context, perhaps a vital hydrocarbon quenching species is present in the FPD but absent in the RFD. Thus it should, in fact, be interesting to collect, analyze and compare organic effluents from doped RFD-type glows and FPD-type flames (just as in the flame photometric reactor [Ch.3]).

Indeed, most of the above speculations could be easily

confirmed or denied by subjecting the pliant RFD system to some fairly obvious and - at least from the present point of view - quite promising experiments. Such experiments are, however, beyond the simple chromatographic and analytical confines of the current study, and would be resorted to only when or if necessary.

## **6. REACTIVE FLOW - FLAME IONIZATION DETECTION**

### **6.1 Introduction**

Recalling from chapter 4, the reactive flow is situated below and dependent upon a flame atop the capillary: extinguishing it would mean extinguishing the reactive flow beneath it.

The flame thus performs a dual function: it provides the reactive flow with free-radical sustenance, and it gets rid of its excess hydrogen. These chores accomplished, though, it just might become a sensor of its own, generating ion pairs from chromatographic peaks. In other words, its role would be that of an additional, flame ionization detector type channel, fed directly by the reactive flow.

All this because the flame has one crucial quality: it is air-rich and, while certainly not optimized for FID duty, should yield much better ionization performance than the hydrogen-rich flame of the FPD. The latter has, of course, been used for its conductivity as well: Several FPD manufacturers offer the easily installed and inexpensive option of an electrical channel (Ch.1). Unfortunately, the FPD's electrical background current and noise in the flame is rather large. It is therefore not surprising that the detection limit for carbon compounds by ionization in that flame is nowhere near that of the FID proper.

On the other hand, many types of FPD-based analyses do benefit from - and may even require - an additional FID

channel: for that, the petroleum, perfume, and pesticide industries (to name but three) offer abundant examples. There, the column effluent is usually divided between two independent detectors, with all the drawbacks such an arrangement entails in terms of split ratio constancy, peak correlation, and detection limits. Still, two detectors are usually preferable to a single detector with two channels<sup>[94]</sup>.

In this context, a very recent, sequential-detection development should be mentioned because it might prove competitive with the common parallel-detection approach. The pulsed flame photometric detector (Ch.1) has been described in which the hydrogen-rich effluents from one *pulse* flow into a second chamber and are mixed there with additional air, to be recombusted by the subsequent pulse. The electrical conductivity of the second chamber thus provides FID-type response<sup>[114]</sup>.

Industrial interests aside, our group has for the past few years dabbled in dual- or multiple-channel detector systems for the determination of signal ratios and subtraction, correlation, and response-ratio chromatograms<sup>[60,61,102]</sup>. For this purpose, amplitudinally independent but temporally concurrent channels offer the most basic and accessible systems to investigate. The already existing flame atop the RFD sits well with such endeavours.

The question is only to what qualitative and quantitative

degree the (chemically corrosive) reactive flow would deliver to the flame the (FID-active parts of) various analytes; i.e. the degree to which the flame atop the reactive flow would be able to respond like a conventional flame ionization detector being fed the same (but intact) analyte molecules. Some ionic conductivity could probably be obtained. But how much and from what compounds?

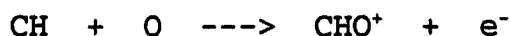
Short of running the actual experiment, the answer to that question does not come easy and, furthermore, is of an ambiguous nature. But to postulate at the beginning will be a useful way of introducing the problems implicit in such an attempt.

On one hand, the column effluent has to travel a few centimeters in a reactive flow that - as is obvious from its generation of mono-, di- and tri-atomic luminescers (including  $\text{CH}^*$  from pure hydrocarbons) - must have the ability to break analytes apart.

On the other hand, if earlier experience regarding effluents collected from the flame photometric reactor (Ch.3) provides any indication, some hydrocarbon molecules could escape the reactive flow unscathed. For instance, recall that up to 82 % of doped-in n-pentane could be recovered from the reactor. Hydrocarbons are more resistant, than are hetero-organics, to a hydrogen-rich environment (particularly in a diffusion as opposed to a premixed flame). How closely their fates in the reactor and the RFD parallel one another

is, however, still an open question.

Even if hydrocarbons were to break down completely in the glowing reactive-flow column, electrical conductivity in the top flame might still be obtained from suitable fragments. As stated in chapter 5, the reaction most often considered to provide the FID with its chemiionization response is



and CH would seem a plausible and relatively stable product of carbon compounds traversing the reactive flow.

As well, the degradation mechanisms that generate the particular carbon species responsible for the "equal-carbon" response behavior of the FID are still open to debate. In the present context, the hydrogen-atom induced decomposition<sup>[93]</sup> pathway seems attractive: if it does indeed represent the main route to analyte degradation in the air-rich FID flame, then the same analyte in the hydrogen-rich RFD flow - or in the hydrogen-rich FPD flame - should be even more prone to take that route. The concept of H-atom cracking processes is also useful as a working hypothesis because it fits some preliminary evidence that was obtained in effluent-collecting experiments with the flame photometric reactor, and in (unrelated) quenching experiments with the FPD<sup>[83,86]</sup>.

The results of the latter seem to favor chemiluminescence and quenching mechanisms that are similar for most FPD-active

elements; for instance mechanisms that both use hydrogen atoms and that hence both correlate with the rapidly interacting, quasi-equilibrium mixture of free radicals in the flame. Recall from chapter 1 that this has been described as the quencher quenching the exciting flame rather than the excited analyte. The excitation of optical emitters by the recombination of flame radicals is, of course, a commonly invoked process in "spectroscopic" flames<sup>[66]</sup>.

If the (hydrogen-rich) reactive flow leaves some hydrocarbons intact; transforms others to species like  $\text{CH}_4$ ,  $\text{CH}_3$ ,  $\text{CH}_2$  and  $\text{CH}$ ; and delivers this mixture to the top (air-rich) flame, then the latter should be capable of FID-type response. In fact, it seems possible to contend, hope against hope, that the air-rich flame, when fed by a reactive flow, may produce even higher ion yields than the conventional FID. This is because a typical, well-performing FID yields only about 0.015 Coulomb per gram of "effective" carbon, i.e. about one ion pair per 500,000 "effective" carbon atoms<sup>[91,92]</sup>.

While most of the seemingly poor ion yield of the FID may be due to a relatively small cross-section of the chemiionization vs. the other reaction channels, and/or to a relatively small steady-state concentration of the required oxygen species, it may also be argued that, in a conventional FID flame, perhaps not all carbon is in its proper, suitably hydrogenated precursor state. If the reactive flow could

provide more of this precursor; and if, perhaps, it could even hydrogenate some of the groups for which the "effective carbon number" (ECN)<sup>[91,92]</sup> is substantially smaller than unity; then one could indeed imagine that the air-rich flame sitting atop of, and being fed by, a hydrogen-cracking, reducing flow containing chemiionization-prone analyte fragments, may produce more ions than an otherwise comparable, conventional FID flame being fed by an inert gas stream containing intact analyte molecules.

These, then, are the reasons for attempting to use the flame of the RFD as a chemiionization channel: the chance, admittedly low, that it would lead to a better performing FID; the possibility, only marginally higher, that it might shed some light on FID or RFD mechanisms; and the probability, much higher, that it would offer the RFD a direct, efficient, and complementary - i.e. chemically orthogonal - second channel. Yet the most important reason for the present effort is that the second channel is consistently in-situ: the flame is already in place; the additional collecting and polarizing electrodes are part of the old FID whose base the RFD occupies; and, best of all, the whole arrangement takes very little time to test - at least for an answer to the cardinal question whether the RFD-fed FID does or does not produce FID-like response to carbon compounds.

### 6.2 Evaluating the (RFD)FID

The primary question of this study is obviously whether the flame produces chemiionization when carbon compounds enter it through the reactive flow. The answer is clearly yes. The only exceptions - as expected by analogy - are carbon compounds (such as CO) that are known to respond only feebly or not at all in the conventional FID.

This raises immediately a series of secondary questions:

- (1) What is the relationship between the (gas supply) regime under which analytes produce maximum electrical conductivity in the air-rich flame, versus the one under which they produce maximum optical emission in the hydrogen-rich reactive flow?
- (2) Does the presence of the reactive flow exert a beneficial or a detrimental influence on the response of analytes in the FID flame above it? How does its effect on analytes compare with that of a hydrogen-rich flame?
- (3) Does the presence of the reactive flow alter the relative FID responses of different types of compounds, e.g. stable vs. labile, luminescing vs. non-luminescing ones?
- (4) Similarly, what are the analytical figures of merit for the FID flame in the presence and in the absence of a reactive flow below it? How do they compare in terms of linear range, and detection limit?

#### **Optimizing FID vs. RFD**

Testing FID responses is obviously restricted to conditions at which the reactive flow can exist. Within the stability region of the reactive flow, then, photometric

responses (for sulfur and phosphorus compounds) had been strongest at relatively low hydrogen and air flow rates, but they fell off dramatically at high flow rates (Ch.4).

As shown in figure 25, the reactive-flow luminescence of a carbon compound (n-dodecane) follows a similar path. So, roughly but still surprisingly, does the flame ionization current. This "(RFD)FID" response is superimposed in figure 25 on the photometric RFD profile (which was obtained, simultaneously and gratuitously, by the RFD-FID functioning in the dual-channel mode for which it was designed). Though far from being perfect, the similarity of the two chemically and physically disparate channels is striking. But why do the two responses follow similar trends?

Chemiiionization and chemiluminescence are known to correlate frequently in flames<sup>(92)</sup> -although the reason for this correlation, more often than not, remains obscure. However, the present case is clearly different in nature: The chemiiionization is observed in the flame, the chemiluminescence in the reactive flow. The RFD-FID thus seems to separate optical from electrical responses: At typical operating conditions, the flame shows only insignificant luminescence compared to the reactive flow; conversely, the reactive flow shows only negligible ionization compared to the flame.

The latter does make sense, at least to a degree. If the chemiiionization needs CH (or a similar reactant) to function,

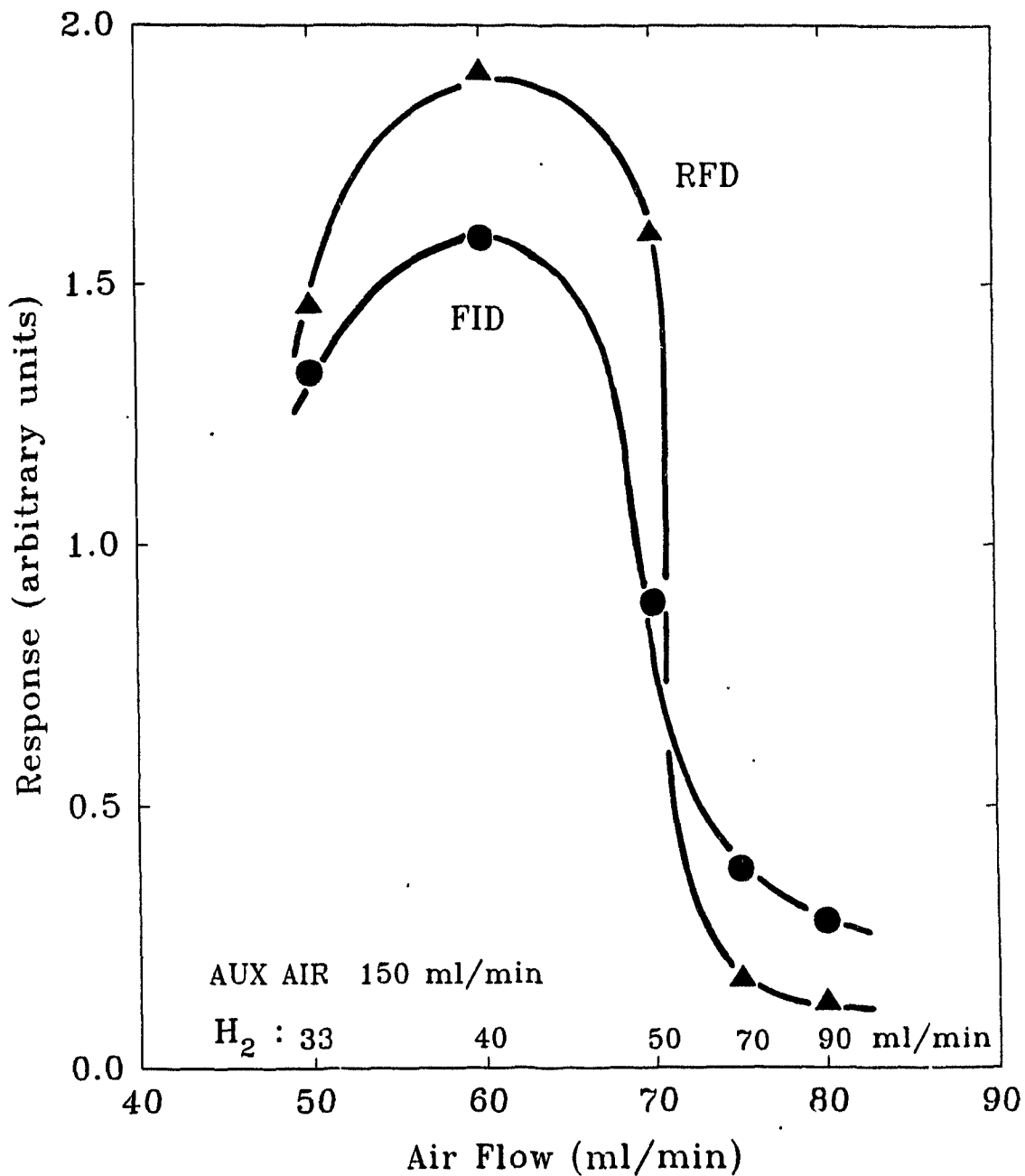


**Figure 25:** Simultaneous optical (RFD) and electrical (FID) responses from 100 ng injections of n-dodecane within stability range of reactive flow.

and if its product is  $\text{CHO}^+$  (or a similar oxygenated product not subject to further chemiionization), then the virtual absence of ionization in the reactive flow indicates that it is possible for CH (or similar species, precursor, etc.) to be passed on in sufficient amounts to the flame, there to produce typical FID response. This also seems to agree with the quenching (or lack thereof) discussion from chapter 5.

A certain amount of congruity between the RFD and the FID response profiles could also have been expected from the fact that the conventional FID, as has been known since its inception, displays a characteristic carbon response maximum at relatively low hydrogen flows.

It is, however, not known - although it would be quite interesting to know - to what extent, or even to what products ( $\text{H}_2\text{O}$  vs.  $\text{H}_2\text{O}_2$ , for instance) premixed hydrogen and air (i.e. oxygen) combine in the reactive flow, and whether the extent and/or the products change with different flow rates and compositions. It is obvious from figure 25 that the reactive-flow mixture is hydrogen-richer at high than at low flow rates. At the same time, high flow rates contain more - though also more diluted - oxygen. This increased supply of oxygen, ready to combine with carbon, may work to pre-empt later FID-type responses.

The curvature of the (RFD)FID response in Figure 25 seems more pronounced than the typical FID profile at different hydrogen flows. Other effects - e.g. the increased oxidation

at higher air inputs speculatively mentioned above - may also play a role. The system could undoubtedly be further investigated, e.g. by measuring spatially resolved data for chemical composition, spectral emission and electrical conductivity (if any) along the length of the capillary holding the reactive flow. But, given the essential concurrence of RFD and FID maxima, and the primarily analytical motivation of this study (for which coinciding maxima are far more important than correlating mechanisms), such consolidating measurements were not carried out.

#### **Single and Double Flames vs. the Reactive-flow**

Another consolidating measurement was, however, carried out - even though it included conditions removed from those of the response maximum and, indeed, the reactive flow region. The incentive for the measurement came from a (seemingly) simple question: Given that the hydrogen-rich reactive flow passes on structures capable of later chemiionization, could not a hydrogen-rich flame behave likewise? If so, that would have implications both analytic (e.g., the feasibility of a dual-flame FPD-FID) and mechanistic (e.g., the distinction between a reactive flow and a flame).

The measurement is easy to carry out - although it suffers, as most experiments in this area do, from the fact that certain phenomena can be obtained and observed only within certain flow regimes; and that, therefore, the desired perfect comparability can often not be achieved.

Given a constant flow of hydrogen, a reactive flow (a glowing column) can be obtained only for a certain flow range of premixed air. If the flow of air is lower, the reactive flow ceases to exist - but the flame on top, sustained by auxiliary air, still burns. If the flow of air is higher, the reactive flow retracts toward, and a (hydrogen-rich) flame appears at, the capillary restriction. Again, the (air-rich) flame on top keeps burning.

Visually at least, the increasing amounts of air fed into the capillary appear to cause the "inner cone" of the air-rich flame to extend downwards, then fill the capillary evenly, then coalesce and contract into a second flame burning at the restriction (see Ch.4-fig.10). The resulting dual-flame arrangement is, in fact, reminiscent of the Smithells separator<sup>[110]</sup> and its modern descendants<sup>[66,82]</sup>; but - in contrast to the reactive  $H_2/O_2$  flow which has, to our knowledge, no forebears - we did not investigate the optical or electrical properties of the lower flame.

For instance: would this hydrogen-rich flame, which sits on the bottom of the capillary, show - in contrast to the reactive flow - ionization response toward carbon? FPD analogy suggests that it should. If it did, could such response perhaps be used to answer one or the other mechanistic question, or could it possibly serve as a non-visual criterion for distinguishing a reactive flow from a real flame?

The three reactive-flow/flame regimes can be successively entered by increasing the supply of premixed air: the air-rich flame on top is first being fed by intact analyte; then by the effluent of the adjacent hydrogen-rich reactive flow; then by the effluent of the hydrogen-rich flame burning way below it. This simple increase of premixed air thus tests the important transfer of electrical response properties. Figure 26 shows the interesting result - for two different levels of nitrogen flow, and for both aromatic and aliphatic test compounds.

Higher nitrogen flows shift the curves to higher ion yields. This could have been predicted by analogy to the conventional FID. If, as is common today, the conventional FID is fed by capillary columns, nitrogen is routinely added: not just for preserving chromatographic resolution but also for increasing detector response<sup>[91]</sup>. A similar effect pertains here, except that the different jet dimension and the high hydrogen flow rate (for an FID) slightly distort the familiar picture. The constant flow of hydrogen used, 40 mL/min, is convenient for accessing the reactive-flow regime; however, it is a bit too high for conventional FID operation.

Note that the response maximum of the conventional-FID analogue - i.e. of a single, air-rich hydrogen diffusion flame burning on the same jet as the RFD-FID, but without the additional nitrogen and oxygen of the premixed air - occurs at 18 mL/min hydrogen. This maximum is more than twice as high

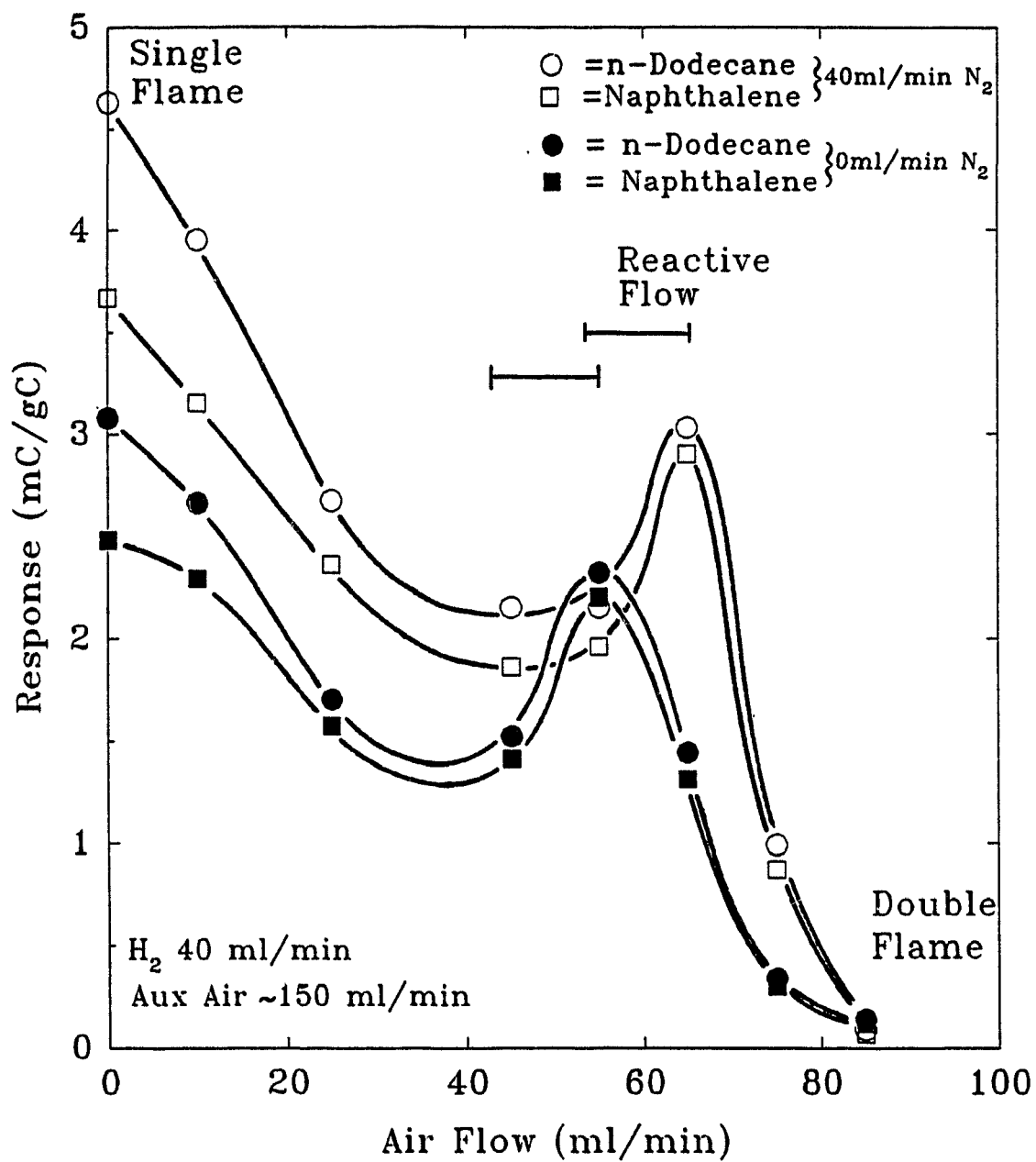


**Figure 26:** Ionization response profiles for varying stages of a reactive flow. 100 ng injections each of n-dodecane and naphthalene.

as the response obtained under the same conditions but - in the "FID-only" mode - at 40 mL/min hydrogen.

Considering the circumstances, the overall response intensity shown in figure 26 is reasonable compared to the roughly 15 millicoulomb per gram effective carbon that a top commercial FID will yield. No doubt the FID performance of the RFD-FID could be further improved, for instance by forcing the auxiliary air closer to the top flame, by polarizing the jet itself, or possibly even changing the capillary dimensions. However, comparative response is neither the most important nor the most interesting feature of figure 26.

Of much greater interest is the response maximum that is located roughly in the reactive-flow region. The region where full reactive flow exists - as judged by a clearly visible, stable, full-length glowing column (when doped) - is marked on figure 26. Less stable and/or partial glowing columns persist close to both sides of this range. Were it not for this local maximum, the response curves of figure 26 might have descended monotonically from single flame to double flame. So why the maximum?

The answer - for now but a speculative one - is that the maximum is indeed associated with the reactive flow; and that this is so because the reactive flow "assists" in producing and/or conveying into the flame the carbon-based species on which chemiionization depends. Thus, although operation of the FID mode at the reactive-flow maximum does not quite match

the ion yield of the pure diffusion flame, the introductory musings on the possibly beneficial effect of a hydrogen-rich reactive flow may not have been entirely unreasonable. Perhaps conditions and dimensions could be found at which operation at reactive-flow conditions would even exceed conventional FID response. However, efforts to find these were never in progress nor planned.

#### **Response Correlations**

Table 5 presents three types of response for various types of compounds, including some typical FID and FPD analytes. The same set of flow conditions - selected to give good photometric response - was used for all compounds. While repeatedly injecting a particular test compound, the reactive flow under the FID was switched on and off by adding or deleting the air premixed into the hydrogen flow. The comparison between the two FID modes with and without a precluding reactive flow was thus imperfect, since the (in the case of the reactive flow even unknown) composition of the gas entering the FID flame changed during switch-overs. However, this was as close to an ideal comparison as could be performed.

That the reactive-flow was indeed "on" when it was supposed to be was affirmed by the presence of a photometric response via the image conduit. This also provided some interesting comparisons of its own. Note, however, the case of tin: for purpose of a consistent experimental protocol, and

**Table 5: RESPONSE OF DIFFERENT COMPOUNDS IN THREE DETECTOR MODES**

Compound	FID Response		RFD Response
	RF off	RF on	
Dodecane	3.3	1.5	4.1 x10 <sup>9</sup> (C)
Naphthalene	2.3	1.2	3.2 x10 <sup>9</sup> (C)
Ethyl decanoate	2.3	1.2	4.0 x10 <sup>9</sup> (C)
p-Methyl-benzophenone	2.2	0.95	4.1 x10 <sup>9</sup> (C)
1,3,5- Trioxane	0.39	0.06	1.7 x10 <sup>9</sup> (C)
1,4- Dioxane	0.55	0.12	1.9 x10 <sup>9</sup> (C)
Pyrazine	0.44	0.22	3.3 x10 <sup>10</sup> (N)
Pyridine	0.61	0.32	3.0 x10 <sup>10</sup> (N)
Thianaphthene	2.0	1.0	3.6 x10 <sup>13</sup> (S)
Di-t-butyl-disulfide	3.0	1.2	4.5 x10 <sup>13</sup> (S)
Di-n-hexyl-sulfide	1.6	0.97	2.1 x10 <sup>13</sup> (S)
Methylcyclopentadienyl manganese tricarbonyl	1.6	0.57	9.7 x10 <sup>12</sup> (Mn)
Tetramethyl-tin	0.87	0.58	1.1 x10 <sup>14</sup> (Sn)
Tetra-n-butyltin	1.8	1.0	1.9 x10 <sup>14</sup> (Sn)
Tris (penta-fluorophenyl) phosphine	3.0	1.2	1.1 x10 <sup>14</sup> (P)

All compounds injected in 100-ng amounts, except 1 µg for the two oxanes. Electrical responses for reactive flow ("RF") off or on are given in millicoulombs per gram carbon injected; optical responses are given in arbitrary (but internally consistent) peak height units per gram of the element shown in parentheses. Flows in mL/min: premix hydrogen 40, air 60, column nitrogen 12; auxiliary air 150. Optical channel filterless, with R-268 photomultiplier tube at -800 V.

by analogy with the complicated spectral mix of FPD emitters<sup>(31)</sup>, the injected amounts of the two stannanes may have exceeded the linear photometric range.

The FID responses are given in "mC/gC", i.e. in millicoulomb peak area per gram of carbon injected, for the obvious purpose of comparison with other absolute or relative response data. Given the extent to which both vary in the conventional-FID literature<sup>(92)</sup>, the absolute numbers of Table 5 for FID-only response (i.e. with the reactive flow turned off) do not present much of a surprise.

Of somewhat greater interest is the comparison between the responses of single compounds with the reactive flow turned off and on. Note that while the absolute response value of a compound can be compromised by on-column decomposition or sample impurity, its response ratio - in the absence versus the presence of the reactive flow - cannot. To strengthen the following argument, the ionization data of Table 5 are replotted in Figure 27, with elemental symbols included.

In this graph, the FID response as fed by the reactive flow appears a more or less constant fraction of the FID response as fed by the intact analyte. (The line is drawn at exactly slope 1/2.) It does not seem to matter whether the compounds are hydrocarbons, hetero-organics or organometallics; whether they contain this or that hetero-element; whether they are relatively stable or

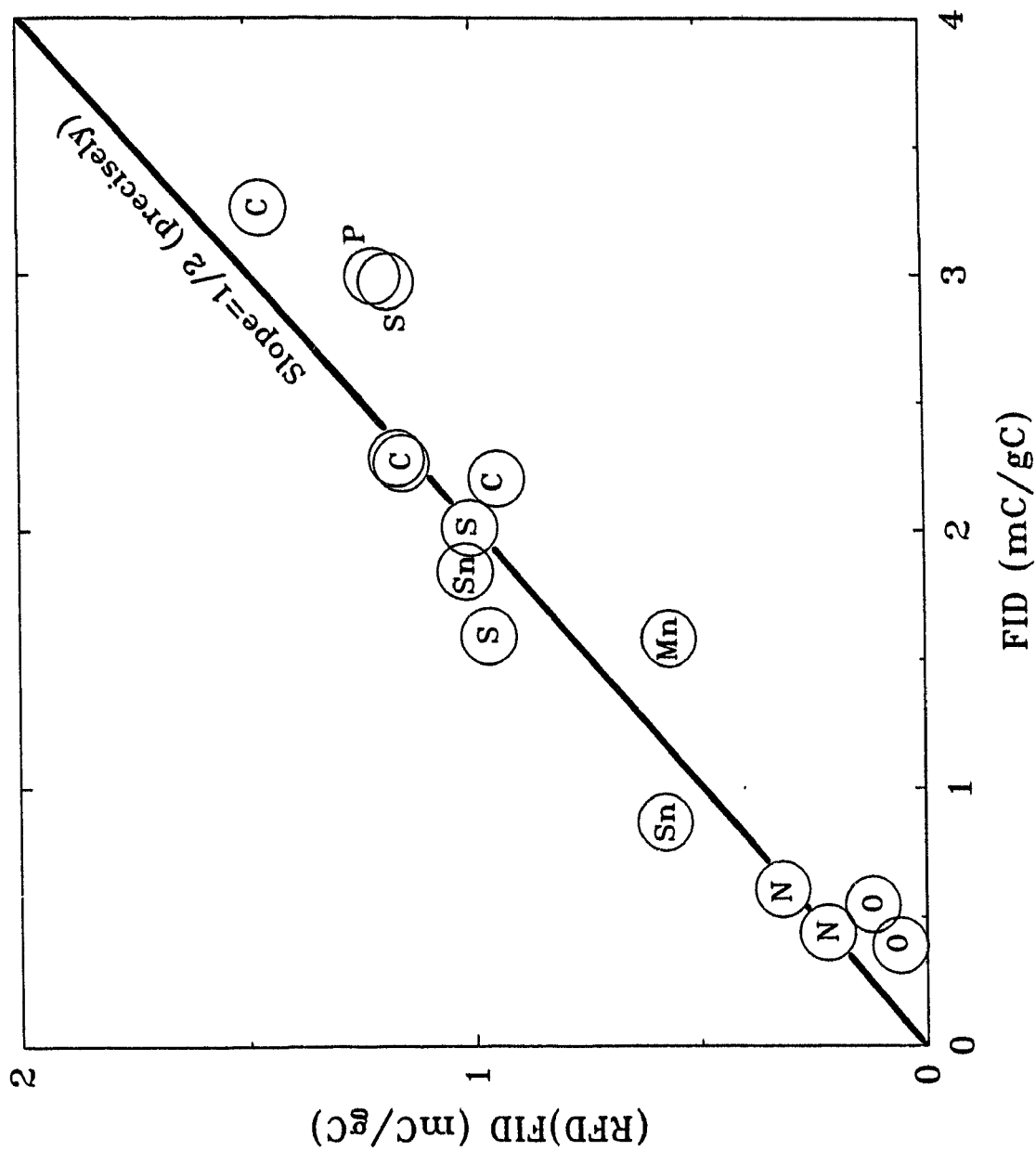


**Figure 27:** Ionization efficiency for different types of compounds with or without passage through a reactive flow. (Illustration via Table 5.)

unstable; and whether they yield weak or strong photometric response. The latter may be irrelevant to the discussion, except that strong RFD response from mono-, di- or triatomic emitters presupposes a significant extent of structural damage to the precursor analyte.

Figure 27 succeeds in suggesting a general relationship between the respective sets of data and, by extension, between the respective degradation mechanisms of the reactive flow and the flame. (One rare type of exception will be discussed later.) The air-rich flame atop the RFD can hence be considered to behave like a conventional FID flame; thereby offering a new, practically simultaneous and, by all evidence, chemically orthogonal response channel. This should make the RFD-FID a convenient and sensitive system for the response ratio studies and correlation chromatograms mentioned earlier.

Although luminescence was monitored only because the photometric channel was already in place, and because it provided unambiguous information on the presence or absence of the reactive flow, it is still interesting to look at some of the gratuitously obtained, relative RFD responses.

Of the four carbon compounds listed at the top of Table 5, three yield very similar responses per gram carbon, with only naphthalene being slightly lower. This is interesting because, in the FPD, naphthalene responds significantly stronger than n-dodecane<sup>[39]</sup>. This would agree with a scenario in which all carbon compounds in the reactive flow would

produce the same, single-carbon, hydrogen-containing luminescer - say CH - with roughly similar efficiency. (Recall the essentially superimposable spectra of n-dodecane and naphthalene from chapter 4.)

Clearly, however, many more compounds would have to be run before such a relationship could be proposed with confidence. Since the absolute responses, as opposed to the response ratios, are subject to bias from, e.g., impure standards and premature decomposition (causes of bias that are too laborious to check and control for so trivial an answer), the measured numbers should not be used to draw conclusions on whether the RFD response is or is not, in particular cases, element-specific.

An apparent exception to the more or less constant ratio of (RFD)FID and FID-only responses appears to be the behavior of two compounds that are included here simply because interesting FID data have already been collected on one of them. Blades<sup>(115)</sup> used 1,3,5-trioxane as an indicator of thermal decomposition (pyrolysis having been suggested earlier as a possible FID degradation scheme). This because the thermal decomposition of trioxane yields methanal: as it happens, the former yields significant, the latter insignificant response in the conventional FID.

Similar to Blades' results, which were obtained on a conventional FID, trioxane yielded a low but still sizable response on our setup when the reactive flow was turned off.

When the reactive flow was turned on, however, trioxane response dropped to almost zero. Whether the product of the degradation was formaldehyde, and to what degree the degradation was thermal, is unclear. In Blades' study, trioxane disintegrated in a Pyrex tube between 300 and 400 °C. In comparison, the reactive flow showed thermocouple temperatures between 200 and 230 °C when measured on an opened detector of otherwise ambient temperature. (The temperature under typical RFD-FID operating conditions was not measured but would, of course, be considerably higher.)

In any case, the reactive flow seems unable to convert trioxane carbon into an FID-active species. It is interesting to note in this context that the photometric response of trioxane is also reduced (as compared to that of other oxygenates) - although not to the same extent as the conductometric response. Such similarity is consistent with the earlier assumption of CH being the predominant emitter. If so, the same species (albeit in different locations) would be responsible for both the chemiionization and the chemiluminescence responses of carbon compounds.

#### **Response Linearity and Detection Limits**

Since the reactive flow "modifies" gas chromatographic effluents before they enter the top flame, it may be reasonably asked whether that process could become subject to chemical exhaustion by a very large analyte influx.

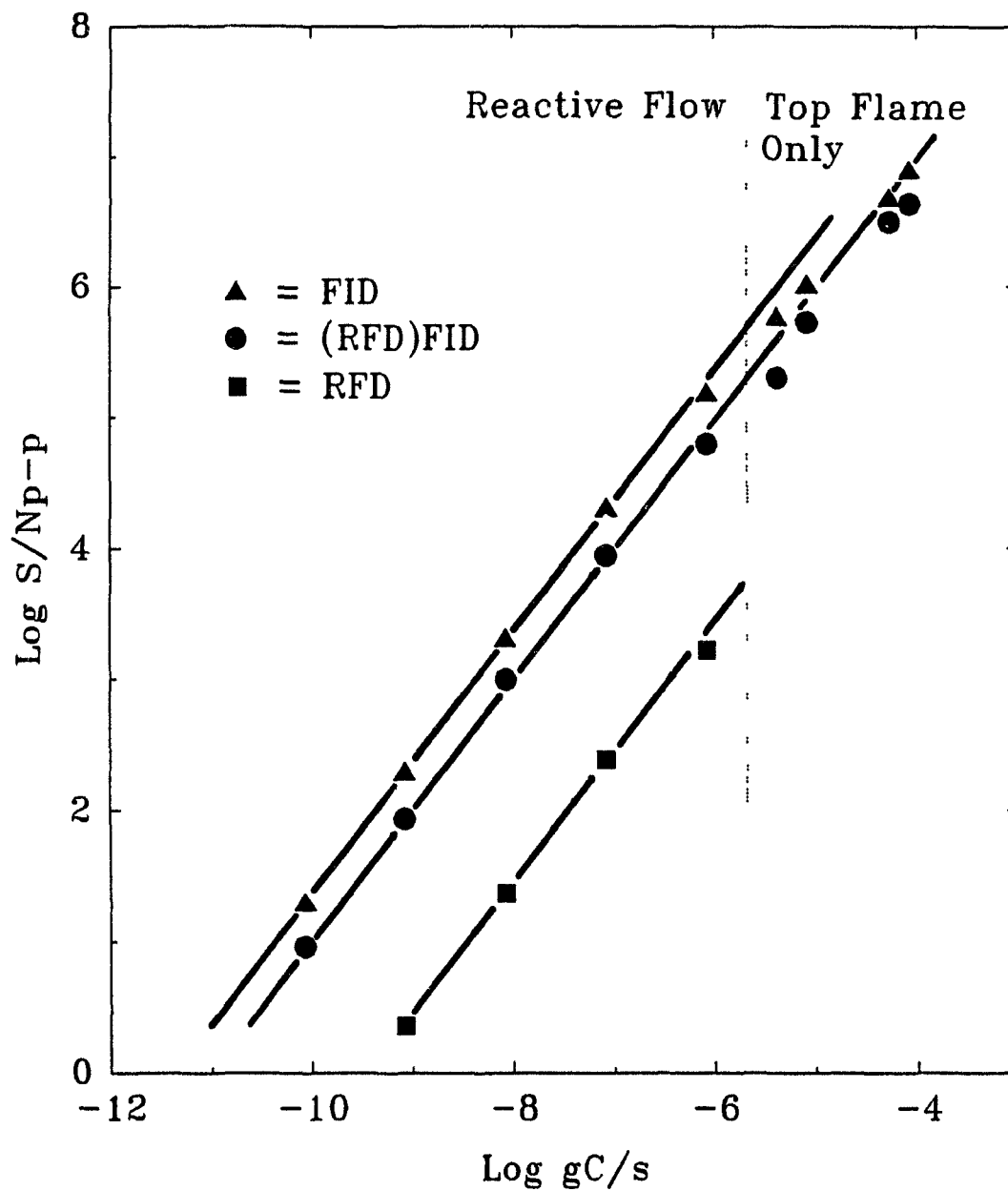
Essentially is the (RFD)FID as linear a detector as is the FID?

Figure 28 shows n-dodecane calibration curves for both the "FID" and the "(RFD)FID" ionization responses (as well as for the simultaneous RFD photometric response). The linear ranges for the two ionization channels are similar, thus affirming the conventional FID behavior of the (RFD)FID channel. Naturally the two channels draw closer together when the reactive flow is terminated by analyte overload, i.e. when the only difference between them is the absence or presence of air in the capillary.

At this overload point the RFD response terminates and the (RFD)FID data deviate most noticeably from the straight. Note that the calibrations of Figure 28 are drawn straight and at exactly unity slope to help the viewer assess the degree and extent of deviation from linearity.

Thus the linear FID range is not quite as clean as expected of conventional FID detectors, and the minimum detectable carbon flow is not quite as low. The (RFD)FID line in Figure 28 yields  $2 \times 10^{-11}$  g C/s for a  $S/N_{p-p} = 2$ .

It is interesting to note that visual inspection of both (RFD)FID and FID traces suggested noise with some genuinely lower frequency components. Since both electrical modes show the effect while the photometric mode does not, (incidentally neither did the original Tracor commercial FID) it can only be attributed to the happenstance construction and condition of



**Figure 28:** FID vs. (RFD)FID response linearity for n-dodecane along with the RFD channel.

the prototype RFD-FID. Hence, while the symptom is recognized, the cause is not understood and, despite its curiously dampened appearance, further investigation of this, within the framework of a deliberately simple, introductory study, was bypassed.

The (RFD)FID's (in comparison with modern FID's) somewhat depressed performance can also be considered a consequence of detector construction and conditions. Overall priority had been given to a design that was fast and facile to test and would allow the reactive flow to persist and yield maximum luminescence, rather than to one that would yield maximum ionization. For these reasons, the relevant comparison is that between the "(RFD)FID" and the "FID" (rather than the conventional FID).

Given that the RFD-FID is optimized for stability of the reactive flow and for optical, not electrical response, this performance of its FID channel (degraded in terms of signal by about a factor of two) is quite satisfactory. It is, in any case, far better than that of a conventional FPD. Furthermore, suitable modifications - i.e. optimization of the capillary's dimensions - could still improve (RFD)FID performance. For meeting particular tasks, though - i.e., for obtaining dual channel RFD-FID response ratios and correlation chromatograms - the detector is already more than adequate.

## 7. A FINAL NOTE: THE SINGING FLAME DETECTOR

### 7.1 Singing In The Flame

Along with describing the reactive flow's photometric properties, chapter 4 also mentioned the artifact of characteristic sounds being produced by the burner under certain conditions. These sounds were initially observed, in benchtop experiments, when an influx of solvent would surge through the capillary and temporarily displace the reactive flow from the tube. As the flame cascaded inward and the reactive flow was being recreated, a sound wave of decreasing pitch and intensity could be easily heard by the operator. As this was further investigated, it became clear that this phenomenon occurred everytime a reactive flow was created, whether solvent was present or not. As more air was dialled into the capillary, as in figure 10's creation of a reactive flow, this same sound profile was always witnessed.

As familiarity was gained with the system, it was found to produce sounds approaching the audible extremes (~15 to 20000 Hz for human ears)<sup>[116]</sup>. Certain variations in the forming of a reactive flow (i.e. tube diameter) could cause a repetitive pop of very low pitch and intensity at the mouth of the burner or, if much larger quantities of air were premixed after a flame landed at the lower restriction of the capillary, a piercing, high-pitched whistle was obtained. While it was interesting and somewhat entertaining to trifle with this property, such an *instrument* has been

played upon in many different systems of the past.

Singing flames have been known since the 1800's and their existence has been well characterized along with other sensitive flames and oscillating phenomena that certainly demonstrate the effect of sound waves on combustion processes<sup>(109)</sup>. It is believed that singing flames are related to a resonance between some vibration of the flame on its burner and a surrounding enclosure. While perhaps not identical, the traditional description of a combustion tube and resonant cavity in singing flames, seems very analogous to the capillary and detector housing, or even the restriction and the capillary itself, in the reactive flow detector. Furthermore, the classical profile of a singing flame, showing continuous crashing and rebuilding of the flame front on its burner, may also be related to the change in flame front shape as a reactive flow is formed (i.e. when the flame can be heard singing). However, detailed flame profiles of the system are required before this can be soundly established.

The analytical viability of this event was not recognized until a large amount of hydrocarbon analyte happened to elute closely with the solvent peak, while the flame was still singing. As the analyte traversed the detector, the flame was not overloaded and a very noticeable change in pitch was heard, which seemed to vary with the concentration profile of the chromatographed sample.

Subsequent trials of this event, with an intentional singing flame (produced by increasing the premixed air to a point just below that which will create a reactive flow) yielded the same result. This finding suggested measuring the change and perhaps putting the singing flame to use.

For several years acoustic emission analysts have measured sound waves in different media, for a variety of purposes, and the method is gaining much attention<sup>[117]</sup>. Belchamber and Horlick observed a correlation between the response variation and nebulizer spray chamber pressure of an inductively coupled plasma<sup>[118]</sup>, and later employed acoustic emission to monitor the plasma's operating conditions in an attempt for use as an internal standard<sup>[119]</sup>. A laser has been used to induce pressure waves, by exciting sodium atoms in a premixed air-acetylene flame, and this sound was measured for their subsequent determination<sup>[120]</sup>. Others have measured pressure waves in flames to correlate sound with flame instability and noise<sup>[109]</sup>. Hence, the measurement of sound has been used in varying applications, the history of which is quite considerable.

For the present case of gas chromatographic detection, the author is unaware of any employment of a singing flame, other than Graiff<sup>[99]</sup>, who used one for ionization detection, as mentioned in the introduction. For monitoring sound, however, there appears to be no precedent in the GC detector literature. This is understandable when one considers that,

even though such a flame may have periodically arisen in many systems, singing flames are generally considered somewhat of a nuisance due to their inherent fluctuation. Thus, it seemed that the further characterization of this "side effect" of the reactive flow detector, may hold potential for becoming a unique GC analyzer of its own.

### **7.2 Characterization**

The nature of the sound produced by the singing flame was the first thing investigated. A microphone placed near the mouth of the detector housing was used to listen to the flame, on which an FID was simultaneously operated. Placing the detector housing over the burner provided the advantage of projecting the sound towards the microphone (it was more audible than the capillary by itself) and the ability to alter the flame's ambient air supply. The sound was monitored on an oscilloscope, as outlined in the experimental section.

Figure 29 recreates an oscilloscope trace of the microphone output typically observed in these experiments, and its appearance is generally similar to some of the other acoustic signals referred to above. The singing flame appears to be a series of pressure waves (heard as "pops"), each of which is followed by some sort of decay. For a given singing flame, lowering the auxiliary air increases the intensity (amplitude) of the initial pressure wave, while

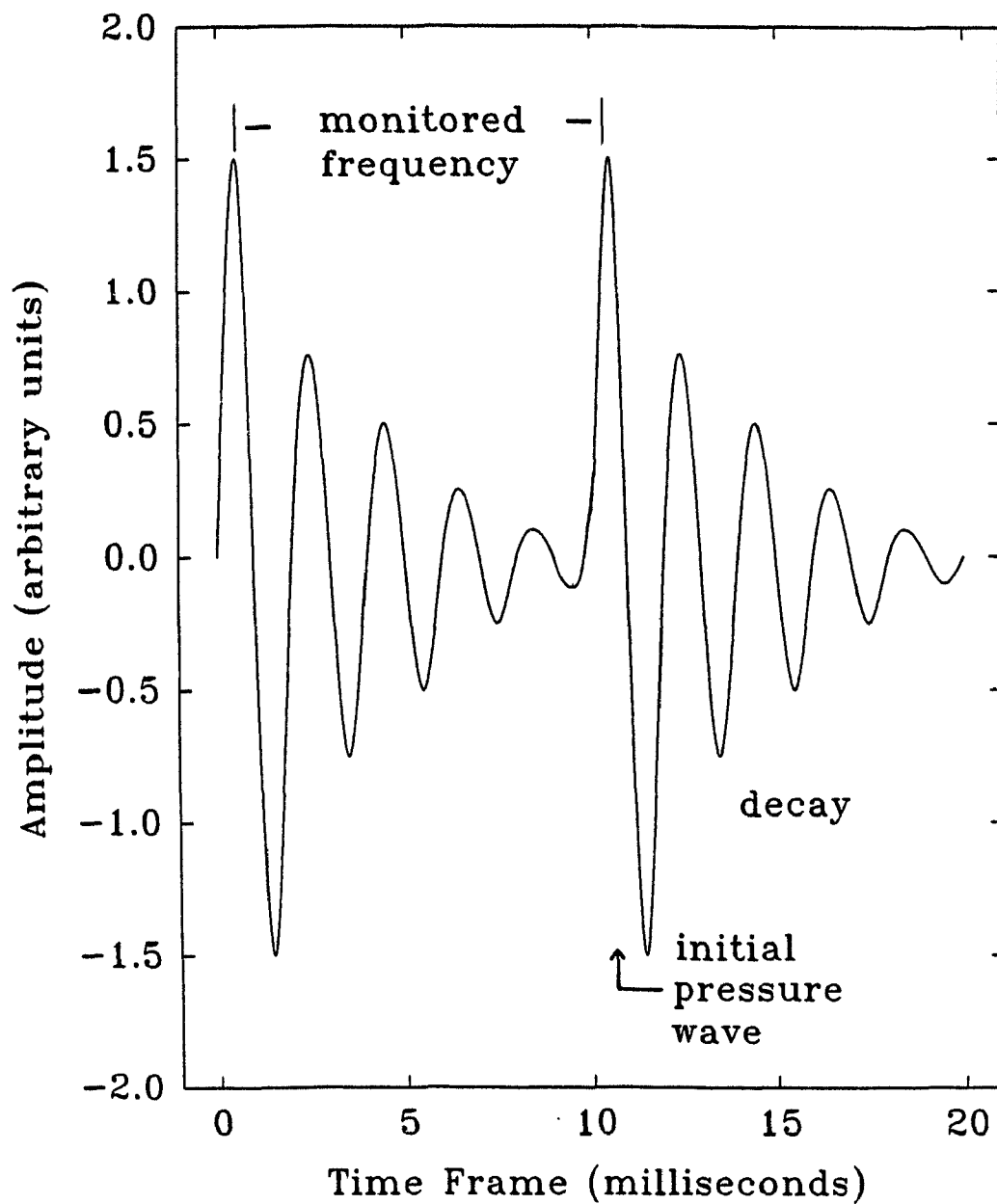


**Figure 29:** Recreation of typical oscilloscope trace of microphone response to the singing flame.

decreasing its pitch (frequency), until the flame is eventually extinguished. Likewise, increasing the auxiliary air will decrease the intensity of this signal, while increasing its frequency, to a point where the flame no longer sings. While the amplitude of the decay is affected by the auxiliary air in the same manner as the initial pressure wave, its frequency remains constant with these changes and seems to be governed by a physical parameter. This could perhaps be attributed to a system "ringing", following the initial pressure wave, as it was by Howard and Greenhalgh<sup>(120)</sup>. Thus it appeared that the phenomenon actually heard was represented by the initial pressure wave and this is what was used for measurement in all subsequent studies.

Another point of interest in qualifying the singing flame concerns the inside diameter of the burner on which it sings. Initial experiments involved the, now standard, 1.8 mm i.d. capillary, but it would be useful to know how other sizes perform. A simple test was designed in which a set of gas flows, forming a singing flame on the 1.8 mm i.d. capillary, were held constant. Then burners of different inside diameters were put in place and the flame they gave rise to was monitored.

For capillaries of 3 and 4 mm i.d., the intensity dropped dramatically and could not be heard. Moderate adjustments in the gas flow, however, did produce a very small response, at a much lower frequency. A 1 mm i.d.

burner, on the other hand, could not create a singing flame at any condition. This was expected in a sense though, as in chapter 4 it was described how this same capillary could not retreat a flame into producing a reactive flow with hydrogen and air. While it was able to create a reactive flow with hydrogen and oxygen, it was much more erratic in behavior and, even though such an arrangement may be capable of forming a singing flame, the potential trouble associated with it was cause enough to bypass this experiment in the current investigation. Thus it appeared that, by coincidence or perhaps original descent, the 1.8 mm i.d. capillary was the best suited for use in further endeavours.

It should be understood that in all of these experiments there was allowed some room for optimization by ear, although wherever possible, measurements with the microphone were made. This pairing allowed for a quick sense of the system and illustrated gas flows that were pointless to measure (i.e. where no sound could be heard).

As previously mentioned, a hydrocarbon analyte in the detector caused the singing flame to change its pitch, through what sounded like a maximum. This, along with the much more pronounced effect that a solvent peak had on the sound seemed to suggest that the singing was sensitive to carbon flow. This was checked with the FID and a frequency counter. As the injected hydrocarbon came through the singing flame, its pitch increased to a maximum point that

corresponded to the apex of the simultaneously measured FID peak. It then decreased back down to the initial frequency. Hence, it seemed reasonable to try and optimize this response for carbon. n-Dodecane, which gave the initially observed response, and naphthalene were used for optimizing in this study.

Optimizing the response of the singing flame now concerned the three main gas flows: premixed hydrogen and air, and auxiliary air. Methodically, the premixed gases seem to provide the conditions for a singing flame, while a rough check by ear, revealed the auxiliary air to have the most profound effect on the response. Thus, for the investigation, a set hydrogen flow was premixed with air to a point where the flame started singing ( $H_2/air \sim 1.3$  in most cases of the 1.8 mm i.d. capillary) and then the carbon response was checked for various settings of auxiliary air. For all of the gas flows studied, both hydrocarbons produced approximately the same resultant change in frequency of the singing flame. The intensity, however, did decrease considerably with the overall gas flow. This suggested that the operator need only choose a gas flow region where the signal was large enough to monitor on the oscilloscope. Subsequently, higher gas flows were chosen for experiments, as they gave a much more intense response.

### 7.3 The Singing Flame Detector

A better understanding of how the system responds towards different experimental variations, allowed for a test of more pressing analytical concern: the singing flame's response to different amounts of injected analyte. Figure 30 shows a calibration curve of n-dodecane in a singing flame supplied with hydrogen, premixed air, and auxiliary air gas flows of 50, 40, and 100 ml/min respectively.

The line in figure 30 is drawn at a slope of 1 and the points that scatter about it imply that the singing flame's response to carbon is linear over almost 2 orders of magnitude. The intensity of the signal remains unchanged over most of the linear portion of the plot, but begins to alter at the upper end. At this point the flame was beginning to be overloaded, and when the carbon flow became sufficient enough to cause it to temporarily stop singing (i.e. the last two points on the curve) this was defined as the upper limit to the linear range. This upper limit is close, but slightly larger than that of the reactive flow's tolerance to carbon. This seems reasonable considering how close in succession that they occur to one another.

The plot in figure 30 is given as signal vs. carbon flow. Signal, in this case, was the frequency at the apex of the carbon peak, minus the frequency prior to the peak's arrival (i.e. the background subtracted response). While the

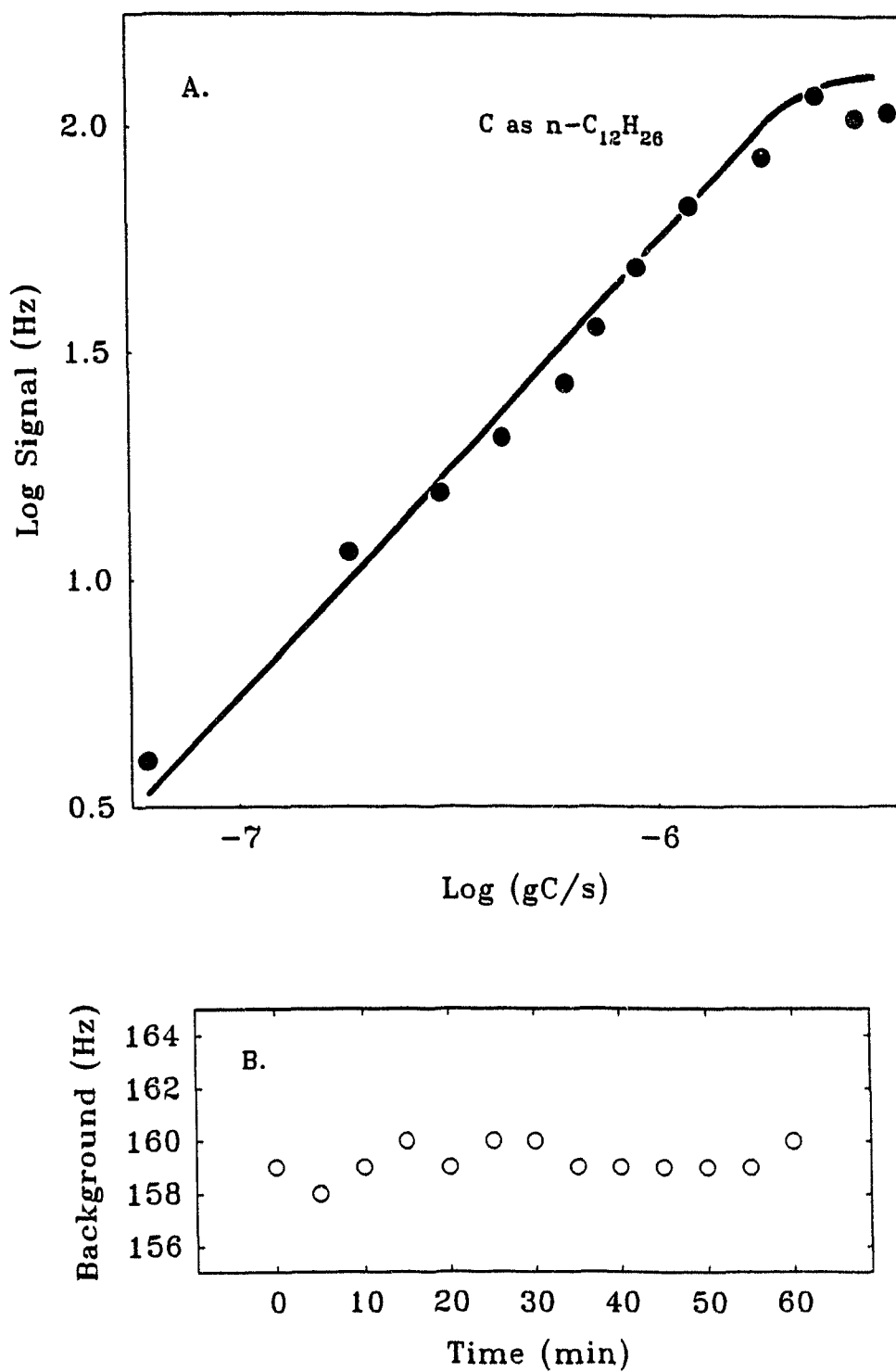


**Figure 30:** Singing flame calibration curve of n-dodecane (A.) and background measurements over time (B.).

lowest amount injected on the curve could be easily distinguished by the operator, it was approaching the background frequency of the singing flame. An accurate depiction of fluctuations in this background frequency is difficult with the present experimental design, and hence, so is a detection limit.

For consideration of the reader, a second plot in figure 30 shows background measurements, of the same flame used in the calibration curve, taken over a period of time. If the outer boundaries of these points are considered to represent the noise on the background, then the minimum detectable amount of carbon (for  $S/N = 2$ ) is about 60 ng/s. If the standard deviation of these measurements is considered then the detection limit improves slightly. However, the background plot in figure 30 is only intended to give the reader a general idea of the stability of the background response over time, and should not be implied to give an accurate illustration of the noise on the signal. In working with the system, it is felt that the detection limit is closer to 40 ng/s of carbon, but this is trivial, pure speculation at present and requires further investigation to conclusively establish the true limit of detection.

One final area that was quickly investigated for this novel system, now dubbed the "singing flame detector", was its response to a series of selected heteroelements. Injections of S, P, Mn, Sn, and Pb were performed and their

subsequent responses showed little difference from what that of the pure hydrocarbon would have yielded. Manganese did, however, give another notable result.

Upon the first injection of manganese (as MMT) the background rose to approximately ten times what a regular hydrocarbon would have caused. Unfortunately it never returned, indicating that the manganese likely deposited on the mouth of the burner. Subsequent injections on this new background gave a typical hydrocarbon response. An increase of the original nature can probably be attributed to the anti-knock properties of manganese but also possibly to variations in the distribution of heat around the rim of the burner. As well, lead and perhaps tin, may have also shown such behavior, but manganese was put through the detector first and subsequent cleaning and reinvestigation of these elements was not carried out in the current study.

Clearly, at this stage, the singing flame detector's sensitivity to carbon is less of a phenomenon than the flame itself, and it cannot compete with that of the FID. Although it is better than one might have expected, in view of some traditionally larger spectroscopic burners and the quantities of solvent that might be required to produce a noticeable change in their singing flames. As well, there appears no particular selectivity in this system (with the exception of manganese and possibly others which show presently unusable potential), but only a few elements were

sampled in this study and perhaps others may behave differently. Furthermore, the singing flame detector may be able to be used in conjunction with an FID to perhaps elucidate mechanistic scenarios of either detector's response. This is mentioned only because quite often the simultaneous FID traces of the singing flame gave negative and oddly appearing peaks for the carbon compounds introduced.

Regardless of its present application, characterizing and establishing the singing flame detector sets a useful precedent for future experiments, which are currently planned, and other researchers who may wish to further tune the performance of this technique.

## **8. CONCLUSION**

The current study has demonstrated the advantages of constructing a large, low-temperature fuel-rich flame reactor for studying quenching related processes in the similar, but smaller flame of the FPD. The flame photometric reactor has shown that diffusion flames discriminate against n-alkane carbon number, in terms of decomposition, whereas premixed flames do not. Furthermore, heterocyclic organic compounds were broken down much more than their pure hydrocarbon analogue. The high capacity and substantial light intensity of the reactor imply that its involvement in many other future studies may lead to spectroscopic, mechanistic, and possibly synthetic advancements.

The newly observed, elongated glow beneath a premixed hydrogen/air flame, was later named a "reactive flow" and was incorporated in the reactive flow detector; a new photometric sensor for gas chromatography. The RFD exhibits elemental sensitivities that are about as good as, or better than those of the FPD, and does so under a single set of conditions. It also does not suffer from response quenching and has been adapted for in-situ flame ionization detection whose sensitivity is only a factor of two lower than that of a comparable FID. Future system optimization, investigations of other elemental responses, and adaptation for a third, in-series analyzer, the electron-capture detector, seems very promising for extending the capabilities of the RFD.

The singing flame detector was established from what was originally thought to be just a side-effect of the reactive flow. The change in pitch of the singing flame, as a result of hydrocarbons travelling through it, relays into an approximate sensitivity to carbon of 60 ng/s, possibly lower. Further experiments may help to refine this technique and disclose new information regarding its use.

In all, the new systems that have been constructed and characterized in this thesis, show significant advantages over previous methods, and have established a foundation from which future works and other scientists may further benefit.

## REFERENCES

1. H.W. Grice, M.L. Yates, and D.J. David, *J. Chromatogr. Sci.*, 8 (1970) 90.
2. M. Krejčí and M. Dressler, *Chromatog. Rev.*, 13 (1970) 1.
3. D.F.S. Natusch and T.M. Thorpe, *Anal. Chem.*, 45 (1973) 1185A.
4. E.R. Adlard, *Crit. Rev. Anal. Chem.*, May (1975) 13.
5. M. Dressler, *Selective Gas Chromatographic Detectors*, *J. Chrom. Library*, Vol.36, Elsevier, Amsterdam, 1986.
6. C.F. Poole and S.A. Schuette, *Contemporary Practice of Chromatography*, Elsevier, Amsterdam, 1984, 185.
7. R.S. Hutte and J.D. Ray, *Detectors for Capillary Chromatography*, Ed., H. Hill and D.G. McMinn, *Chemical Analysis Series*, 121, John Wiley and Sons, Inc., New York, 1992, 195.
8. S. Kapila, D.O. Duebelbeis, S.E. Manahan, and T.E. Clevenger, *Environmental Analysis Using Chromatography Interfaced With Atomic Spectroscopy*, Ed., R.M. Harrison and S. Rapsomanikis, John Wiley and Sons, Inc., New York, 1989, Ch.3.
9. M.T. Shakeer and R.M. Harrison, *ibid*, Ch.12.
10. R. Pigliucci, W. Averill, J.E. Purcell, and L.S. Ettre, *Chromatographia*, 8 (1975) 165.
11. W. Wardencki and B. Zygmunt, *Anal. Chim. Acta*, 255 (1991) 1.

12. P.C. Uden, *Anal. Proc.*, 30 (1993) 405.
13. H. Hill, *Anal. Chem.*, 66 (1994) 626R.
14. W. Thornburg and H. Beckman, *Anal. Chem.*, 41 (1969) 140R.
15. S.O. Farwell and C.J. Barinaga, *J. Chromatogr. Sci.*, 24 (1986) 483.
16. M.L. Selucky, *Chromatographia*, 4 (1971) 425.
17. W.A. Aue, *J. Chrom. Sci.*, 13 (1975) 329.
18. R.F. Zainullin and V.G. Berezkin, *Crit. Rev. Anal. Chem.*, 22 (1991) 183.
19. J. Sevcik, *J. Gas Chromatography Library, Detectors In Gas Chromatography*, 4, Elsevier, Amsterdam, 1986.
20. S.S. Brody and J.E. Chaney, *J. Gas Chromatogr.*, 4 (1966) 42.
21. M.C. Bowman and M. Beroza, *J. Chromatogr. Sci.*, 7 (1969) 484.
22. Y.-Z. Tang and W.A. Aue, *J. Chromatogr.*, 408 (1987) 69.
23. M.C. Bowman, M. Beroza, and G. Nickless, *J. Chromatogr. Sci.*, 9 (1971) 44.
24. E.J. Sowinski and I.H. Suffet, *J. Chromatogr. Sci.*, 9 (1971) 632.
25. R. Ross and T. Shafik, *J. Chromatogr. Sci.*, 11 (1973) 46.
26. C.A. Burgett and L.E. Green, *Spectrochim. Acta.*, 30B (1975) 55.
27. W.A. Aue and C.G. Flinn, *Anal. Chem.*, 52 (1980) 1537.

28. W.A. Aue and C.G. Flinn, *J. Chromatogr.*, 142 (1977) 145.
29. W.A. Aue and C.G. Flinn, *J. Chromatogr.*, 186 (1979) 299.
30. W.A. Aue and C.G. Flinn, *J. Chromatogr. Sci.*, 18 (1980) 136.
31. W.A. Aue and C.G. Flinn, *Can. J. Spectr.*, 25 (1980) 141.
32. W.A. Aue and C.G. Flinn, *J. Chromatogr.*, 153 (1978) 49.
33. W.A. Aue and C.G. Flinn, *J. Chromatogr.*, 158 (1978) 161.
34. W.A. Aue and C.R. Hastings, *J. Chromatogr.*, 87 (1973) 232.
35. X.Y. Sun and W.A. Aue, *J. Chromatogr.*, 467 (1989) 75.
36. X.Y. Sun and W.A. Aue, *Can. J. Chem.*, 67 (1989) 897.
37. X.Y. Sun and W.A. Aue, *Mikrochim. Acta.*, I (1990) 1.
38. W.A. Aue, B. Millier, and X.Y. Sun, *Anal. Chem.*, 62 (1990) 2453.
39. X.Y. Sun, B. Millier, and W.A. Aue, *Can. J. Chem.*, 70 (1992) 1129.
40. I.H. Williams, R. Kore, and D.G. Findlayson, *J. Agri. Food Chem.*, 19 (1971) 456.
41. M. Beroza and M.C. Bowman, *Envir. Sci. and Tech.*, 2 (1968) 450.
42. M.C. Bowman and M. Beroza, *J. Agri. Food Chem.*, 16 (1968) 399.
43. C.W. Stanley and J.I. Morrison, *J. Chromatogr.*, 40 (1969) 289.
44. D.A. Clay, C.H. Rodgers, and R.H. Jungers, *Anal. Chem.*, 49 (1977) 126.

45. A.P. Bentz, *Anal. Chem.*, 48 (1976) 454A.
46. M.E. Garza Jr. and J. Muth, *Envir. Sci. and Tech.*, 8 (1974) 249.
47. Y. Hoshika and Y. Iida, *J. Chromatogr.*, 134 (1977) 423.
48. C.D. Pearson, *J. Chromatogr. Sci.*, 14 (1976) 154.
49. A.R. Baig, C.J. Cowper, and P.A. Gibbons, *Chromatographia*, 16 (1982) 297.
50. R.S. Braman, J.M. Ammons, and J.L. Bricker, *Anal. Chem.*, 50 (1978) 992.
51. R.E. Baumgardner, T.A. Clark, and R.K. Stevens, *Anal. Chem.*, 47 (1975) 563.
52. W.L. Crider, *Amer. Lab.*, 1(11) (1969) 10.
53. L. Blomberg, *J. Chromatogr.*, 125 (1976) 389.
54. M.J. Prager and W.R. Seitz, *Anal. Chem.*, 47 (1975) 148.
55. D. Nurok, J.W. Anderson, and A. Zlatkis, *Chromatographia*, 11 (1978) 188.
56. M. Kawabata, K. Ohtsuki, H. Kokura, and Y. Wakahara, *Agric. Biol. Chem.*, 41 (1977) 2285.
57. A.R. Blanchette and A.D. Cooper, *Anal. Chem.*, 48 (1976) 729.
58. H. Kaji, M. Hisamura, N. Saito, and M. Murao, *J. Chromatogr.*, 145 (1978) 464.
59. W.A. Aue, B. Millier, and X.Y. Sun, *Anal. Chem.*, 63 (1991) 2951.
60. W.A. Aue, X.Y. Sun, and B. Millier, *J. Chromatogr.*, 606 (1992) 73.

61. X.Y. Sun, W.A. Aue, *J. Chromatogr.*, 667 (1994) 191.
62. R.L. Shearer, D.L. O'Neal, R. Rios, and M.D. Baker, *J. Chrom. Sci.*, 28 (1990) 24.
63. R.L. Shearer and E.B. Poole, *J. Chrom. Sci.*, 31 (1993) 82.
64. T.G. Chasteen, G.M. Silver, J.W. Birks, and R. Fall, *Chromatographia*, 30 (1990) 181.
65. S.E. Eckert-Tilotta, S.B. Hawthorne, and D.J. Miller, *J. Chromatogr.*, 591 (1992) 313.
66. P.T. Gilbert, in *Analytical Flame Spectroscopy*, Ed., R. Mavrodineanu, MacMillan, London, 1970, Ch.5.
67. M. Lau Thanh and M. Peyron, *J. Chim. Phys.*, 60 (1963) 1289.
68. A. Syty and J.A. Dean, *Appl. Optics*, 7 (1968) 1331.
69. M.C. Bowman and M. Beroza, *Anal. Chem.*, 40 (1968) 1448.
70. T. Sugiyama, Y. Suzuki, and T. Takeuchi, *J. Chromatogr.*, 77 (1973) 309.
71. A.G. Gaydon and G. Whittingham, *Proc. Roy. Soc. London, Ser. A*, 189 (1947) 313.
72. T.M. Sugden and A. Demerdache, *Nature*, 195 (1962) 596.
73. A. Attair, R. Forgey, J. Horn, and W.H. Corocoran, *J. Chromatogr. Sci.*, 15 (1977) 222.
74. T. Sugiyama, Y. Suzuki, and T. Takeuchi, *J. Chromatogr. Sci.*, 11 (1973) 639.
75. T.J. Cardwell and P.J. Marriot, *J. Chromatogr. Sci.*, 20 (1982) 83.

76. W.A. Aue and X.Y. Sun, *J. Chromatogr.*, 633 (1993) 151.
77. W.L. Crider, *Anal. Chem.*, 41 (1969) 534.
78. W.E. Rupprecht and T.R. Phillips, *Anal. Chim. Acta.*, 47 (1969) 439.
79. T. Sugiyama, Y. Suzuki, and T. Takeuchi, *J. Chromatogr.*, 80 (1973) 61.
80. G.H. Liu and P.R. Fu, *Chromatographia*, 27 (1989) 159.
81. P.L. Patterson, *Anal. Chem.*, 50 (1978) 345.
82. P.L. Patterson, R.L. Howe, and A. Abu-Shumays, *Anal. Chem.*, 50 (1978) 339.
83. W.A. Aue and X.Y. Sun, *J. Chromatogr.*, 641 (1993) 291.
84. K.A. Goode, *J. Inst. Pet.*, 56 (1970) 33.
85. C.A. Burgett and L.E. Green, *J. Chromatogr. Sci.*, 12 (1974) 356.
86. Y.-Z. Tang, Ph.D. Thesis, Dalhousie University, 1988.
87. H.A. Moye, *Anal. Chem.*, 41 (1969) 1717.
88. R. Mavrodineanu and H. Boiteux, *Flame Spectroscopy*, John Wiley and Sons, London, (1965) Ch.5.
89. E. Atar, S. Chekis, and A. Amirav, *Anal. Chem.*, 63 (1991) 2061.
90. S. Chekis, E. Atar, and A. Amirav, *Anal. Chem.*, 65 (1993) 539.
91. H. Hill and D.G. McMinn, *Detectors for Capillary Chromatography*, Chemical Analysis Series, 121, John Wiley and Sons, Inc., New York, 1992, Ch.2.
92. P. Boček and J. Janák, *Chromatogr. Rev.*, 15 (1971) 111.

93. A.T. Blades, *J. Chromatogr. Sci.*, 11 (1973) 251.
94. R.S. Braman, *Anal. Chem.*, 38 (1966) 734.
95. J. Sevčik, *Chromatographia*, 4 (1971) 195.
96. H.W. Grice, M.L. Yates, and D.J. David, *J. Chromatogr. Sci.*, 8 (1970) 90.
97. G. Castello, G. D'Amato, and M. Nicchia, *J. Chromatogr.*, 521 (1990) 99.
98. H. Hill and W.A. Aue, *J. Chromatogr. Sci.*, 12 (1974) 541.
99. L.B. Graiff, *Nature*, 203 (1964) 856.
100. S.V. Olesik, L.A. Pekay, and E.A. Paliwoda, *Anal. Chem.*, 61 (1989) 58.
101. C.E. Sängler-van de Griend, Ch.E. Kientz, and U.A.Th. Brinkman, *J. Chromatogr.*, 673 (1994) 299.
102. B. Millier, X.Y. Sun, and W.A. Aue, *J. Chromatogr.*, 675 (1994) 155.
103. K.M. Aldous, R.F. Browner, R.M. Dagnall, and T.S. West, *Anal. Chem.*, 42 (1970) 939.
104. P.J. Padley and T.M. Sugden, *Proc. Roy. Soc. London, Ser. A*, 248 (1958) 248.
105. R.M. Dagnall, B. Fleet, T.H. Risby, and D.R. Deans, *Talanta*, 18 (1971) 155.
106. R.S. Hobbs, G.F. Kirkbright, M. Sargent, and T.S. West, *Talanta*, 15 (1968) 997.
107. C.F. Cullis and M.F.R. Mulcahy, *Combustion and Flame*, 18 (1972) 225.

108. J.A. Barnard and J.N. Bradley, *Flame and Combustion*, Chapman and Hall, London, 1984.
109. A.G. Gaydon and H.G. Wolfhard, *Flames*, Chapman and Hall, London, 1970.
110. A. Smithells and H. Ingle, *J. Chem. Soc. Trans.*, 61 (1892) 204.
111. R.M. Dagnell, K.C. Thompson, and T.S. West, *Analyst*, 93 (1968) 72.
112. V.A. Joonson and E.P. Loog, *J. Chromatogr.*, 120 (1976) 285.
113. X.Y. Sun and W.A. Aue, unpublished research, (1993).
114. A. Amirav and N. Tzanany, *The Combined Pulsed Flame Photometric Ionization Detector*, Abstract 664, Pittsburgh Conference, 1994.
115. A.T. Blades, *J. Chromatogr. Sci.*, 22 (1984) 120.
116. M. Baxter, *The Rock-N-Roll Singer's Survival Manual*, Hal Leonard Publishing Corporation, Milwaukee, 1990, 40.
117. A.P. Wade, D.B. Sibbald, M.N. Bailey, R.M. Belchamber, S. Bittman, J.A. McLean, and P.D. Wentzell, *Anal. Chem.*, 63 (1991) 497A.
118. R.M. Belchamber and G. Horlick, *Spectrochim. Acta*, 36B (1981) 581.
119. R.M. Belchamber and G. Horlick, *Spectrochim. Acta*, 37B (1982) 17.
120. A.G. Howard and D.A. Greenhalgh, *Anal. Chim. Acta*, 106 (1979) 361.